CARBON AND LIPID METABOLISM IN *MYCOBACTERIUM TUBERCULOSIS*

A Dissertation

Presented to the Faculty of the Graduate School

of Cornell University

In Partial Fulfillment of the Requirements for the Degree of

Doctor of Philosophy

by

Wonsik Lee

January 2014

CARBON AND LIPID METABOLISM IN *MYCOBACTERIUM TUBERCULOSIS*

Wonsik Lee, Ph. D.

Cornell University 2014

Mycobacterium tuberculosis is an air borne, facultative intracellular bacterial pathogen that resides in the phagosome of host cells. Virulence of *M. tuberculosis* is related to its abilities to respond to environmental cues encountered during infection and reprogram its metabolism to adapt to them. Nutrients derived from the host are key factors contributing to shape the carbon metabolism of *M. tuberculosis* during infection. This metabolic shift involves activation of fatty acid and cell wall lipids metabolism of the bacterium; however, the mechanistic interplay between them is undefined. In this study, to understand the metabolic adaptation on propionyl-CoA 3-carbon product of cholesterol in *M. tuberculosis*, the propionate detoxification and methyl-branched (MB) lipid synthesis pathways were investigated. The data presented here shows that excess propionyl-CoA was toxic to *M. tuberculosis*, as the propionyl-CoA inhibited pyruvate dehydrogenase (PDH) and acetate or fatty acid rescued the toxicity through providing acetyl-CoA the product of PDH. A mechanistic insight was revealed by metabolic labeling with radioactive propionate and fatty acids: the given fatty acids facilitate propionyl-CoA incorporation into a key MB lipid PDIM by serving as acyl-primers required for its biosynthesis. Additionally, to further define genes required for propionate and fatty acid metabolism an approach exploiting propionate toxicity and TraSH analysis was employed. The data from the genetic

profiling by TraSH confirms our model for the fatty acids rescue from the propionate toxicity and suggests putative roles for uncharacterized genes in MB lipids synthesis and fatty acid metabolism. This model was also validated by using lipid droplet loaded macrophage where *M. tuberculosis* exploited fatty acids from the host lipid droplet to synthesis PDIM resulting in reduction of the propionate stress. Data presented in this work demonstrates that the propionyl-CoA processing is a significant problem for survival in the host cell, and that the routing of propionyl-CoA into MB cell wall lipids plays an important role for limiting the metabolic stress derived from propionate. And, the data also demonstrates that the fatty acids from lipid droplets in the host macrophage may provide a well-balanced diet that retains appropriate level of acetyl-CoA and propionyl-CoA.

BIOGRAPHICAL SKETCH

Wonsik Lee earned his Bachelor of Science in Biological Engineering from Inha University in 2001 and a Master of Science in Biological Science from Korea Advanced Institute of Science and Technology in 2003. He worked in industry on metabolic flux analysis to develop industrial strains in South Korea before joining Cornell University for his Ph.D. in 2008. He was awarded the Fulbright Fellowship for Graduate Study in 2008. At Cornell University, his dissertation research in *Mycobacterium tuberculosis* was supervised by Dr. David Russell.

To my wife, Dayeon Jung

ACKNOWLEDGMENTS

First and foremost I would like to thank my Ph.D. advisor, Dr. David G Russell for his enthusiasm, expertise and great patience at all times. It has been my honor to be his student. I would also like to thank Dr. John D Helmann and Dr. Brian R Crane for their guidance on my doctoral graduate committee. I would also like to thank many past and present members of the Russell Lab for their help and direction. Foremost I need to thank Dr. Brian VanderVen for his contribution of ideas, time, and stimulating discussion. Special thanks to Linda Bennett for supporting us and maintaining the lab. I also thank Dr. Sunchang Kim at KAIST and Dr. Jaeseong So at Inha University for their helpful advice and guidance.

Finally, and most importantly, I would like to thank my parents, Kwangjin Lee and Jungwon Hur for support and encouragement. Words can never express adequately the depth of my feelings of gratitude. To my sister Wonae and brother Wonjong, thank you for all their support and warmth. Thanks to my dear parents-in-law Kyubong Jung and Pangeun Ann, for being so supportive.

To my wife, Dayeon Jung, this dissertation would not be possible without her support and patience. I am grateful for sharing all this time together with her.

TABLE OF CONTENTS

Chapter two
Evaluation of propionate toxicity and detoxification in *M. tuberculosis*

Chapter Three
Phenotypic profiling for defining genes essential for propionate and fatty acid metabolism

LIST OF FIGURES

LIST OF TABLES

LIST OF ABBREVIATIONS

AMP	Adenosine monophosphate
APC	Antigen presenting cells
BCG	Bacillus Camette-Guerin
CD	Cluster of differentiation
CFU	Colony forming units
DAT	Diacyltrehalose
DC-SIGN	Dendritic Cell-Specific Intercellular adhesion molecule-3-Grabbing Non-integrin
HIV	human immunodeficiency virus
ICD	Isocitrate dehydrogenase
ICL	Isocitrate lyase
INF- γ	Interferon-gamma receptor
LD	Lipid droplet
LDL	Low-density lipoproteins
LOS	Lipo-oligosaccharides
MB-lipid	Methylbranched lipid
MCC	Methylcitrate cycle
MDR-TB	Multidrug-resistant *M. tuberculosis*
MM-CoA	Methylmalonyl-CoA
MMP	Methylmalonyl-CoA pathway
MOI	Multiplicity of infection

MTBC	*M. tuberculosis* complex
NADH	Nicotinamide adenine dinucleotide
NADPH	Nicotinamide adenine dinucleotide phosphate
NALP	NACHT, LRR and PYD domains-containing protein
NOD	Nucleotide-binding oligomerization domain-containing protein
NOS	Nitrate oxidase
ORF	Open reading frames
PAT	Polyacyltrehalose
PDH	Pyruvate dehydrogenase
PDIM	Phthiocerol dimycocerosates
RNI	Reactive nitrogen intermediates
ROI	Reactive oxygen intermediates
SL-1	Sulfolipid-1
TAG	Triacylglyceride
TAT	Triacyltrehalose
TB	Tuberculosis
TCA	Tricarboxylic acid cycle
TDM	Trehalose Dimycolate
TLC	Thin layer chromatography
TLR	Toll-like receptors

TNF	Tumor necrosis factor
TraSH	Transposon site hybridization
VitB12	Vitamin B12
XDR-TB	Extensively drug resistant strains of *M. tuberculosis*

CHAPTER ONE

Introduction

1.1 History of tuberculosis

Tuberculosis has plagued human beings throughout human known history and prehistory. Skeletal analysis suggests that TB was present in Africa as early as 50,000 years ago. Archeological evidences for TB, including Pott`s deformities found in Egyptian mummies, can be documented more than 5,000 years ago. Just as in Egypt, evidence for various manifestation of TB are also found in America and all across Europe throughout the human history [1-4]. Written documentation of patients with TB-like symptoms first appeared in the seventh century B.C [5]. By the early of 19th century, TB was devastating European countries claiming close to 1,000 lives per million people annually. Throughout the centuries, scientists and medical practitioners had sought to understand the origin of TB. In 1865, a French physician, Jean-Antoine Villemin demonstrated the contagious nature of TB by showing transmission of TB to laboratory rabbits from tuberculosis tissue from a patient who died of tuberculosis. 20 years later, in 1882, Robert Koch changed the history of tuberculosis through his identification of *Mycobacterium tuberculosis* as the causative agent of TB, and the development of a standardized set of parameters required for the identification of the causative agent of all infectious diseases (Koch-Henle postulates) [6].

Over 130 years later, despite efforts, TB is still one of the deadliest infectious diseases; one-third of the world population is latently infected with *M. tuberculosis* and 1.8 million people die annually from TB, including 0.5 million deaths in

individuals co-infected with human immunodeficiency virus (HIV) (WHO). The emergence of drug resistant strains and HIV associated tuberculosis has complicated the current tuberculosis pandemic [7]. Although our current chemotherapy is effective for the control of TB, it is hampered by the vast reservoir of latently infected people and frequent non-compliance in anti-mycobacterial therapy, which is associated with the development of drug resistant strains. Thus, understanding of the *M. tuberculosis* physiology underlying survival of *M. tuberculosis* both inside and outside the host is central to design of more effective drugs.

1.2 *M. tuberculosis,* the bacillus

M. tuberculosis is a gram positive, rod shaped bacillus in the family *Mycobacteriaceae*. It comes from the genus *Mycobacterium*, which is composed of close to 100 recognized species [8]. Although most of bacteria in the genus *Mycobacterium* are non-pathogenic, *M. tuberculosis* is a well adapted human pathogen and, along with *M. africanum*, *M. canettii*, *M. bovis*, and *M. microti*, it comprises the *M. tuberculosis* complex (MTBC) [9].

M. tuberculosis has complex lipid-loaded cell wall containing unique, long chain mycolic acid that is responsible for formation of acid-stable complexes when the carbol fushin dyes are added (acid fast). It is believed that this complex lipid coat forms a gram negative like outer membrane [10] (Figure 1.1B). *M. tuberculosis* is a slow growing bacteria with 16-24 hour generation time and is highly aerobic and requires high levels of oxygen. Its genome is distinguished by 65.5% G+ C rich and

contains approximately 4,000 open reading frames (ORF), with hypothetical functions annotated for over 40% of these genes [11]. Classical virulence factors, such as type III effector proteins, are missing in the *M. tuberculosis* genome. However, its genome contains 250 genes (8% of its genome) involved in fatty acid metabolism, with 39 of these involved in the polyketide metabolism generating the extremely hydrophobic coat [11]. Such large numbers of genes show the evolutionary importance of the lipid coat to its survival in the host. Indeed, the lipid coat provides a hydrophobic barrier to antibiotics [12], and the biosynthetic pathway of such lipids has been targeted by anti-mycobacterial drugs as shown by the mode of action of isoniazid on *inhA* of mycolic acid biosynthesis [13].

M. tuberculosis is characterized by a range of complex lipids based on multimethyl-branched fatty acids (Figure 1.1A). These lipids include the dimycocerosates of the phthiocerol family (PDIMs), a family of sulfated acyl-trehaloses (SL), diacyl trehalose (DAT), and a heavily acylated trehalose, pentaacyl trehalose (PAT) [14, 15]. These methyl-branched lipids build a characteristic *M. tuberculosis* outer membrane by interaction with the monolayer of mycolic acids [16]. Other members of the mycobacteria appear to have alternative characteristic dimycocerosates of glycolipids: *M. bovis* BCG, *M. microti*, and *M. marinum* produce a phenolic glycolipid [17], mycoside B [18], and lipooligosaccharides (LOS) [19], respectively. The biosynthesis of these multimethyl-branched lipids involves processing and elongation of fatty acid acyl-chains by over 20 *pks* genes in *M. tuberculosis* [15]. Because theses lipids are believed to be key virulence factors, their

regulations and carbon metabolism involved in their biosynthetic pathways have been studied extensively over the last few decades [20].

1.3 Tuberculosis and current drug regimens

When humans are exposed to *M. tuberculosis*, 5-10% develop progressive disease, which is characterized by weight loss, fibrosis and persistent coughing. The majority of remaining infected individuals (~90%) develop a latent infection, with no apparent clinical symptoms for decades [21]. Although latently infected people are non-infectious and resistant to re-infection on repeated exposure, these constitute a large reservoir of potential infections. Among these latent infections, there is a ~5% risk of developing active disease during the remaining life time [22]. However, the risk of reactivation of latent infection increases significantly with HIV co-infection or in an immunocompromised condition. Approximately 13% of active tuberculosis is related to co-infection with HIV [23].

Current anti-tuberculosis vaccine was developed in the 1930s by using an attenuated *M. bovis* Bacillus Camette-Guerin (BCG) strain [24]. While the BCG vaccine provides partial protection against disseminated forms of TB during early childhood, it has limited efficacy in preventing tuberculosis in adult; on the basis of controlled clinical trial, an overall protective effect in adult is approximately 50% [25, 26]. Nevertheless, currently it is the most widely used vaccine; it continues to be administered in infants in countries where TB is endemic [27].

A

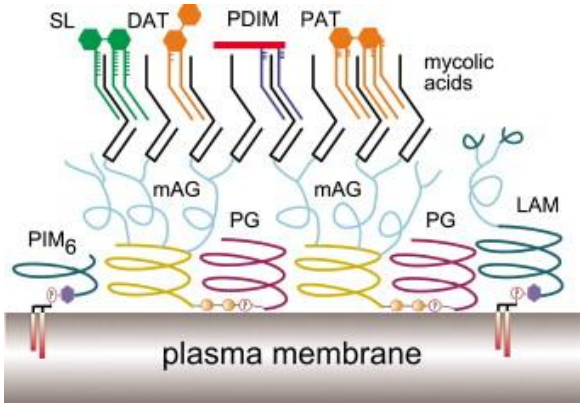

B

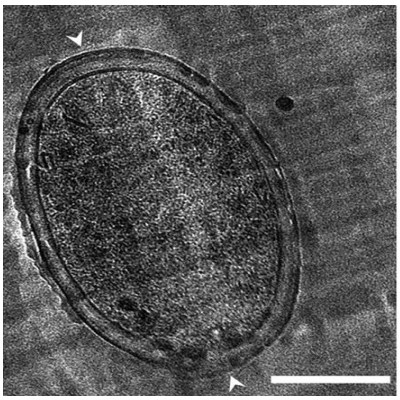

Figure 1.1 ***M. tuberculosis*** **cell wall** (A) components in the cell envelope [15]. the PDIMs, dimycocerosates of the phthiocerol family; SL, sulfated acyl-trehaloses; DAT, diacyl trehalose; PAT, pentaacyl trehalose; mAG, mycolyl ararbinogalactanp; PG, peptidoglycan; LAM, lipoarabinomannan; PIM, phophatidylinositol pentamannoside. (B) double layer of the cell envelope[10].

To replace BCG, more than 30 candidate vaccines are under development, some of them showed close to 40% efficacy for prevention of TB in HIV-infected adults [21].

Because of the limited protection of BCG vaccine, the main TB treatment relies on chemotherapy. For patients with active pulmonary tuberculosis, current standard drug treatment regimens include four first-line drugs, isoniazid, rifampin, pyrazinamide, and ethambutol. Treatment requires at least 6 months [28]. People with latent *M. tuberculosis* infection also require preventive drug treatment; the current recommended regimen is isoniazid alone administrated for 9 months. With early diagnosis and administration of effective regimens, the current treatment achieves more than 95% cure rate [22]. However, the treatment is compromised by the emergence of multidrug-resistant *M. tuberculosis* (MDR-TB). In 2012 alone, 440,000 new cases of TB were estimated globally [23]. Patients infected with the MDR-TB are treated with second-line drugs or combination regimens of these and first-line drugs for 20-30 months (WHO guideline). These second–line drugs include fluoroquinolone, ethionamide, cycloserine, and para-aminosalicylic acid [29]. However, the second-line drugs are highly toxic and are not well-tolerated, rendering treatment difficult. Moreover, the recent emergence of extensively drug resistant strains of *M. tuberculosis* (XDR-TB), which is resistant to isoniazid, rifampin, and even second-line drugs, increases the threat to current TB control. Therefore, there is an urgent need to find new strategies to combat *M. tuberculosis*.

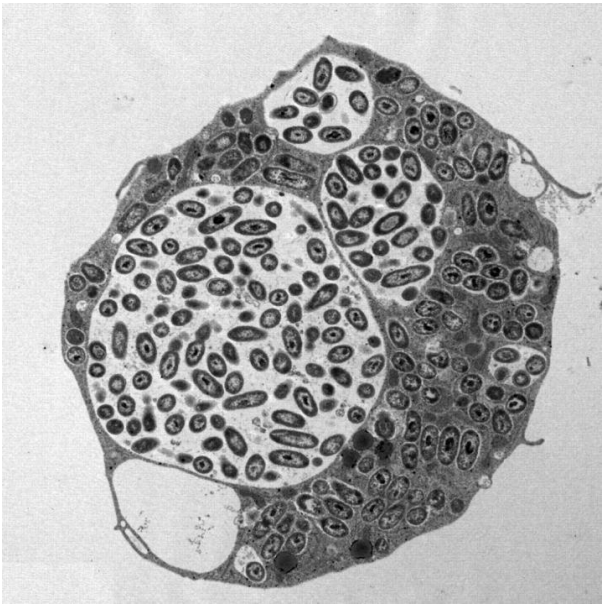

Figure 1.2 Electron micrograph of a human alveolar macrophage infected with *M. tuberculosis* [30]

1.4 *M. tuberculosis* pathogenesis

1.4.1 Overview

TB infection is initiated when *M. tuberculosis*, inhaled as aerosol droplets, are engulfed by alveolar macrophages mainly (Figure 1.2), but it is also possible that the bacilli can be ingested by alveolar epithelial pneumocytes or dendritic cells in the lung [31, 32]. Following phagocytosis, the infected host cells recruit monocytes, lymphocytes, and neutrophils from neighboring blood vessel through a proinflammatory response that is highly dependent on the production of tumor necrosis factor (TNF) by infected macrophage [4, 31]. These cells form the early granuloma, which is the pathogenic feature of tuberculosis: the granulomas are composed of infected macrophages surrounded by macrophage-derived giant cells, foamy macrophages, epithelioid macrophages and lymphocytes [33-36]. Through this process, containment of *M. tuberculosis*, host is achieved, which blocks the spread of the bacteria. This contained infection is referred as latent tuberculosis, in which the host stays asymptomatic and in a non-transmissible state until the host immune state changes. When host immunity is compromised by immunosuppressive conditions such as HIV co-infection, the center of the granulomas become caseous, and necrotic. Following such a change the bacteria become reactivated and are thought to replicate in the liquefied center of granuloma. Then, these granulomas release the reactivated, infectious bacilli into the airways or blood vessel, which allow *M. tuberculosis* to escape from 'the containment' and spread to neighboring lung tissue and even to other

organs. This state is referred to as active pulmonary tuberculosis and represent the transmission stage of the infection [31].

1.4.2 Host immune response

During the early innate immune response, the phagocytes initiate internalization of *M. tuberculosis* through the recognition of components of the bacilli. These host receptors include toll-like receptors (TLR) 2, TLR4, and phagocytic receptors such as C-type lectin receptors, the mannose receptors, and DC-SIGN [37-42]. In addition to membrane bound receptors, the cytosolic recognition receptors, NOD2 [43] and NLRP3 [44] also recognize mycobacterial peptidoglycan and secreted protein ESAT-6 respectively [45]. Following recognition the infected cells employ anti-microbial strategies to limit the growth of *M. tuberculosis*, including acidification of phagosome, autophagy [46, 47], and apoptosis [48]. But, *M. tuberculosis* has evolved multiple mechanisms to survive within the host cells. *M. tuberculosis* modulates the trafficking and maturation of its phagosome, allowing it to avoid the hostile environment of the lysosome. This is accomplished by preventing the recruitment of the vacuolar ATPase and maintaining a pH of 6.4 within its phagosome [49]. As such, the phagosome containing *M. tuberculosis* appears to be arrested at an early stage of its maturation. Several mycobacterial effectors have been implicated in this inhibition of phagosome maturation: (1) the bacterial lipids: lipoarabinomannan [50-52], trehalose dimycolate [53-56], and the sulfolipids[57], (2) the bacterial proteins: secreted acid phosphatase (*sapM*) [58], Zinc metalloprotease (*zmp1*) [59] and protein kinase G (*pknG*) [60].

Also, by regulating apoptotic and necrotic cell death, *M. tuberculosis* can generate a productive cellular niche; inhibiting host cell apoptosis allows for expansion of bacterial population in a single cell, but also for prolonged survival of infected cells before the cell dies [61-63]. Cell death does appear to be a bacteria-driven phenomenon and ESX1 induces the necrotic death of infected macrophage and the recruitment of other macrophages to serve as new host cells [64].

In the early stages of granuloma formation, inflammatory cytokines, TNF and INF-γ are primary mediators of cellular immune response [65-68]. These cytokines are required to control *M. tuberculosis* infection and for the formation of organized granuloma, which is impaired in TNF or INF- γ deficient mice [66, 68]. Activation of the infected host cells with INF- γ leads extensive changes in the intracellular environment: delivering the bacilli into lysosomes through the acidification of bacterium containing phagosome (to pH5.2) [69], oxidative killing through reactive nitrogen and oxygen intermediates [70]. Primarily, these cytokines are produced by T cells. As such, it is believed that the *M. tuberculosis* infection is controlled by a variety of T cells, including CD4, CD8, and CD1 T cells [71, 72]. Following infection, the activation of *M. tuberculosis* specific CD4 T cells is observed prior to stimulation of CD8 T cells. CD4 T cells recognizes mycobacterial protein (or peptide) antigens presented in antigen presenting cells (APC), and produces high levels of INF-γ, which in turn activates infected macrophages [73]. This observation is validated by the finding that HIV patients with the depleted CD4 T cells were susceptible to tuberculosis [74]. In addition to CD1 T cells, both CD8 T cells and CD1 restricted T cells also contribute to controlling *M. tuberculosis* infection through INF- γ production

and cytolytic activity [75-78]. CD1 restricted T cells recognize non-peptide antigens such as lipid and glycolipid antigens presented in CD1 molecules [79, 80].

1.5 Intracellular environment and adaptation

Despite the fact that *M. tuberculosis* arrests normal phagosomal maturation and resides in a compartment that resembles an early endosome [81, 82], the intracellular environment of the macrophage phagosome is still hostile. Moreover, activation of the infected macrophage or induction of autophagy in the cells leads to phagosome maturation, resulting in delivery of *M. tuberculosis* containing vacuole to an acidic, hydrolytically competent lysosome. In addition to this acidification, during infection, *M. tuberculosis* can encounter other anti-microbial strategies of the host, including an increase in reactive oxygen and nitrogen intermediates, excess metal ions, and antimicrobial peptides. *M. tuberculosis* has however evolved to adapt and exploit this hostile environment.

1.5.1 Acidification of the phagosome

Among these intracellular challenges generated by host, it appears that phagosomal acidification is a central cue to *M. tuberculosis*. During the infection, the bacterium resides in a phagosome with around pH 6.4, which drops close to pH 5.2 as the phagosome matures in the activated macrophage. Indeed, *M. tuberculosis*'s responses to this pH shift were revealed by transcriptional profiling; it was observed that 30 out of 68 genes which are induced 2 hours post-infection were related to

phagosomal acidification[83, 84]. Primarily, *M. tuberculosis* senses and responds to pH shift through a two-component signal transduction system, *phoPR*.

Transcriptional profiling suggests that *phoPR* regulates 64 genes constituting *phoPR* regulon, 44 of which are involved in lipid metabolism and the synthesis of *M. tuberculosis* cell envelope components [84]. For example, *phoPR* induces *pks2* and *pks3*, which encodes enzymes involved in production of virulence-associated acyl-trehaloses, such as sulfolipids, polyacyltrehalose (PAT) and diacyltrehalose (DAT). At low pH, a *phoP* mutant lacks these acyl-trehalose, but produces more phthiodiolone and phthiocerol A (PDIMs) [85-87]. In addition, *aprA* which is also regulated by *phoP* was shown to regulate expression of genes involved in PDIM biosynthesis. At low pH, in contrast to the *phoP* mutant, production of PDIMs was decreased in mutants lacking *aprA* [88].

Together, these suggest a link between the *phoPR* regulon and *M. tuberculosis* lipid metabolism in response to a pH shift indicating that *M. tuberculosis* uses pH to sense the host environment and remodel its cell wall to enhance intracellular survival.

1.5.2 Toxic molecules: ROS, RNI, and metal ions

Phagocytes also employ diverse toxic molecules to limit the infection. These include ROI by the NADPH oxidase (Phox), RNI by nitrate oxidase (NOS2), and excess metal ions such as copper.

Among them, radical-mediated killing is likely the primary antimicrobial mechanism [89]. Indeed, mice deficient in both Phox and NOS2 are markedly susceptible to a variety of infections [90]. However, *M. tuberculosis* has evolved a

variety of resistance mechanisms against oxidative stresses. For example, *M. tuberculosis* maintains an antioxidant defense mechanism through a NADH-dependent peroxidase and peroxynitrite reductase which is constituted by dihydrolipoamide dehydrogenase (*lpd*), dihydrolipoamide succinyl-transferase (*sucB*), alkyl-hydroperoxide reductase (*ahpC*), and *ahpD*. Also, mycobacterial catalase (*katG*) and superoxide dismutases (*sodA* and *sodC*) enhance tolerance to oxidative stress [91]. Additionally, *M. tuberculosis* also produces an anti-oxidant, mycothiol, which serves similar functions to glutathione [92, 93]. Synergistically, these series of mechanisms provide protection for mycobacterial proteins and DNA damage from ROI and RNI during infection.

In addition to toxic RNI and ROI, the mammalian host utilizes Cu as an antimicrobial agent exploiting the catalytic capacity of the metal through its redox chemistry: as a redox active metal, Cu reacts with H_2O_2, resulting in the generation of toxic hydroxyl radical and hydroxyl anion [94, 95]. Indeed, upon activation of the macrophage, Cu levels in the phagosomes containing mycobacteria increase dramatically [96]; the macrophage elevates Cu concentration through a high affinity Cu importer (Ctr1) and ATPase Cu pump (AP7A) [97]. Cu is an essential component of large number of microbial enzymes involved in a wide variety of cellular process, such as cell growth, stress response, and survival during infection [98, 99]. However, excess Cu is toxic. In order to minimize the Cu toxicity generated by host cells, *M. tuberculosis* encodes two Cu-responsive regulons known as CsoR system and RicR regulon [100, 101], including P-type ATPase metal transporter (*ctpV*) [101, 102] and mycobacterial cooper transporter B (*mctB*) [103, 104].

1.5.3 Starvation

In addition to these toxic molecules, the hosts also employ starvation mechanisms to restrict the growth of *M. tuberculosis*. It has been demonstrated that activated macrophages starve the bacterium of nutrients such as amino acids, carbohydrates, and essential metal ions.

During the infection, starvation of amino acids in phagosome has been shown through analysis of auxotrophic strains. Lysine, proline, leucine, and tryptophan auxotrophs are all attenuated in mice [105-108]. In order to efficiently replicate in an amino acid depleted environment *M. tuberculosis* has evolved to retain the biosynthetic pathways for 20 amino acids [11] and independently synthesize its own amino acids regardless of the host environment [84, 109]. In addition to amino acid depletion, host cells can also deplete intracellular iron through iron sequestration for defense against mycobacterial infection [110]. Activated macrophages exhibit low iron levels within the phagosomes [111]. Since iron is an essential redox cofactor of enzymes required for essential cellular process, iron acquisition is important to maintain infection. *M. tuberculosis* employs siderophores and mycobactin to compete for iron with host. Mycobactin is synthesized by the *mbtA-N* locus under iron-limited conditions [112]. Finally, it has long been believed that the host macrophage may restrict carbohydrate availability to *M. tuberculosis* within its phagosome. In bacterial cell, if exogenous glucose is limited, 6-carbon intermediate such as glucose 6-phosphate is generated through gluconeogenesis, rendering the bacterium dependent on the gluconeogenesis [113]. Among enzymes involved in this *de novo* synthesis is

phosphoenolpyruvate carboxykinase (*pckA*) that converts oxaloacetate to phosphoenolpyruvate. Indeed, using bacterial transcriptional analysis, it has been demonstrated that the expression of *pckA* was elevated during mice infection and this result was directly validated using *ΔpckA* mutant [114-116]. While *M. tuberculosis* is challenged by carbohydrate depletion during infection, it is likely that the bacterium is exposed to sufficient amount of host lipids and appears to shift its metabolism to exploit them [117].

1.6 Lipid diet during *M. tuberculosis* infection

1.6.1 Host tissue remodeling to support infection

In recent studies, the strong association of lipid loaded foamy macrophages with tuberculosis granulomas has been demonstrated and it is likely that the foamy cells provide a lipid rich micro-environment for intracellular *M. tuberculosis* [118, 119]. Using electron microscopy, several groups have shown that, in foamy macrophages, phagosomes containing *M. tuberculosis* are tightly apposed to lipid bodies, which suggests that the bacterium may have access to host lipids and metabolize them [119] (Figure 1.3). The induction of these lipid droplets in macrophages has been observed in many bacterial or viral infections [118]. Primarily, in infection, lipid bodies in the cells are accumulated through the activation of toll like receptors and proinflamatory cytokines. Macrophages can also induce lipid bodies to store lipids when they are exposed to a high concentration of fatty acids or lipoproteins such as low-density lipoproteins (LDLs) [120]. Dysregulation of LDL processing through genes involved

in cholesterol efflux, was shown to lead to accumulation of lipid bodies in macrophages. Indeed, in *M. tuberculosis infection*, this was validated by the transcriptional profiling of human TB granulomas, which revealed a significant dysregulation in lipid metabolism [121]. The mycobacterial cell wall lipid TDM has been shown to drive the formation of foamy macrophages during infection [122]. Recently, macrophages were also shown to accumulate lipid bodies under hypoxic conditions in culture, which is thought to mirror the microaerophilic environment in the human TB granuloma [123-125].

1.6.2 Bacterial metabolic reprogramming

This lipid rich environment of the host shapes the carbon metabolism of *M. tuberculosis*. During infection, strong induction of genes involved in fatty acid degradation has been shown by transcriptional profiling, suggesting the preferential utilization of fatty acids as a carbon source [84, 117, 126-128]. These genes include 18 genes involved in beta-oxidation of fatty acids and several genes involved in metabolic pathways for products of fatty acid breakdown, such as isocitrate lyase (*icl*) of the glyoxylate cycle (acetyl-CoA) and Rv1130-Rv1131 of methylcitrate cycle (propionyl-CoA) [129]. This theme has been observed in several independent studies. Perhaps, this metabolic shift to a lipid-based diet is due to availability of host lipids surrounding *M. tuberculosis* during infection. This is consistent with the early observation that the bacterium from infected mice preferentially utilizes fatty acids over carbohydrates [130]. Because of this host lipid environment, *M. tuberculosis*

appears to have become enriched for genes involved in fatty acid metabolism [11]. Many of these genes play important roles in metabolic and cell wall envelop remodeling, which are required for survival in host cells. For example, isocitrate lyase is required for survival in macrophage and mice [131, 132]. The glyoxylate cycle gated by the isocitrate lyase is a variation of the tricarboxylic acid cycle, and as an anabolic pathway (conversion of acetyl-CoA to succinate), allows the bacterium to utilize carbon source generating acetyl-CoA [133]. Since fatty acids breakdown through β-oxidation yield acetyl-CoA, the glyoxylate cycle is indispensable in a fatty acid based growth condition.

1.7 *M. tuberculosis* and propionate

1.7.1 Cholesterol during infection

Mass spectrometric analysis of the lipids present in the caseum from human tuberculosis granulomas revealed the major lipid contents, including triacylglycerol, cholesterol, and cholesterol ester [121]. Among these abundant lipids, cholesterol in particular has been thought to be an important carbon source for intracellular *M. tuberculosis*. Mutants defective in cholesterol transporter (*mce4*) exhibited reduced virulence in INF-γ activated and in the chronic phase of murine infection [116, 134].

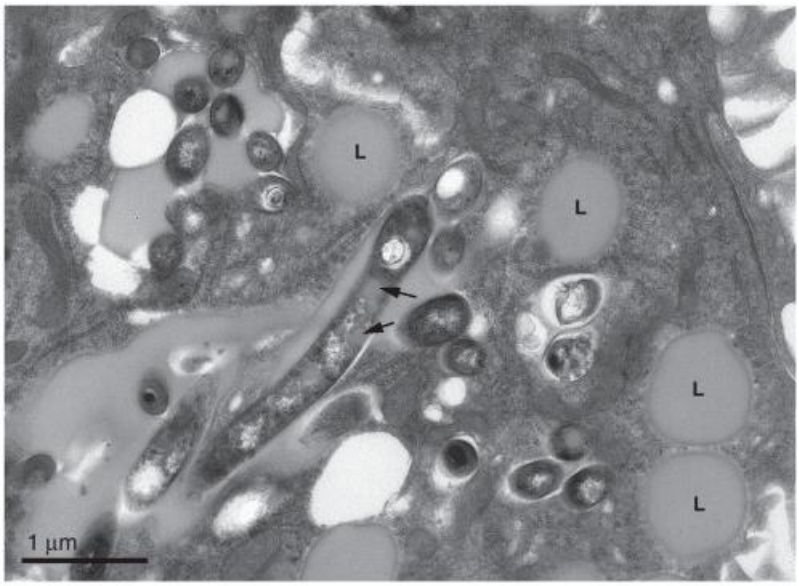

Figure 1.3 *M. tuberculosis* containing phagosomes in contact with lipid bodies in foamy macrophages[36]

Moreover, this phenotype of *Δmce4* mutant is very similar to the phenotype of *Δicl* mutants [131, 132]. This is significant because in *M. tuberculosis* isocitrate lyase plays a role in the methylcitrate cycle, which is an essential pathway to reduce the toxicity of propionyl-CoA produded during the breakdown of cholesterol by the bacterium. Together, the phenotypes of the mutant *Δicl* or *Δmce4* suggest that *M. tuberculosis* is exposed to host-derived cholesterol and the bacterium utilizes it as carbon source during infection.

1.7.2 Propionate metabolism during infection

In addition to cholesterol, propionyl-CoA can be also generated by β-oxidation of odd (or branched) chain fatty acids and catabolism of branched chain amino acids such as valine [135]. During infection, *M. tuberculosis* appears to become exposed to a significant concentration of propionyl-CoA [136]. Propionate, the 3 carbon fatty acid, has long been used as antimicrobial and antifungal agent because of its growth inhibitory effects [137] and there are several studies into its mechanisms of the toxicity [138-140]. However, despite the importance of propionate metabolism in mycobacteria, the targets of the propionyl-CoA or mechanisms of its toxicity have yet to be revealed.

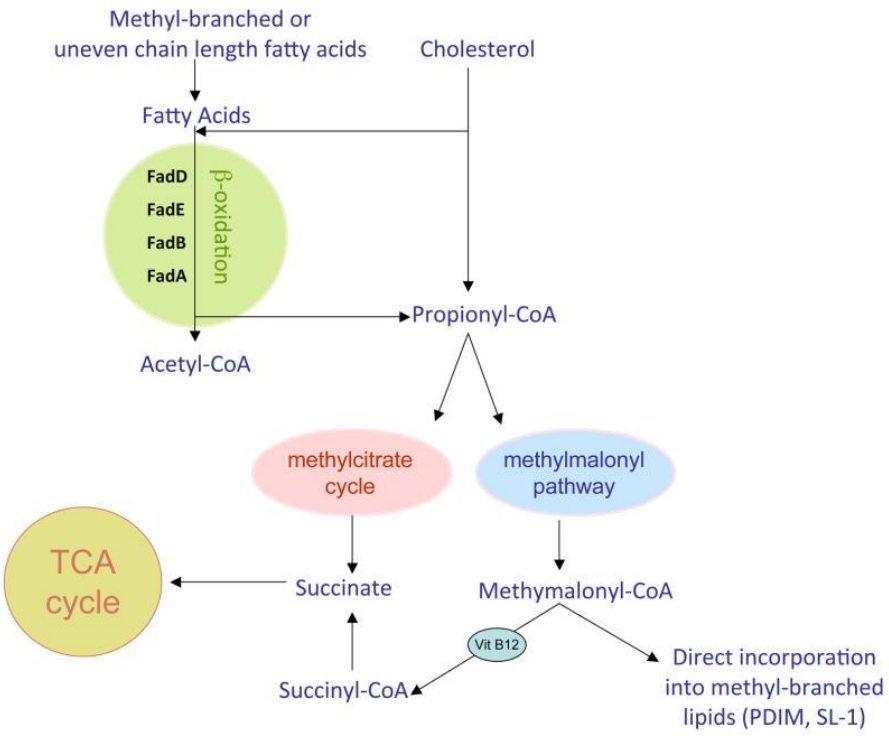

Figure 1.4 Pathway for lipid metabolism in *M. tuberculosis* [141]

In *M. tuberculosis*, three biochemical pathways have been proposed to facilitate propionyl-CoA metabolism: the methylcitrate cycle, the methylmalonyl pathway, and the biosynthesis of methyl-branched polyketides such as PDIM, PAT, and SL-1 (Figure 1.4). The latter pathways in particular, have been implicated in virulence of *M. tuberculosis*. Propionyl-CoA carboxylase in the methyl-malonyl pathways converts propionyl-CoA to methyl-malonyl-CoA, which can be fed into biosynthetic pathways of methyl-branched polyketides [15]. Since polyketides are produced by iterative condensation of acetyl-CoA (or longer acyl-CoA) and methyl-malonyl-CoA, the balance between the 2 carbon units (acetyl-CoA) and 3 carbon units (propionyl-CoA) is likely critical to their synthesis. This connection between propionate metabolism and polyketide biosynthesis has been demonstrated by the elevated production of PDIMs or SL-1 of *M. tuberculosis* grown on propionate [142]. In addition to this direct link, propionate metabolism is also connected to polyketide metabolism through the transcriptional regulator *whiB3*, which senses redox changes in the bacterial cytosol and regulates the biosynthesis of cell wall lipids including the methyl branched polyketides and triacylglycerol [143]. A mutant defective in *whiB3* exhibited resistance to elevated levels of propionate and had enhanced levels of PDIMs *in vitro*. This is significant because, *whiB3* seems to help *M. tuberculosis* to deal with metabolic stresses such as propionate toxicity and redox imbalance through the elevation of β-oxidation upon metabolic shift to lipid based carbon source. These data demonstrate the importance of propionate metabolism in adaptation to host lipid-derived carbon sources. However, these connections need to be validated through genome wide approaches to evaluate the contribution of the different metabolic

pathways to propionate detoxification and methyl-branched polyketide synthesis in *M. tuberculosis*.

1. 8 Aims of this study

The purpose of the following work is to understand carbon metabolism in *M. tuberculosis*

I. Understand the metabolic stress induced by propionyl-CoA

II. Identify the entire set of *M. tuberculosis* genes required for propionate metabolism

III. Understand the metabolic adaptations to handle excess propionate

IV. Use a macrophage infection model to understand the coupled metabolic reprogramming in *M. tuberculosis* and its host cell.

1.9 References

1. Zink, A.R., et al., *Characterization of Mycobacterium tuberculosis complex DNAs from Egyptian mummies by spoligotyping.* J Clin Microbiol, 2003. **41**(1): p. 359-67.
2. Crubezy, E., et al., *Identification of Mycobacterium DNA in an Egyptian Pott's disease of 5,400 years old.* C R Acad Sci III, 1998. **321**(11): p. 941-51.
3. Daniel, T.M., *The history of tuberculosis.* Respir Med, 2006. **100**(11): p. 1862-70.
4. Russell, D.G., *Who puts the tubercle in tuberculosis?* Nat Rev Microbiol, 2007. **5**(1): p. 39-47.
5. Smith, I., *Mycobacterium tuberculosis pathogenesis and molecular determinants of virulence.* Clin Microbiol Rev, 2003. **16**(3): p. 463-96.
6. Keshavjee, S. and P.E. Farmer, *Tuberculosis, drug resistance, and the history of modern medicine.* N Engl J Med, 2012. **367**(10): p. 931-6.
7. Dye, C., et al., *Worldwide incidence of multidrug-resistant tuberculosis.* J Infect Dis, 2002. **185**(8): p. 1197-202.
8. Cole, S., et al., *Tuberculosis and the Tubercle Bacillus*. ASM Press. 2005. 143-182.
9. Brosch, R., et al., *A new evolutionary scenario for the Mycobacterium tuberculosis complex.* Proc Natl Acad Sci U S A, 2002. **99**(6): p. 3684-9.
10. Hoffmann, C., et al., *Disclosure of the mycobacterial outer membrane: cryo-electron tomography and vitreous sections reveal the lipid bilayer structure.* Proc Natl Acad Sci U S A, 2008. **105**(10): p. 3963-7.

11. Cole, S.T., et al., *Deciphering the biology of Mycobacterium tuberculosis from the complete genome sequence.* Nature, 1998. **393**(6685): p. 537-44.

12. Camacho, L.R., et al., *Analysis of the phthiocerol dimycocerosate locus of Mycobacterium tuberculosis. Evidence that this lipid is involved in the cell wall permeability barrier.* J Biol Chem, 2001. **276**(23): p. 19845-54.

13. Rawat, R., A. Whitty, and P.J. Tonge, *The isoniazid-NAD adduct is a slow, tight-binding inhibitor of InhA, the Mycobacterium tuberculosis enoyl reductase: adduct affinity and drug resistance.* Proc Natl Acad Sci U S A, 2003. **100**(24): p. 13881-6.

14. Karakousis, P.C., W.R. Bishai, and S.E. Dorman, *Mycobacterium tuberculosis cell envelope lipids and the host immune response.* Cell Microbiol, 2004. **6**(2): p. 105-16.

15. Minnikin, D.E., et al., *The methyl-branched fortifications of Mycobacterium tuberculosis.* Chem Biol, 2002. **9**(5): p. 545-53.

16. Brennan, P.J. and H. Nikaido, *The envelope of mycobacteria.* Annu Rev Biochem, 1995. **64**: p. 29-63.

17. Puzo, G., *The carbohydrate- and lipid-containing cell wall of mycobacteria, phenolic glycolipids: structure and immunological properties.* Crit Rev Microbiol, 1990. **17**(4): p. 305-27.

18. Thurman, P.F., et al., *Possible intermediates in the biosynthesis of mycoside B by Mycobacterium microti.* Eur J Biochem, 1993. **212**(3): p. 705-11.

19. Ren, H., et al., *Identification of the lipooligosaccharide biosynthetic gene cluster from Mycobacterium marinum.* Mol Microbiol, 2007. **63**(5): p. 1345-59.

20. Jackson, M., G. Stadthagen, and B. Gicquel, *Long-chain multiple methyl-branched fatty acid-containing lipids of Mycobacterium tuberculosis: biosynthesis, transport, regulation and biological activities.* Tuberculosis (Edinb), 2007. **87**(2): p. 78-86.

21. Rook, G.A., K. Dheda, and A. Zumla, *Immune responses to tuberculosis in developing countries: implications for new vaccines.* Nat Rev Immunol, 2005. **5**(8): p. 661-7.

22. Zumla, A., et al., *Tuberculosis.* N Engl J Med, 2013. **368**(8): p. 745-55.

23. *Global tuberculosis report*. 2012, World Heath Organization

24. Calmette, A., *Preventive Vaccination Against Tuberculosis with BCG.* Proc R Soc Med, 1931. **24**(11): p. 1481-90.

25. Fine, P.E., *Variation in protection by BCG: implications of and for heterologous immunity.* Lancet, 1995. **346**(8986): p. 1339-45.

26. Kaufmann, S.H., *Future vaccination strategies against tuberculosis: thinking outside the box.* Immunity, 2010. **33**(4): p. 567-77.

27. Russell, D.G., C.E. Barry, 3rd, and J.L. Flynn, *Tuberculosis: what we don't know can, and does, hurt us.* Science, 2010. **328**(5980): p. 852-6.

28. LoBue, P.A., D.A. Enarson, and T.C. Thoen, *Tuberculosis in humans and its epidemiology, diagnosis and treatment in the United States.* Int J Tuberc Lung Dis, 2010. **14**(10): p. 1226-32.

29. Ginsberg, A.M., *Tuberculosis drug development: progress, challenges, and the road ahead.* Tuberculosis (Edinb), 2010. **90**(3): p. 162-7.

30. Russell, D.G., H.C. Mwandumba, and E.E. Rhoades, *Mycobacterium and the coat of many lipids.* J Cell Biol, 2002. **158**(3): p. 421-6.

31. Russell, D.G., *Mycobacterium tuberculosis: here today, and here tomorrow.* Nat Rev Mol Cell Biol, 2001. **2**(8): p. 569-77.

32. Bermudez, L.E. and J. Goodman, *Mycobacterium tuberculosis invades and replicates within type II alveolar cells.* Infect Immun, 1996. **64**(4): p. 1400-6.

33. Dorhoi, A., S.T. Reece, and S.H. Kaufmann, *For better or for worse: the immune response against Mycobacterium tuberculosis balances pathology and protection.* Immunol Rev, 2011. **240**(1): p. 235-51.

34. Jouanguy, E., et al., *IL-12 and IFN-gamma in host defense against mycobacteria and salmonella in mice and men.* Curr Opin Immunol, 1999. **11**(3): p. 346-51.

35. Ramakrishnan, L., *Revisiting the role of the granuloma in tuberculosis.* Nat Rev Immunol, 2012. **12**(5): p. 352-66.

36. Russell, D.G., *The evolutionary pressures that have molded Mycobacterium tuberculosis into an infectious adjuvant.* Curr Opin Microbiol, 2013. **16**(1): p. 78-84.

37. Armstrong, J.A. and P.D. Hart, *Phagosome-lysosome interactions in cultured macrophages infected with virulent tubercle bacilli. Reversal of the usual nonfusion pattern and observations on bacterial survival.* J Exp Med, 1975. **142**(1): p. 1-16.

38. Downing, J.F., et al., *Surfactant protein a promotes attachment of Mycobacterium tuberculosis to alveolar macrophages during infection with*

human immunodeficiency virus. Proc Natl Acad Sci U S A, 1995. **92**(11): p. 4848-52.

39. Gaynor, C.D., et al., *Pulmonary surfactant protein A mediates enhanced phagocytosis of Mycobacterium tuberculosis by a direct interaction with human macrophages.* J Immunol, 1995. **155**(11): p. 5343-51.

40. Schlesinger, L.S., *Macrophage phagocytosis of virulent but not attenuated strains of Mycobacterium tuberculosis is mediated by mannose receptors in addition to complement receptors.* J Immunol, 1993. **150**(7): p. 2920-30.

41. Schlesinger, L.S., et al., *Phagocytosis of Mycobacterium tuberculosis is mediated by human monocyte complement receptors and complement component C3.* J Immunol, 1990. **144**(7): p. 2771-80.

42. Zimmerli, S., S. Edwards, and J.D. Ernst, *Selective receptor blockade during phagocytosis does not alter the survival and growth of Mycobacterium tuberculosis in human macrophages.* Am J Respir Cell Mol Biol, 1996. **15**(6): p. 760-70.

43. Brooks, M.N., et al., *NOD2 controls the nature of the inflammatory response and subsequent fate of Mycobacterium tuberculosis and M. bovis BCG in human macrophages.* Cell Microbiol, 2011. **13**(3): p. 402-18.

44. Deretic, V., *Autophagy as an innate immunity paradigm: expanding the scope and repertoire of pattern recognition receptors.* Curr Opin Immunol, 2012. **24**(1): p. 21-31.

45. Mishra, B.B., et al., *Mycobacterium tuberculosis protein ESAT-6 is a potent activator of the NLRP3/ASC inflammasome.* Cell Microbiol, 2010. **12**(8): p. 1046-63.

46. Kim, J.J., et al., *Host cell autophagy activated by antibiotics is required for their effective antimycobacterial drug action.* Cell Host Microbe, 2012. **11**(5): p. 457-68.

47. Mostowy, S., *Autophagy and bacterial clearance: a not so clear picture.* Cell Microbiol, 2013. **15**(3): p. 395-402.

48. Behar, S.M., M. Divangahi, and H.G. Remold, *Evasion of innate immunity by Mycobacterium tuberculosis: is death an exit strategy?* Nat Rev Microbiol, 2010. **8**(9): p. 668-74.

49. Sturgill-Koszycki, S., et al., *Lack of acidification in Mycobacterium phagosomes produced by exclusion of the vesicular proton-ATPase.* Science, 1994. **263**(5147): p. 678-81.

50. Fratti, R.A., et al., *Mycobacterium tuberculosis glycosylated phosphatidylinositol causes phagosome maturation arrest.* Proc Natl Acad Sci U S A, 2003. **100**(9): p. 5437-42.

51. Vergne, I., J. Chua, and V. Deretic, *Tuberculosis toxin blocking phagosome maturation inhibits a novel Ca2+/calmodulin-PI3K hVPS34 cascade.* J Exp Med, 2003. **198**(4): p. 653-9.

52. Hmama, Z., et al., *Quantitative analysis of phagolysosome fusion in intact cells: inhibition by mycobacterial lipoarabinomannan and rescue by an 1alpha,25-*

dihydroxyvitamin D3-phosphoinositide 3-kinase pathway. J Cell Sci, 2004. **117**(Pt 10): p. 2131-40.

53. Behling, C.A., et al., *Induction of pulmonary granulomas, macrophage procoagulant activity, and tumor necrosis factor-alpha by trehalose glycolipids.* Ann Clin Lab Sci, 1993. **23**(4): p. 256-66.

54. Crowe, L.M., et al., *Interaction of cord factor (alpha, alpha'-trehalose-6,6'-dimycolate) with phospholipids.* Biochim Biophys Acta, 1994. **1194**(1): p. 53-60.

55. Perez, R.L., et al., *Cytokine message and protein expression during lung granuloma formation and resolution induced by the mycobacterial cord factor trehalose-6,6'-dimycolate.* J Interferon Cytokine Res, 2000. **20**(9): p. 795-804.

56. Spargo, B.J., et al., *Cord factor (alpha,alpha-trehalose 6,6'-dimycolate) inhibits fusion between phospholipid vesicles.* Proc Natl Acad Sci U S A, 1991. **88**(3): p. 737-40.

57. Goren, M.B., et al., *Prevention of phagosome-lysosome fusion in cultured macrophages by sulfatides of Mycobacterium tuberculosis.* Proc Natl Acad Sci U S A, 1976. **73**(7): p. 2510-4.

58. Vergne, I., et al., *Mechanism of phagolysosome biogenesis block by viable Mycobacterium tuberculosis.* Proc Natl Acad Sci U S A, 2005. **102**(11): p. 4033-8.

59. Muttucumaru, D.G., et al., *Mycobacterium tuberculosis Rv0198c, a putative matrix metalloprotease is involved in pathogenicity.* Tuberculosis (Edinb), 2011. **91**(2): p. 111-6.

60. Cowley, S., et al., *The Mycobacterium tuberculosis protein serine/threonine kinase PknG is linked to cellular glutamate/glutamine levels and is important for growth in vivo.* Mol Microbiol, 2004. **52**(6): p. 1691-702.

61. Divangahi, M., et al., *Eicosanoid pathways regulate adaptive immunity to Mycobacterium tuberculosis.* Nat Immunol, 2010. **11**(8): p. 751-8.

62. Hinchey, J., et al., *Enhanced priming of adaptive immunity by a proapoptotic mutant of Mycobacterium tuberculosis.* J Clin Invest, 2007. **117**(8): p. 2279-88.

63. Velmurugan, K., et al., *Mycobacterium tuberculosis nuoG is a virulence gene that inhibits apoptosis of infected host cells.* PLoS Pathog, 2007. **3**(7): p. e110.

64. Pym, A.S., et al., *Loss of RD1 contributed to the attenuation of the live tuberculosis vaccines Mycobacterium bovis BCG and Mycobacterium microti.* Mol Microbiol, 2002. **46**(3): p. 709-17.

65. Bean, A.G., et al., *Structural deficiencies in granuloma formation in TNF gene-targeted mice underlie the heightened susceptibility to aerosol Mycobacterium tuberculosis infection, which is not compensated for by lymphotoxin.* J Immunol, 1999. **162**(6): p. 3504-11.

66. Cooper, A.M., et al., *Disseminated tuberculosis in interferon gamma gene-disrupted mice.* J Exp Med, 1993. **178**(6): p. 2243-7.

67. Flesch, I.E. and S.H. Kaufmann, *Activation of tuberculostatic macrophage functions by gamma interferon, interleukin-4, and tumor necrosis factor.* Infect Immun, 1990. **58**(8): p. 2675-7.

68. Flynn, J.L., et al., *Tumor necrosis factor-alpha is required in the protective immune response against Mycobacterium tuberculosis in mice.* Immunity, 1995. **2**(6): p. 561-72.

69. Via, L.E., et al., *Effects of cytokines on mycobacterial phagosome maturation.* J Cell Sci, 1998. **111 (Pt 7)**: p. 897-905.

70. Darwin, K.H., et al., *The proteasome of Mycobacterium tuberculosis is required for resistance to nitric oxide.* Science, 2003. **302**(5652): p. 1963-6.

71. North, R.J. and Y.J. Jung, *Immunity to tuberculosis.* Annu Rev Immunol, 2004. **22**: p. 599-623.

72. Roura-Mir, C. and D.B. Moody, *Sorting out self and microbial lipid antigens for CD1*. Microbes Infect, 2003. **5**(12): p. 1137-48.

73. Cooper, A.M., *Cell-mediated immune responses in tuberculosis.* Annu Rev Immunol, 2009. **27**: p. 393-422.

74. Havlir, D.V. and P.F. Barnes, *Tuberculosis in patients with human immunodeficiency virus infection.* N Engl J Med, 1999. **340**(5): p. 367-73.

75. Flynn, J.L., et al., *Major histocompatibility complex class I-restricted T cells are required for resistance to Mycobacterium tuberculosis infection.* Proc Natl Acad Sci U S A, 1992. **89**(24): p. 12013-7.

76. Lalvani, A., et al., *Human cytolytic and interferon gamma-secreting CD8+ T lymphocytes specific for Mycobacterium tuberculosis.* Proc Natl Acad Sci U S A, 1998. **95**(1): p. 270-5.

77. Stenger, S., et al., *An antimicrobial activity of cytolytic T cells mediated by granulysin.* Science, 1998. **282**(5386): p. 121-5.

78. Tan, J.S., et al., *Human alveolar T lymphocyte responses to Mycobacterium tuberculosis antigens: role for CD4+ and CD8+ cytotoxic T cells and relative resistance of alveolar macrophages to lysis.* J Immunol, 1997. **159**(1): p. 290-7.

79. Beckman, E.M., et al., *Recognition of a lipid antigen by CD1-restricted alpha beta+ T cells.* Nature, 1994. **372**(6507): p. 691-4.

80. Sieling, P.A., et al., *CD1-restricted T cell recognition of microbial lipoglycan antigens.* Science, 1995. **269**(5221): p. 227-30.

81. Clemens, D.L. and M.A. Horwitz, *The Mycobacterium tuberculosis phagosome interacts with early endosomes and is accessible to exogenously administered transferrin.* J Exp Med, 1996. **184**(4): p. 1349-55.

82. Russell, D.G., J. Dant, and S. Sturgill-Koszycki, *Mycobacterium avium- and Mycobacterium tuberculosis-containing vacuoles are dynamic, fusion-competent vesicles that are accessible to glycosphingolipids from the host cell plasmalemma.* J Immunol, 1996. **156**(12): p. 4764-73.

83. Gonzalo-Asensio, J., et al., *PhoP: a missing piece in the intricate puzzle of Mycobacterium tuberculosis virulence.* PLoS One, 2008. **3**(10): p. e3496.

84. Rohde, K.H., R.B. Abramovitch, and D.G. Russell, *Mycobacterium tuberculosis invasion of macrophages: linking bacterial gene expression to environmental cues.* Cell Host Microbe, 2007. **2**(5): p. 352-64.

85. Chesne-Seck, M.L., et al., *A point mutation in the two-component regulator PhoP-PhoR accounts for the absence of polyketide-derived acyltrehaloses but not that of phthiocerol dimycocerosates in Mycobacterium tuberculosis H37Ra.* J Bacteriol, 2008. **190**(4): p. 1329-34.

86. Gonzalo Asensio, J., et al., *The virulence-associated two-component PhoP-PhoR system controls the biosynthesis of polyketide-derived lipids in Mycobacterium tuberculosis.* J Biol Chem, 2006. **281**(3): p. 1313-6.

87. Walters, S.B., et al., *The Mycobacterium tuberculosis PhoPR two-component system regulates genes essential for virulence and complex lipid biosynthesis.* Mol Microbiol, 2006. **60**(2): p. 312-30.

88. Abramovitch, R.B., et al., *aprABC: a Mycobacterium tuberculosis complex-specific locus that modulates pH-driven adaptation to the macrophage phagosome.* Mol Microbiol, 2011. **80**(3): p. 678-94.

89. Nathan, C. and M.U. Shiloh, *Reactive oxygen and nitrogen intermediates in the relationship between mammalian hosts and microbial pathogens.* Proc Natl Acad Sci U S A, 2000. **97**(16): p. 8841-8.

90. Shiloh, M.U., et al., *Phenotype of mice and macrophages deficient in both phagocyte oxidase and inducible nitric oxide synthase.* Immunity, 1999. **10**(1): p. 29-38.

91. Bryk, R., et al., *Metabolic enzymes of mycobacteria linked to antioxidant defense by a thioredoxin-like protein.* Science, 2002. **295**(5557): p. 1073-7.

92. Buchmeier, N. and R.C. Fahey, *The mshA gene encoding the glycosyltransferase of mycothiol biosynthesis is essential in Mycobacterium tuberculosis Erdman.* FEMS Microbiol Lett, 2006. **264**(1): p. 74-9.

93. Vilcheze, C., et al., *Mycothiol biosynthesis is essential for ethionamide susceptibility in Mycobacterium tuberculosis.* Mol Microbiol, 2008. **69**(5): p. 1316-29.

94. Samanovic, M.I., et al., *Copper in microbial pathogenesis: meddling with the metal.* Cell Host Microbe, 2012. **11**(2): p. 106-15.

95. Hood, M.I. and E.P. Skaar, *Nutritional immunity: transition metals at the pathogen-host interface.* Nat Rev Microbiol, 2012. **10**(8): p. 525-37.

96. Wagner, D., et al., *Elemental analysis of Mycobacterium avium-, Mycobacterium tuberculosis-, and Mycobacterium smegmatis-containing phagosomes indicates pathogen-induced microenvironments within the host cell's endosomal system.* J Immunol, 2005. **174**(3): p. 1491-500.

97. White, C., et al., *A role for the ATP7A copper-transporting ATPase in macrophage bactericidal activity.* J Biol Chem, 2009. **284**(49): p. 33949-56.

98. Andreini, C., et al., *Occurrence of copper proteins through the three domains of life: a bioinformatic approach.* J Proteome Res, 2008. **7**(1): p. 209-16.

99. Ridge, P.G., Y. Zhang, and V.N. Gladyshev, *Comparative genomic analyses of copper transporters and cuproproteomes reveal evolutionary dynamics of copper utilization and its link to oxygen.* PLoS One, 2008. **3**(1): p. e1378.

100. Liu, T., et al., *CsoR is a novel Mycobacterium tuberculosis copper-sensing transcriptional regulator.* Nat Chem Biol, 2007. **3**(1): p. 60-8.

101. Ward, S.K., E.A. Hoye, and A.M. Talaat, *The global responses of Mycobacterium tuberculosis to physiological levels of copper.* J Bacteriol, 2008. **190**(8): p. 2939-46.

102. Ward, S.K., et al., *CtpV: a putative copper exporter required for full virulence of Mycobacterium tuberculosis.* Mol Microbiol, 2010. **77**(5): p. 1096-110.

103. Wolschendorf, F., et al., *Copper resistance is essential for virulence of Mycobacterium tuberculosis.* Proc Natl Acad Sci U S A, 2011. **108**(4): p. 1621-6.

104. Siroy, A., et al., *Rv1698 of Mycobacterium tuberculosis represents a new class of channel-forming outer membrane proteins.* J Biol Chem, 2008. **283**(26): p. 17827-37.

105. Hondalus, M.K., et al., *Attenuation of and protection induced by a leucine auxotroph of Mycobacterium tuberculosis.* Infect Immun, 2000. **68**(5): p. 2888-98.

106. Parish, T., *Starvation survival response of Mycobacterium tuberculosis.* J Bacteriol, 2003. **185**(22): p. 6702-6.

107. Pavelka, M.S., Jr., et al., *Vaccine efficacy of a lysine auxotroph of Mycobacterium tuberculosis.* Infect Immun, 2003. **71**(7): p. 4190-2.

108. Smith, D.A., et al., *Characterization of auxotrophic mutants of Mycobacterium tuberculosis and their potential as vaccine candidates.* Infect Immun, 2001. **69**(2): p. 1142-50.

109. Talaat, A.M., et al., *The temporal expression profile of Mycobacterium tuberculosis infection in mice.* Proc Natl Acad Sci U S A, 2004. **101**(13): p. 4602-7.

110. Ganz, T., *Iron in innate immunity: starve the invaders.* Curr Opin Immunol, 2009. **21**(1): p. 63-7.

111. Cellier, M.F., P. Courville, and C. Campion, *Nramp1 phagocyte intracellular metal withdrawal defense.* Microbes Infect, 2007. **9**(14-15): p. 1662-70.

112. Rodriguez, G.M., *Control of iron metabolism in Mycobacterium tuberculosis.* Trends Microbiol, 2006. **14**(7): p. 320-7.

113. Munoz-Elias, E.J. and J.D. McKinney, *Carbon metabolism of intracellular bacteria.* Cell Microbiol, 2006. **8**(1): p. 10-22.

114. Collins, D.M., et al., *Production of avirulent mutants of Mycobacterium bovis with vaccine properties by the use of illegitimate recombination and screening of stationary-phase cultures.* Microbiology, 2002. **148**(Pt 10): p. 3019-27.

115. Liu, K., J. Yu, and D.G. Russell, *pckA-deficient Mycobacterium bovis BCG shows attenuated virulence in mice and in macrophages.* Microbiology, 2003. **149**(Pt 7): p. 1829-35.

116. Sassetti, C.M. and E.J. Rubin, *Genetic requirements for mycobacterial survival during infection.* Proc Natl Acad Sci U S A, 2003. **100**(22): p. 12989-94.

117. Schnappinger, D., et al., *Transcriptional Adaptation of Mycobacterium tuberculosis within Macrophages: Insights into the Phagosomal Environment.* J Exp Med, 2003. **198**(5): p. 693-704.

118. Melo, R.C. and A.M. Dvorak, *Lipid body-phagosome interaction in macrophages during infectious diseases: host defense or pathogen survival strategy?* PLoS Pathog, 2012. **8**(7): p. e1002729.

119. Peyron, P., et al., *Foamy macrophages from tuberculous patients' granulomas constitute a nutrient-rich reservoir for M. tuberculosis persistence.* PLoS Pathog, 2008. **4**(11): p. e1000204.

120. Walther, T.C. and R.V. Farese, Jr., *Lipid droplets and cellular lipid metabolism.* Annu Rev Biochem, 2012. **81**: p. 687-714.

121. Kim, M.J., et al., *Caseation of human tuberculosis granulomas correlates with elevated host lipid metabolism.* EMBO Mol Med, 2010. **2**(7): p. 258-74.

122. Geisel, R.E., et al., *In vivo activity of released cell wall lipids of Mycobacterium bovis bacillus Calmette-Guerin is due principally to trehalose mycolates.* J Immunol, 2005. **174**(8): p. 5007-15.

123. Bostrom, P., et al., *Hypoxia converts human macrophages into triglyceride-loaded foam cells.* Arterioscler Thromb Vasc Biol, 2006. **26**(8): p. 1871-6.

124. Daniel, J., et al., *Mycobacterium tuberculosis uses host triacylglycerol to accumulate lipid droplets and acquires a dormancy-like phenotype in lipid-loaded macrophages.* PLoS Pathog, 2011. **7**(6): p. e1002093.

125. Via, L.E., et al., *Tuberculous granulomas are hypoxic in guinea pigs, rabbits, and nonhuman primates.* Infect Immun, 2008. **76**(6): p. 2333-40.

126. Homolka, S., et al., *Functional genetic diversity among Mycobacterium tuberculosis complex clinical isolates: delineation of conserved core and lineage-specific transcriptomes during intracellular survival.* PLoS Pathog, 2010. **6**(7): p. e1000988.

127. Rohde, K.H., et al., *Linking the transcriptional profiles and the physiological states of Mycobacterium tuberculosis during an extended intracellular infection.* PLoS Pathog, 2012. **8**(6): p. e1002769.

128. Timm, J., et al., *Differential expression of iron-, carbon-, and oxygen-responsive mycobacterial genes in the lungs of chronically infected mice and tuberculosis patients.* Proc Natl Acad Sci U S A, 2003. **100**(24): p. 14321-6.

129. Munoz-Elias, E.J., et al., *Role of the methylcitrate cycle in Mycobacterium tuberculosis metabolism, intracellular growth, and virulence.* Mol Microbiol, 2006. **60**(5): p. 1109-22.

130. Bloch, H. and W. Segal, *Biochemical differentiation of Mycobacterium tuberculosis grown in vivo and in vitro.* J Bacteriol, 1956. **72**(2): p. 132-41.

131. Munoz-Elias, E.J. and J.D. McKinney, *Mycobacterium tuberculosis isocitrate lyases 1 and 2 are jointly required for in vivo growth and virulence.* Nat Med, 2005. **11**(6): p. 638-44.

132. McKinney, J.D., et al., *Persistence of Mycobacterium tuberculosis in macrophages and mice requires the glyoxylate shunt enzyme isocitrate lyase.* Nature, 2000. **406**(6797): p. 735-8.

133. Cozzone, A.J., *Regulation of acetate metabolism by protein phosphorylation in enteric bacteria.* Annu Rev Microbiol, 1998. **52**: p. 127-64.

134. Pandey, A.K. and C.M. Sassetti, *Mycobacterial persistence requires the utilization of host cholesterol.* Proc Natl Acad Sci U S A, 2008. **105**(11): p. 4376-80.

135. Ibrahim-Granet, O., et al., *Methylcitrate synthase from Aspergillus fumigatus is essential for manifestation of invasive aspergillosis.* Cell Microbiol, 2008. **10**(1): p. 134-48.

136. Griffin, J.E., et al., *Cholesterol catabolism by Mycobacterium tuberculosis requires transcriptional and metabolic adaptations.* Chem Biol, 2012. **19**(2): p. 218-27.

137. Luck, E., and M. Jager, *Propionic acid, antimicrobial food additives: charateristics, uses, and effects*. 2 ed. 1997, New York, NY: Springer.

138. Brock, M. and W. Buckel, *On the mechanism of action of the antifungal agent propionate.* Eur J Biochem, 2004. **271**(15): p. 3227-41.

139. Man, W.J., et al., *The binding of propionyl-CoA and carboxymethyl-CoA to Escherichia coli citrate synthase.* Biochim Biophys Acta, 1995. **1250**(1): p. 69-75.

140. Maruyama, K. and H. Kitamura, *Mechanisms of growth inhibition by propionate and restoration of the growth by sodium bicarbonate or acetate in Rhodopseudomonas sphaeroides S.* J Biochem, 1985. **98**(3): p. 819-24.

141. Russell, D.G., et al., *Mycobacterium tuberculosis wears what it eats.* Cell Host Microbe, 2010. **8**(1): p. 68-76.

142. Jain, M., et al., *Lipidomics reveals control of Mycobacterium tuberculosis virulence lipids via metabolic coupling.* Proc Natl Acad Sci U S A, 2007. **104**(12): p. 5133-8.

143. Singh, A., et al., *Mycobacterium tuberculosis WhiB3 maintains redox homeostasis by regulating virulence lipid anabolism to modulate macrophage response.* PLoS Pathog, 2009. **5**(8): p. e1000545.

CHAPTER TWO

Evaluation of propionate toxicity and detoxification in *M. tuberculosis*

Adapted from

Intracellular *Mycobacterium tuberculosis* exploits host-derived fatty acids to limit metabolic stress. Lee W, VanderVen BC, Fahey RJ, Russell DG .J Biol Chem. 2013 Mar 8; 288(10):6788-800.

ABSTRACT

Recent data indicate that the nutrients available to *Mycobacterium tuberculosis* inside its host cell are restricted in their diversity. Fatty acids and cholesterol appear more favored, however, their degradation can result in certain metabolic stresses. Their breakdown can generate propionyl-CoA, which gives rise to potentially toxic intermediates. Detoxification of propionyl-CoA relies on the activity of the methylcitrate cycle, the methylmalonyl pathway or incorporation of the propionyl-CoA into methyl-branched lipids in the cell wall. The current article explores carbon flux through these pathways, focusing primarily on those pathways responsible for the incorporation of propionyl-CoA into virulence-associated cell wall lipids. Exploiting both genetic and biochemical rescue we demonstrate that these metabolic pressures are experienced by *M. tuberculosis* inside its host macrophage, and that the bacterium accesses host fatty acid stores to alleviate the pressure. These data have major implications to our appreciation of central metabolism of *M. tuberculosis* during the course of infection.

2.1 Introduction

Mycobacterium tuberculosis, a facultative intracellular pathogen, is an intracellular pathogen. Most like other invasive pathogens, *M. tuberculosis* must acquire host derived nutrients and adapt metabolically to the conditions that are provided by the host over the course of infection. There is a growing body of literature indicating that *M. tuberculosis* utilizes a restricted set of host-derived nutrients to persist within its host cell. Most notably, host lipids appear to be the primary carbon source for *M. tuberculosis in vivo* or in infected macrophages in culture. The reliance on host-derived nutrients such as cholesterol as a major carbon source comes at a cost to *M. tuberculosis*. In addition to the degradation of the A, B, C, and D, rings of cholesterol, the acyl side chain is predicted to be degraded by rounds of β-oxidation, which will give rise to propionyl-CoA [1-3]. *M. tuberculosis* is exquisitely sensitive to increases in the propionyl-CoA pool and the bacterium has three different means of metabolizing this precursor of potentially-toxic metabolite(s) [4-6]. ICL1 functions both as an isocitrate lyase in the glyoxylate shunt as well as a methylisocitrate lyase that catalyzes the last reaction of the methylcitrate cycle (MCC), which converts propionyl-CoA to succinate and pyruvate that feeds into the TCA cycle [4, 7]. Alternatively, propionyl-CoA carboxylase can generate methylmalonyl-CoA that can enter the vitamin B12-dependent, methylmalonyl pathway (MMP) leading to the production of succinyl-CoA [5]. Finally, and of considerable significance to infection, these 3-carbon intermediates in the form of methyl-malonyl-CoA may be used as building blocks for the bacterium's cell wall lipids [8-10]. The complex lipids of the *M. tuberculosis* cell wall form an impressive hydrophobic barrier around the

bacterium and are also known modulators of host cell function, acting as highly potent virulence factors [11]. These bioactive lipids can be esterified with up-to five multiple methyl-branched (MB) long chain fatty acids, which provides an effective "sink" for excess propionyl-CoA. In *M. tuberculosis*, these MB lipids include the phthiocerol dimycocerosates (PDIM), and the trehalose ester families including sulfolipid-1 (SL-1), diacyltrehalose (DAT), triacyltrehaose (TAT), and polyacyltrehalose (PAT) [12]. These *M. tuberculosis*-lipids are synthesized by individual polyketide synthase complexes from malonyl- and methylmalonyl–CoA (MM-CoA), which originate from acetyl-CoA and propionyl-CoA, respectively. Thus, the 3-carbon metabolite propionyl-CoA, plays a significant role in the generation of cell wall lipids known to be required for the modulation of the host at both the level of the host cell and the infected tissue [13-18].

Cholesterol is the best characterized source of 3-carbon metabolites in *M. tuberculosis*. Additionally, degradation of uneven chain length fatty acids or MB-amino acids will all generate propionyl-CoA, therefore the interplay between the assimilatory pathways (MCC and MMP) and the biosynthetic incorporation of MM-CoA into MB-cell wall lipids is critical to minimizing the potential toxicity of these metabolites while maximizing their "usefulness" for either energy production or building blocks for the bacterium's cell wall lipids. In this current study we selectively manipulated carbon flux through the three different propionyl-CoA processing pathways to elucidate both the genetic and biochemical linkages between the pathways, as well as the factors that promote incorporation of 3-carbon intermediates into the cell wall lipids of the bacterium. Moreover, we demonstrate

through biochemical rescue, that *M. tuberculosis* can access and metabolize the lipid stores in its host cell to shunt propionyl-CoA through favored, non-intoxicating routes of degradation or synthesis.

2.2 Materials and Methods

Culture media and Growth conditions

M. tuberculosis strains were maintained in Middlebrook 7H9 medium supplemented with 0.2% glycerol, 10% OADC and 0.05% tyloxapol. Kanamycin (20 μg/ml) or hygromycin (50 μg/ml) were used where necessary. For growth on defined carbon sources, strains were grown without shaking in minimal medium (0.5 g/L asparagine, 1.0 g/L KH_2PO_4, 2.5 g/L Na_2HPO_4, 50 mg/L ferric ammonium citrate, 0.5 g/L $MgSO_4$,$7H_2O$, 0.5 mg/L $CaCl_2$ and 0.1 mg/L $ZnSO_4$, 10 mM glycerol, and 0.05% tyloxapol) [19] containing propionate or fatty acids (Sigma). Prior to addition, fatty acids having longer chain length than butyric acid (C4) were dissolved to 100 mM in a solution of tyloxapol:ethanol (1:1) at 80°C for at least 30 minutes. To overcome the poor solubility of long chain fatty acids (C10-C24), a prewarmed 100 mM stock solution of each long chain fatty acids was added to the medium to a final concentration of 0.05 mM. To activate the MMP, VitB12 was added to a concentration of 10 μg/ml. All chemicals were purchased from Sigma unless otherwise stated.

Growth curve

Mycobacterial cultures of strains grown in the minimal medium were subcultured in 1:100(v/v) in triplicate into 15ml of minimal medium with appropriate supplements. Cultures were incubated in T25 at 37°C without shaking, and the growth was monitored by measuring optical density at 600 nm (Bio-Rad)

Pyruvate Quantification

For pyruvate quantification, the medium from 100ml cultures of the *Δicl1* mutant at OD_{600}=1.0 was concentrated to OD_{600}=10, and released pyruvate was quantified using a pyruvate quantification kit (SIGMA).

Enzyme Assay

Pyruvate dehydrogenase(PDH) was measured as described previously [20, 21]. The assay contained pH8.0 50mM Tris-HCl, 2.5mM cysteine, 2mM NAD, 2mM $MgCl_2$, 0.8mM thiamine pyrophosphate, 2mM pyruvate, and 20μM CoASH in a final volume 1 mL. The assay was started by addition of *M. tuberculosis* cell free lysate and reduction of NAD to NADH was monitored at 340 nm.

Metabolic Labeling and Lipid Analysis

Metabolic radiolabeling of mycobacterial cell wall lipids were performed as described [22-24]. Briefly, bacterial strains were cultured in the 20 ml minimal medium with 4

μCi of [1-^{14}C] sodium propionate, 4 μCi of [1 ^{14}C] stearic acid, or 4 μCi of [1,2-^{14}C] sodium acetate for 2 weeks. Cultures were centrifuged and washed in PBS and the cell wall lipids were extracted twice with $CHCl_3/CH_3OH$ (2:1 v/v). After determination of ^{14}C incorporation by scintillation counter, 10,000 cpm from each lipid extract was loaded onto a TLC plate and resolved by running twice in a petroleum ether: ethyl acetate (98:2, v/v) solvent system. Radiolabelled lipids was detected and visualized by autoradiography with a phosphoimager.

In order to track the fate of the double-labeled stearic acid, [1-^{14}C, 9, 10-^{3}H] stearic acid (Perkin-Elmer) was used. To isolate labeled PDIM, lipid extracts were spotted on TLC and run twice in petroleum ether: ethyl acetate (98:2, v/v) solvent system. The PDIM was visualized by iodine vapor, scraped from the plates, and lipids were extracted in petroleum ether. The relative ratio of ^{3}H and ^{14}C in the isolated PDIM was determined by scintillation counter from 2 biological replicates analyzed in triplicate.

2.3 RESULTS and DISCUSSION

2.3.1 The relative, but not the absolute, abundance of 3-carbon versus 2-carbon metabolites is critical for *M. tuberculosis* fitness

To elucidate the pressures induced by increased concentrations of 3-carbon intermediates we developed approaches to experimentally modulate the concentration of propionyl-CoA and the bacterium's ability to process the metabolite. Propionyl-

CoA, a high energy metabolite, is a key precursor to several cell wall lipids in *M. tuberculosis* [25, 26]; however, the buildup of propionyl-CoA is potentially toxic to the cell. Propionyl-CoA may be metabolized through either the MCC or the MMP, however, transcriptional profiling of *M. tuberculosis* in macrophages indicates that propionyl-CoA is metabolized predominantly through the MCC, leading to the production pyruvate and succinate (Figure 2.1) [27]. Additionally, the MCC genes are transcriptionally induced and key MCC metabolites accumulate when *M. tuberculosis* is grown in the presence of cholesterol indicating enhanced flux of propionyl-CoA carbons through the MCC [1]. ICL1 (Rv0467) functions as a 2-methylisocitrate lyase, and catalyzes that last reaction in the MCC thus, this enzymes is critical in relieving the potential toxicity of propionyl-CoA [28].

It had been shown previously that mutants defective in expression of ICL1 are unable to grow on propionate as a sole carbon source [7, 29]. We modified this approach to demonstrate that the growth of a *Δicl1* mutant was normal in minimal medium with 10 mM glycerol but was inhibited strongly by the addition of increasing concentrations of propionate (Figure 2.2). The growth of wild-type H37Rv was unimpaired under these conditions. This demonstrated that propionate, or its products, were intoxicating the *Δicl1* mutant even in the presence of an alternate carbon source suggesting strongly that a functional MCC is critical to alleviating the increased propionyl-CoA concentration. Savvi and colleagues had shown that the MMP offered

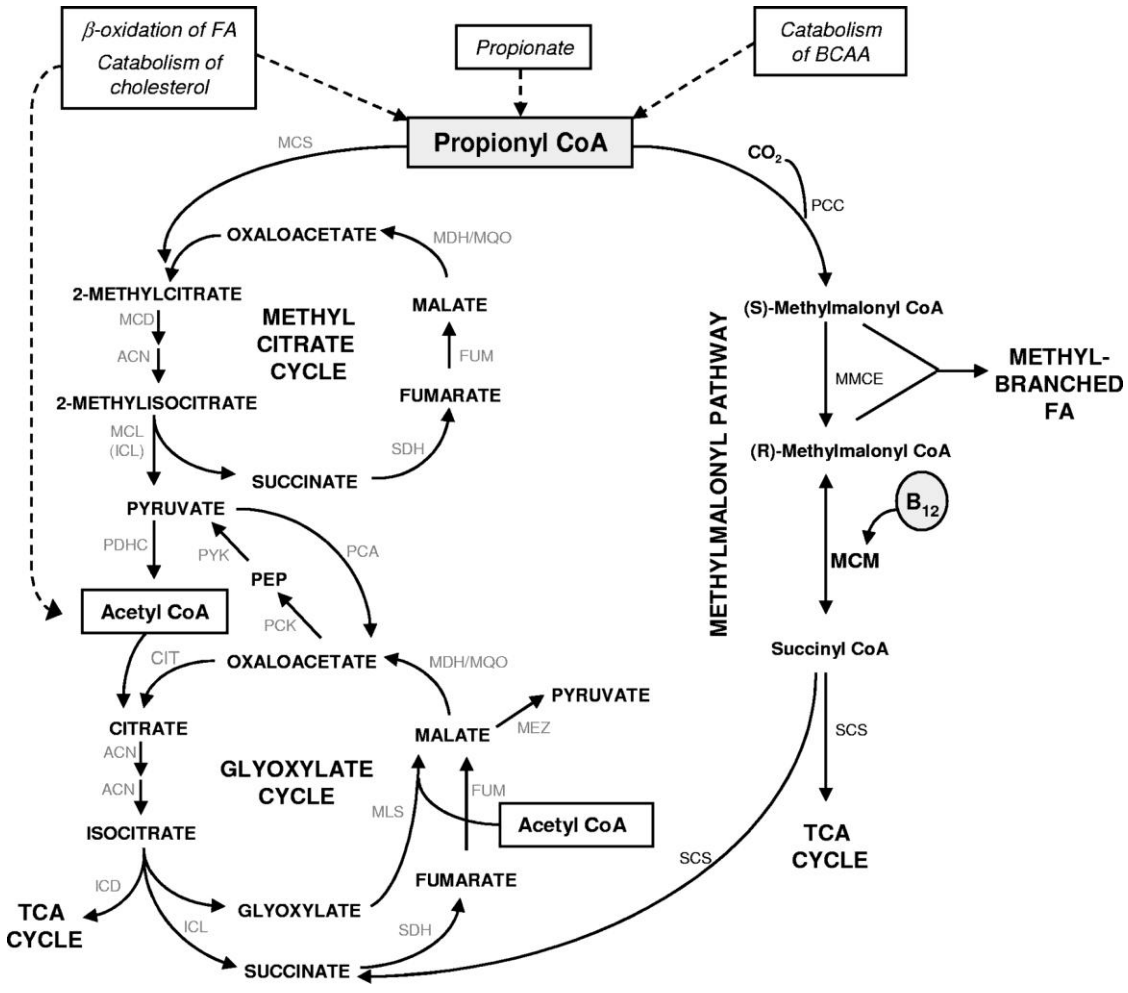

Figure 2.1 Propionate pathways in *M. tuberculosis.* Taken from Savvi et al [5].

an alternate route for propionyl-CoA degradation but that this pathway was dependent on the activity of a MM-CoA synthase, which requires Vitamin B12 (VitB12) as a co-factor [5]. Although *M. tuberculosis* does possess the genes required for synthesis of VitB12 it is likely not produced under normal *in vitro* culture conditions. We found that the addition of VitB12 to the culture medium containing the *Δicl1* mutant rescued the mutant from propionate-mediated intoxication (Figure 2.2), thus further confirming the results of Saavi and colleagues, and demonstrating that both MCC and MMP function to detoxify propionyl-CoA rather than render it usable as an alternative carbon source.

Only acetate supplementation rescued the propionate toxicity (Figure 2.3) and, while we cannot formally prove that *M. tuberculosis* has access to all these intermediates, the data are consistent with the previous study on *Aspergillus*. Much of the acetyl-CoA in *M. tuberculosis* is generated by PDH from pyruvate and to test whether propionate addition impairs PDH activity we monitored the accumulation of extracellular pyruvate in the presence and absence of exogenous propionate in *Δicl1* mutant cultures. As hypothesized, pyruvate rapidly accumulated in the medium in the presence of propionate (Figure 2.4), but pyruvate was almost undetectable in the control culture. To further confirm this phenotype, we grew the *Δicl1* mutant on minimal medium supplemented with 0.05 mM propionate and acetate in increasing concentrations from 0.5-4.0 mM, illustrated in (Figure 2.5). Interestingly, compared to the control culture with no propionate, the bacterial growth rates were similar when the acetate concentration exceeds 4 mM. These findings indicate that propionyl-CoA,

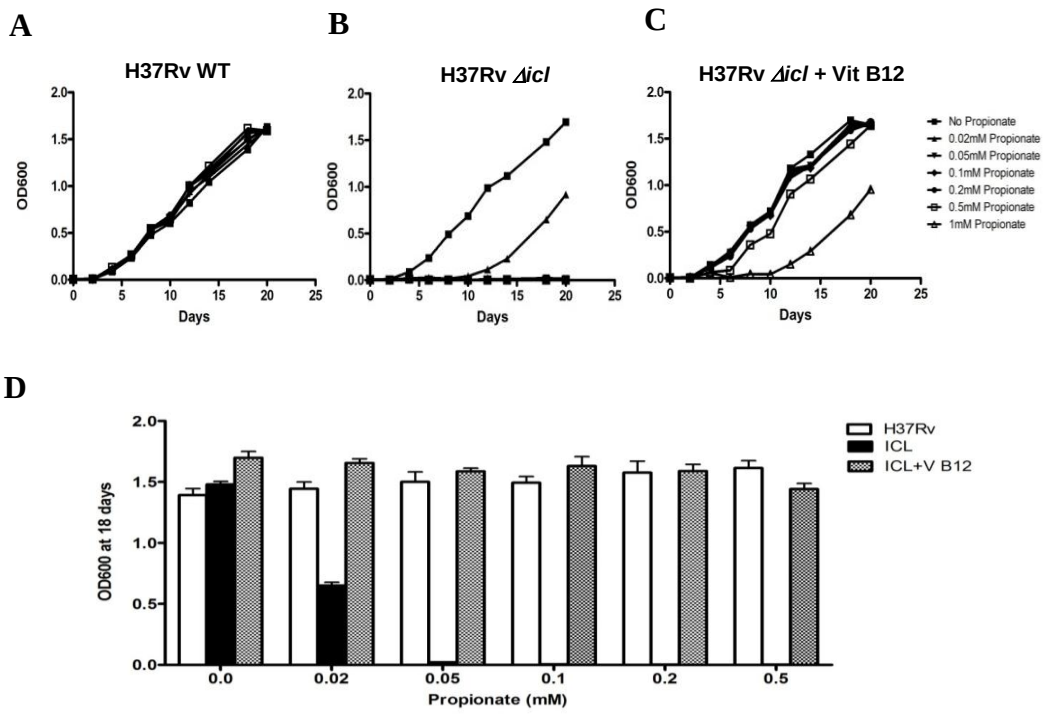

Figure 2.2 Mitigation of propionate toxicity in a *Δicl1* mutant strain by acetate and VitB12. The *Δicl1* mutant strain of *M. tuberculosis* grows poorly in the presence of propionate but growth can be rescued by the addition of either VitB12 or acetate. (A)-(C) Bacterial growth, measured by absorbance at 600 nm, was determined for *M. tuberculosis* H37Rv and *Δicl* strain grown for 18 days in minimal media containing 10mM glycerol as primary carbon source and propionate across the range from 0.02 mM to 1 mM. Vitamin B12 at the concentration of 10 μg/ml reversed the propionate toxicity observed in the *Δicl1* mutant strain. (D) Growth at 18 day was compared. Data are representative of three experiments.

or its products, impair the production of acetyl-CoA, and that the addition of increasing concentrations of acetate relieves this toxicity, which implies that it is the relative balance of 2- and 3-carbon intermediates that is critical for bacterial fitness.

To extend this observation to more physiologically-relevant substrates we examined the ability of longer chain fatty acids to rescue growth of the *Δicl1* mutant in propionate containing medium [16]. We focused on even chain-length fatty acids because odd chain fatty acids and MB-fatty acids, would also yield propionyl-CoA that would elevate propionyl-CoA levels in the bacterium. First we measured the growth of wild-type (wt) *M. tuberculosis* in glycerol containing media in the presence of saturated even-chain fatty acids from acetic acid (C2) to lignoceric acid (C24). As noted previously [30, 31], free fatty acids of intermediate chain length (C10-C16) were toxic to *M. tuberculosis* but the bacterium grew well on either short or longer chain length fatty acids (Figure 2.6). Next, the fatty acids that supported wt *M. tuberculosis* growth were tested for their ability to rescue the *Δicl1* mutant from propionate-mediated toxicity. Growth was restored to the *Δicl1* mutant through supplementing the propionate- and glycerol-containing media with the majority of the fatty acids, except C12, C14, suggesting that the acetyl-CoA pool may also be expanded though β-oxidation of long chain fatty acids (Figure 2.7). Interestingly, the shorter chain fatty acids (C2-C8) supplementation abrogated the propionate-mediated toxicity efficiently, while long chain fatty acids (C18-C24) appeared to sustain growth in propionate following a lag period.

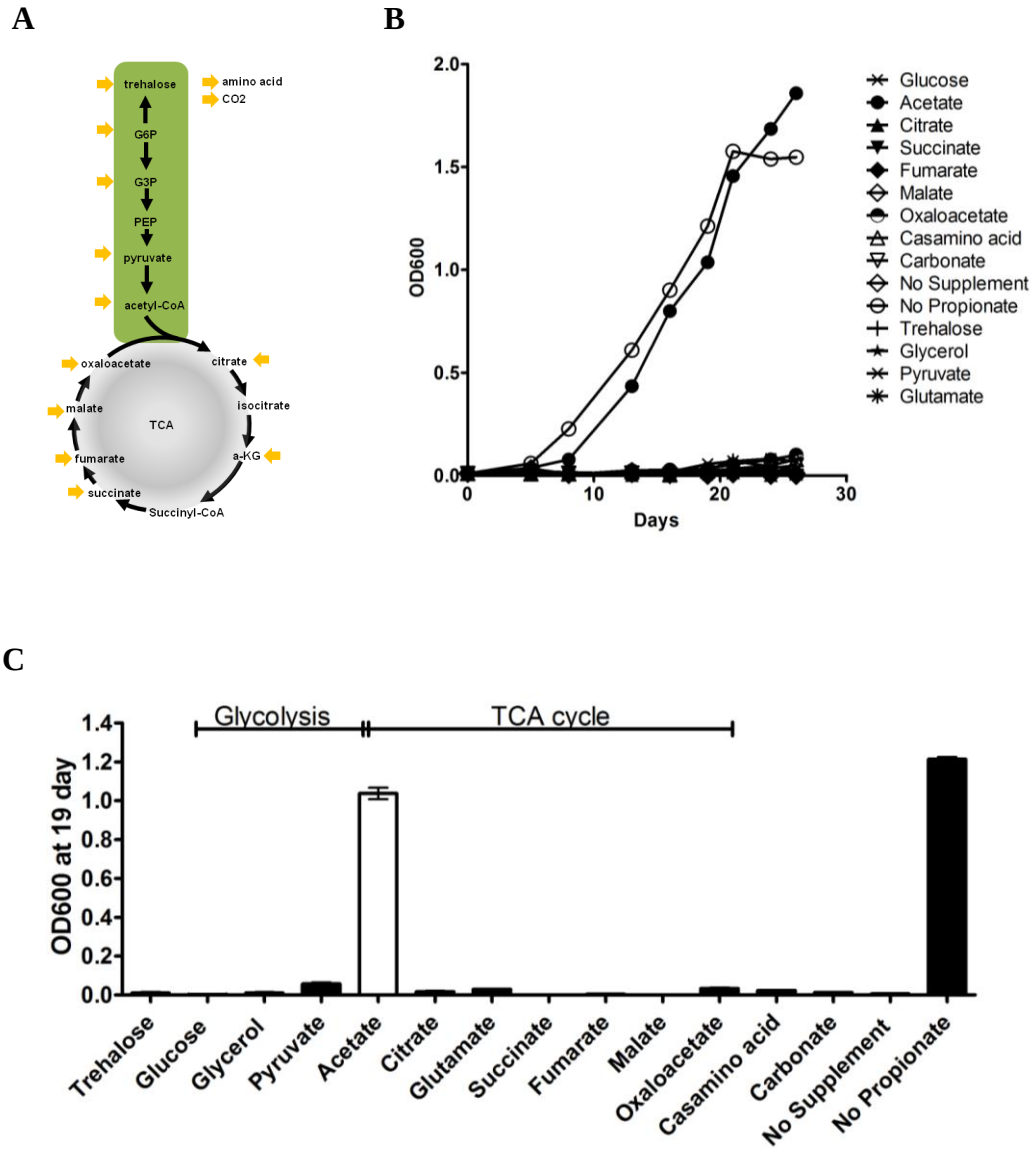

Figure 2.3 Propionate toxicity is rescued in the *Δicl1* mutant strain with acetate. Of the central metabolic intermediates tested only acetate (4 mM) was able to rescue growth of the *Δicl1* mutant strain in the presence of propionate (0.05 mM). Bacterial growth, measured by absorbance at 600 nm, was determined for *M. tuberculosis* H37Rv and *Δicl* strain grown for 19 days in minimal media containing 10mM glycerol as primary carbon source supplemented with central metabolic intermediates. Data are representative of three experiments.

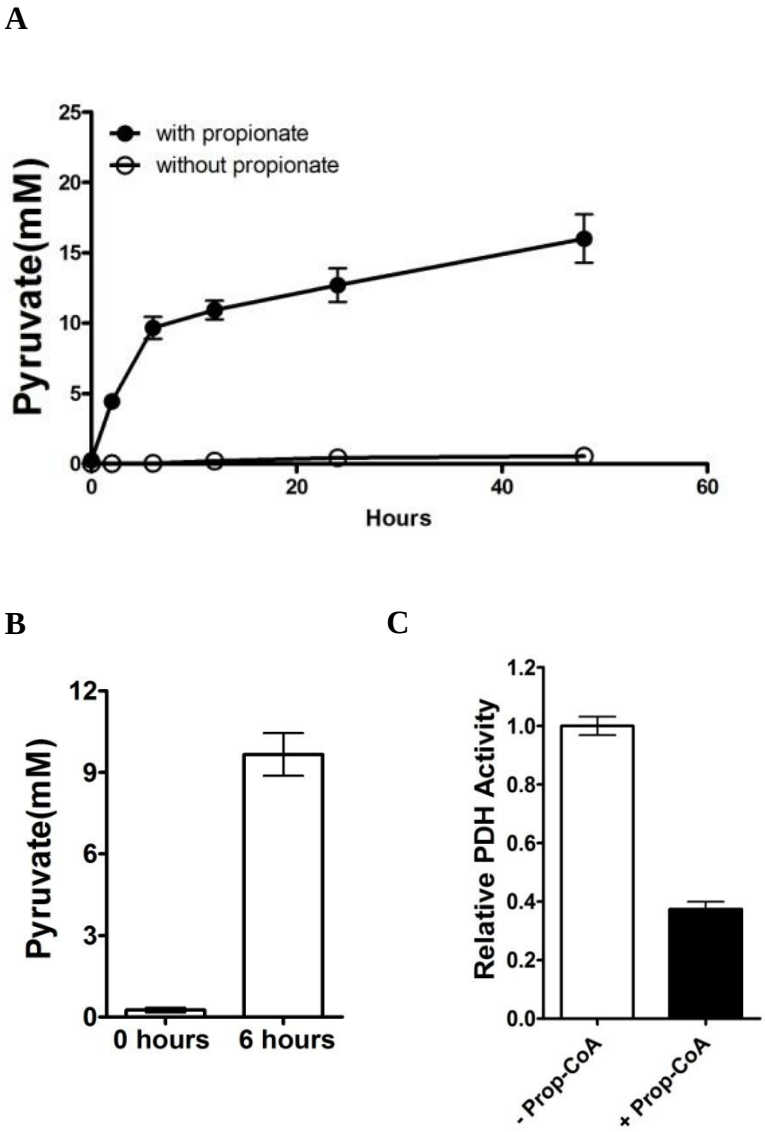

Figure 2.4 Propionyl-CoA or intermediates inhibits pyruvate dehydrogenase (PDH). (A)-(B) pyruvate accumulates and is released from the *icl1* mutant when grown in the presence of propionate over the course of 48 h. (C) the PDH activity of *M. tuberculosis* lysate is reduced by 60% upon addition of propionly-CoA in vitro assay. Data are representative of three experiments. *Error bars*, Standard Deviation.

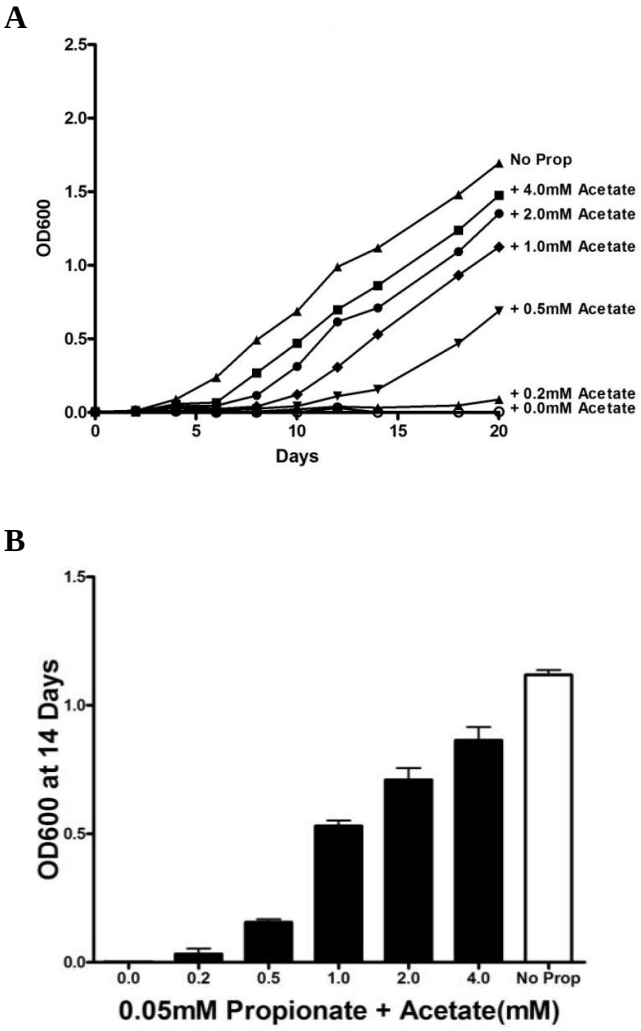

Figure 2.5 Acetate can rescue propionate toxicity in *Δicl1 M. tuberculosis*. (A) and (B) The C2 compound, acetate rescues propionate toxicity of *Δicl1 M. tuberculosis* in a dose dependent manner. Bacteria were grown for 18 days in medium containing 10 mM glycerol (G) and 0.05 mM propionate supplemented with acetate across the range 0.05mM to 4mM. Bacteria were grown for 18 days in medium containing 10 mM glycerol and 0.05 mM propionate supplemented with a range of acetate. Bacterial growth was measured by absorbance at 600 nm and results are representative of 3 replicates.

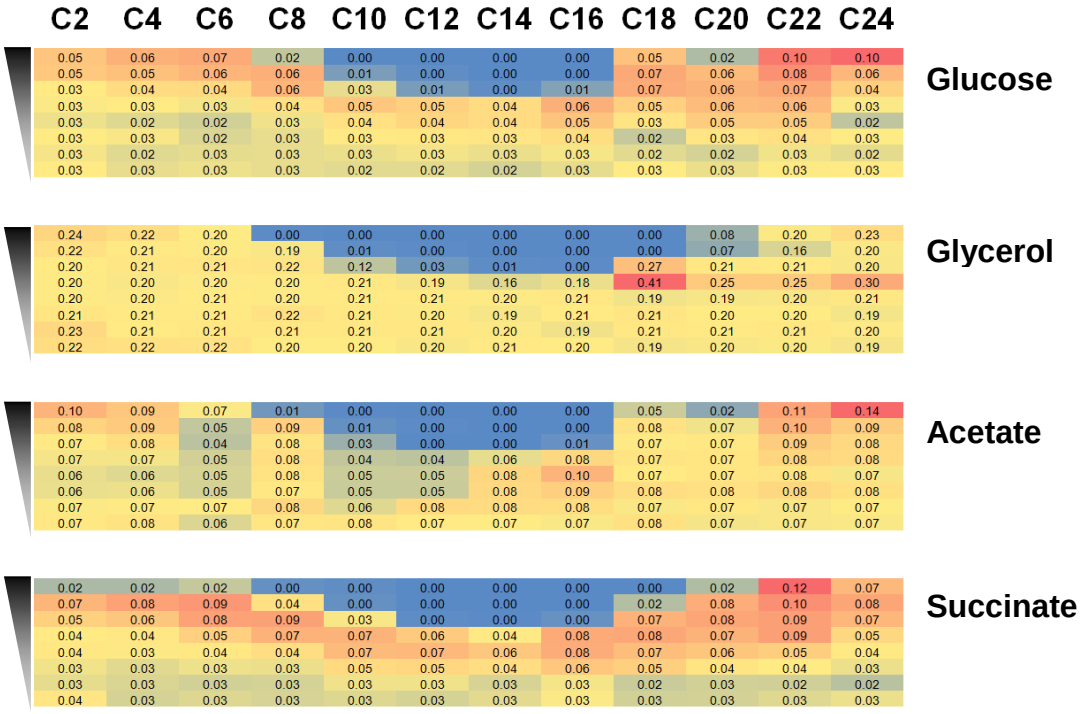

Figure 2.6 Free fatty acids of intermediate chain length (C10-C16) are toxic to *M. tuberculosis*, however the bacterium utilizes fatty acids of shorter or longer chain length. H37Rv wild type was grown in minimal media containing 10mM glycerol (alternatively glucose, acetate, or succinate) primary carbon source and fatty acids from acetate (C2) to lignocerate (C24). Fatty acids were supplemented at concentration range 0.2mM – 0mM by 2-fold serial dilutions in 96 well plates. At 7 days, bacterial growth was measured by absorbance at 600 nm and results are representative of 3 replicates.

A

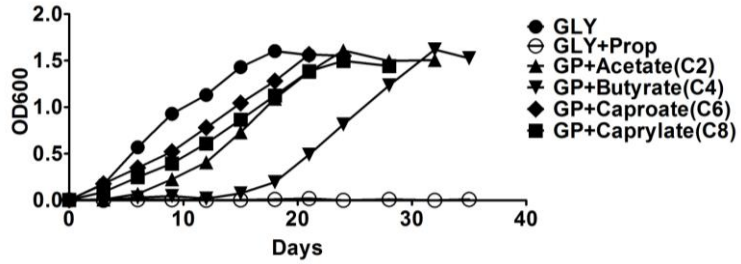
OD600
Days
GLY
GLY+Prop
GP+Acetate(C2)
GP+Butyrate(C4)
GP+Caproate(C6)
GP+Caprylate(C8)

B

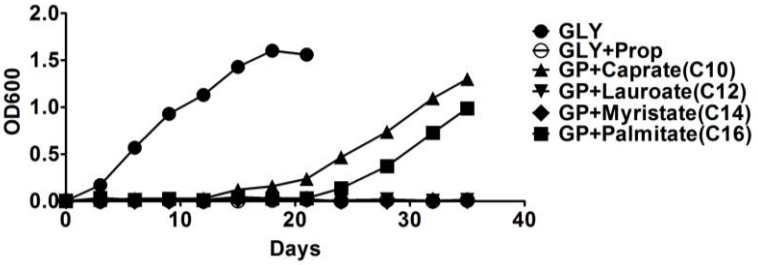
OD600
Days
GLY
GLY+Prop
GP+Caprate(C10)
GP+Lauroate(C12)
GP+Myristate(C14)
GP+Palmitate(C16)

C

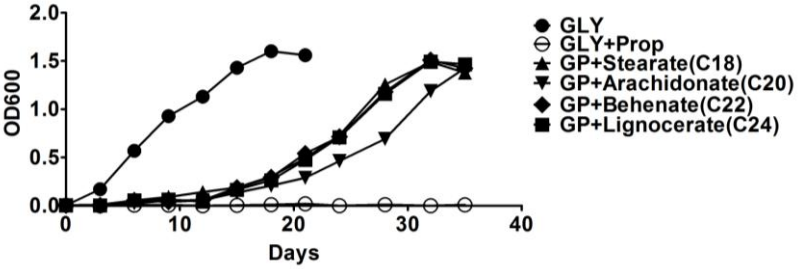
OD600
Days
GLY
GLY+Prop
GP+Stearate(C18)
GP+Arachidonate(C20)
GP+Behenate(C22)
GP+Lignocerate(C24)

D

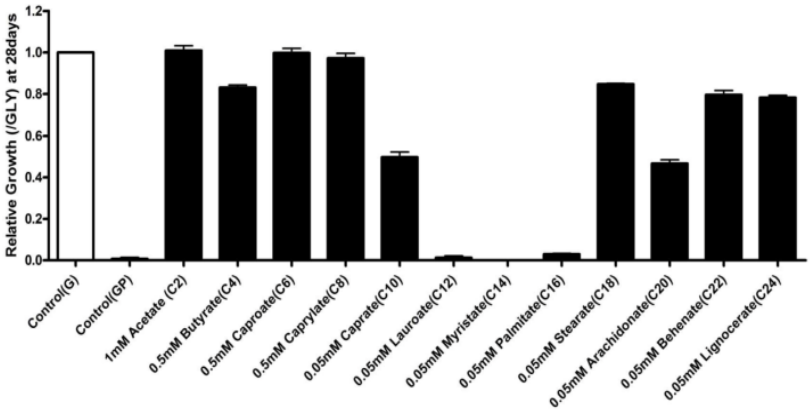
Relative Growth (/GLY) at 28days
Control(G)
Control(GP)
1mM Acetate (C2)
0.5mM Butyrate(C4)
0.5mM Caproate(C6)
0.5mM Caprylate(C8)
0.05mM Caprate(C10)
0.05mM Lauroate(C12)
0.05mM Myristate(C14)
0.05mM Palmitate(C16)
0.05mM Stearate(C18)
0.05mM Arachidonate(C20)
0.05mM Behenate(C22)
0.05mM Lignocerate(C24)

Figure 2.7 Fatty acids of differing chain lengths rescue the *Δicl1* strain from propionate toxicity. Acetate, short-chain fatty acids, and long-chain fatty acids similar to those found in the host macrophage can rescue propionate toxicity in *Δicl1 M. tuberculosis*. Short to mid-length and long chain fatty acids also rescue propionate toxicity in *Δicl1 M. tuberculosis*. Bacteria were grown for 18 days in medium containing 10 mM glycerol and 0.05 mM propionate supplemented (GP) with saturated even-chain length fatty acids (C2-C24) at the following concentrations; acetate (C2) was provided with 1 mM, short chain fatty acids (C4-C8) at 0.5 mM and intermediate and long chain fatty acids (C10-C24) at 0.05 mM. Bacterial growth was measured by absorbance at 600 nm and results are representative of 3 replicates.

Together, these observations support the contention that it is the relative abundance of 2- versus 3-carbon intermediates that plays an important role in protecting *M. tuberculosis* from the potential toxicity of propionyl-CoA.

2.3.2 The methyl branched lipid, PDIM acts as a sink for propionyl-CoA

The third proposed route of detoxification of propionyl-CoA is through its incorporation into the MB-lipids of cell wall lipids. To synthesize MB-lipids, *M. tuberculosis* would require fatty acids to act as primers for the polyketide synthase-catalyzed addition of MM-CoA from propionyl-CoA [32]. In the case of the typical mycocerosic acid in PDIM there is a 4:1 molar ratio of MM-CoA to acyl primer required for synthesis. We therefore hypothesized that under our defined growth conditions, the *Δicl1* mutant grown in minimal medium containing propionate and glycerol in the absence of VitB12 is dependent upon the biosynthesis of MB-lipids as a means of detoxifying excess propionyl-CoA. If correct, then provision of acetate, or longer chain fatty acids, would facilitate synthesis of fatty acid-AMP precursors that would act as acceptors for methylmalonyl-CoA and enable *M. tuberculosis* to incorporate excess propionate into cell wall lipids such as PDIM. This hypothesis would predict that radiolabel in the form of ^{14}C in acetate, long chain fatty acids or propionate should all be incorporated into PDIM.

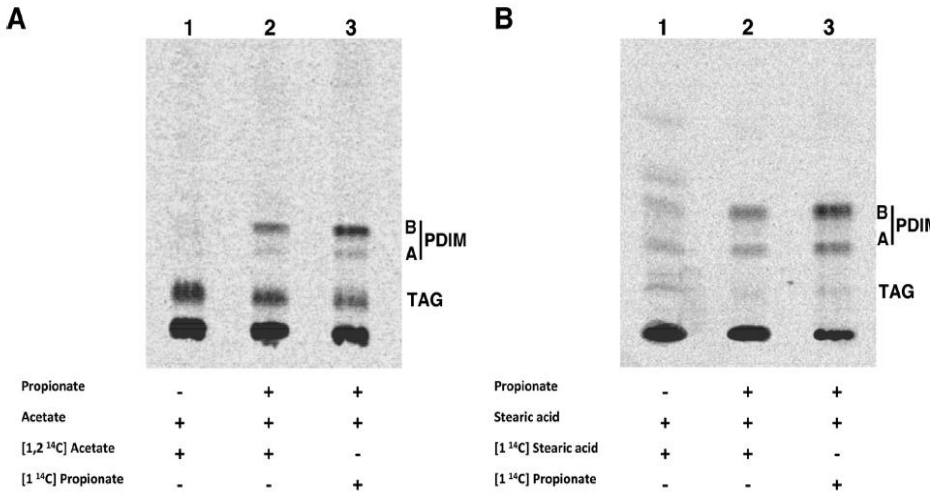

E

Ratio of total PDIM to TAG (PDIM / TAG)

	A			B			C				D			
Lane	1	2	3	1	2	3	1	2	3	4	1	2	3	4
	0.06	0.63	1.46	3.04	8.77	11.82	0.22	0.67	4.94	35.07	0.43	0.36	2.28	39.68

Figure 2.8 Fatty acids rescue propionate toxicity in *M. tuberculosis* through incorporation into methyl-branched lipids such as PDIM, in both the *Δicl1* mutant strain and wild-type *M. tuberculosis*. TLC analysis of the cell lipid lipids indicates that radiolabel derived from [1-^{14}C] propionate, [1, 2-^{14}C] acetate, or [1-^{14}C] stearic acid is incorporated into the cell wall lipid PDIM. ^{14}C incorporation into PDIM is enhanced by 0.05 mM propionate but is a constitutive process in both the *Δicl1* mutant strain, and in the high-PDIM-producing wild-type Erdman strain. Bacteria were grown in glycerol medium containing propionate, acetate and stearic acid as indicated.(A) Lipids from the *Δicl1* mutant (Lane 1) incubated with [1, 2-^{14}C] acetate in absence of propionate; (lane 2) incubated with [1,2-^{14}C] acetate in presence of 0.05 mM unlabeled propionate; or (Lane 3) incubated with [1-^{14}C] propionate in the presence of 0.05 mM unlabeled propionate; (C) lipids from Erdman. (B), (D): (B) The experiment was repeated using the long chain fatty acid, stearic acid (C18) instead of acetate (C2). Lipids from the *Δicl1* mutant (Lane 1) incubated with [1-^{14}C] stearic acid in absence of propionate; (Lane 2) with [1-^{14}C] stearic acid in presence of 0.05 mM unlabeled propionate; (Lane 3) with [1-^{14}C] propionate in the presence of 0.05 mM unlabeled propionate; (D) lipids from Erdman. (E) Ratio of PDIM to TAG. The bands labeled correspond to (1) triacylglycerol, (2) phthiocerol A dimycocerate and (3) phthiodiolone dimycocerate. The identity of the PDIM and TAG bands had been established previously by mass spectrometry [24].

To follow the flow of carbon into PDIM, we metabolically labeled the *Δicl1* mutant and a wild-type (wt) Erdman strain, which produces abundant PDIM, with ^{14}C-propionate, ^{14}C-acetate, and ^{14}C-stearic acid. The peripheral cell wall lipids were isolated and analyzed by thin layer chromatography (TLC). As shown in Figure 2.8, ^{14}C label was incorporated into PDIM in both the *Δicl1* mutant and the wt strain from either ^{14}C-acetate or ^{14}C-stearic acid. The amount of radiolabel incorporated into PDIM from ^{14}C-acetate, and ^{14}C-stearic acid was enhanced in the *Δicl1* mutant in the presence of 0.05 mM unlabeled propionate. In the wt strain, which has an intact MCC, ^{14}C label from ^{14}C-propionate was incorporated into both TAG and PDIM in the presence 0.05 mM unlabeled propionate. Significantly, in the absence of unlabeled propionate, the ^{14}C-propionate tracer was found only in PDIM.

These data indicate that, at least in a high PDIM-producing strain of *M. tuberculosis*, under these *in vitro* conditions, flux of propionyl-CoA into PDIM is the preferred route of detoxification even in the presence of an intact MCC. These data demonstrate that utilization of both long chain fatty acids and the *de novo* synthesis of fatty acids from acetate facilitates formation of the fatty acid-AMP primers to support the incorporation of propionyl-CoA into the MB-cell wall lipid PDIM.

2.3.3 Stearic acid is incorporated into *M. tuberculosis* PDIM without degradation through β-oxidation.

The preceding result does not discriminate between the direct incorporation of stearic acid into PDIM as an acyl-primer, from the incorporation of acetyl-CoA

released by β-oxidation of the stearic acid. To determine whether intact stearic acid is used as a fatty acid primer for PDIM biosynthesis, we metabolically labeled wt Erdman and the *Δicl1* mutant with double isotope labeled, stearic acid [9,10-^{3}H, 1-^{14}C] in the presence of propionate(Figure 2.9). If the stearic acid were catabolized by β-oxidation the 1-^{14}C radiolabel would be released as ^{14}C-acetyl-CoA, which can enter central metabolism or be used as a substrate by the FAS1 system and incorporated into n-fatty acids. Therefore, we predict that if the stearic acid were β-oxidized the ratio of ^{3}H to ^{14}C would change indicating a loss of ^{14}C from stearic acid. However, we found that the ^{3}H: ^{14}C ratio within PDIM was virtually identical to the stearic acid [9,10-^{3}H, 1-^{14}C] standard, Table 1. This result demonstrates that long chain fatty acids, such as stearic acid, can bypass catabolic β-oxidation, and serve as a primer for direct incorporation into PDIM.

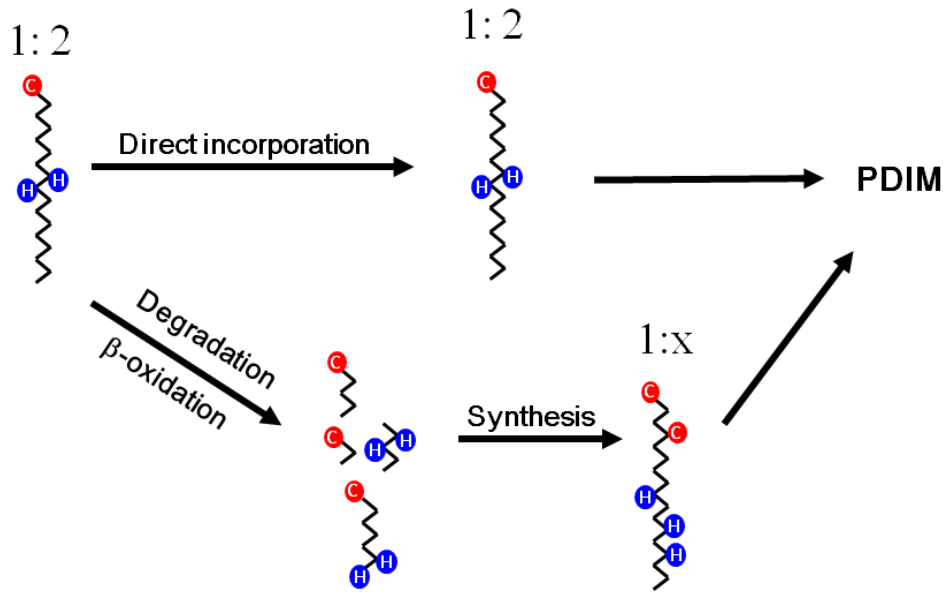

Figure 2.9 Schematic draw for stearic acid incorporation into *M. tuberculosis* PDIM. A specific ratio between isotopes, ^{14}C and ^{3}H in the double isotope stearic acid [9,10-^{3}H, 1-^{14}C] will be presented in the ratio of labeled PDIM by the isotope, when intact stearic acid is incorporated into PDIM. However, if the stearic acid is processed by β-oxidation and synthesis (*M. tuberculosis* FAS-I and FAS-II system), the ratio in *M. tuberculosis* PDIM will be shifted from the specific ratio in the double isotope stearic acid [9, 10-^{3}H, 1-^{14}C].

Table 1.1 Stearic acid is incorporated *M. tuberculosis* PDIM intact, without β-oxidation.

Stearic acid [9,10-^{3}H, 1-^{14}C] Dual Isotope Labeling				
	^{3}H:^{14}C CPM Ratios of H37Rv *Δicl*		^{3}H:^{14}C CPM Ratios of Erdman	
	Experiment 1	Experiment 2	Experiment 1	Experiment 2
Total PDIM	0.2962 ± 0.007	0.3087 ± 0.012	0.2784± 0.001	0.2821± 0.004
Stearic acid [9,10-^{3}H, 1-^{14}C]	0.2932 ± 0.005	0.3130 ± 0.003	0.2898± 0.002	0.2966± 0.002

Double-labeled stearic acid [9,10-^{3}H, 1-^{14}C] was used for metabolic labeling of the *Δicl1* strain or Erdman in minimal medium containing glycerol, 0.05mM propionate, and 0.05mM stearic acid. After 2 weeks incubation, *M. tuberculosis* wall surface lipids were extracted, and PDIM was purified from the PDIM bands by TLC. The ratio of ^{3}H and ^{14}C radioactivity (cpm) was determined for both the starting material and the extracted PDIM bands. Average and standard deviations were calculated from 3 technical replicates from each experiment.

2.4 Concluding remarks

The ability of *M. tuberculosis* to utilize cholesterol as a carbon source during the course of infection has been shown to be critical to its success as a pathogen [19]. However, the degradation of cholesterol expands the propionyl-CoA pool with potentially toxic consequences [5, 6]. In the current study we performed genetic and biochemical manipulation of the methylcitrate cycles (MCC) and methylmalonyl pathways (MMP) to reveal the metabolic requirements for incorporation of propionyl-CoA into PDIM and other virulence-associated lipids of the bacterial cell wall.

The "choices" open to *M. tuberculosis* are both catabolic through the degradation of propionyl-CoA by the MCC and MMP and the incorporation of its products into the TCA cycle, and anabolic through the generation of malonyl-CoA primers to act as acceptors of propionyl-CoA in the synthesis of MB lipids. In the wt Erdman strain we observed the incorporation of propionate into PDIM in both the presence and absence of exogenous propionate, and the incorporation of propionate into TAG only when exogenous propionate was present. This suggests firstly, that *M. tuberculosis* routes propionate into MB lipids by preference, and secondly, because the generation of TAG from propionate requires the MMC, this indicates that the MCC is activated in response to additional pressure from propionate. The "opening" of the MCC has the potential to generate more acetyl-CoA, which in turn could enhance PDIM production. This hypothesis is consistent with the observations of Jain and colleagues who observed that increased levels of methylmalonyl-CoA led to increased synthesis of PDIM and SL-1, and furthermore, impairment in synthesis of these lipids lead to reduced virulence in mice [8]. Finally, transcriptional profiling of

M. tuberculosis in macrophages over an extended period of infection demonstrated that the genes encoding all the steps of the MCC were highly up-regulated throughout the duration of the infection [27]. These data argue strongly that the tightly-coordinated interplay between the MCC, MMP and MB-lipid synthesis is important to *M. tuberculosis* and may represent an "Achilles' heel" in the metabolic network in a bacterium that is highly evolved to survive and persist in its human host.

Acknowledgment

The authors wish to gratefully acknowledge the technical support of Linda Bennett.

2. 5 References

1. Griffin, J.E., et al., *Cholesterol catabolism by Mycobacterium tuberculosis requires transcriptional and metabolic adaptations.* Chem Biol, 2012. **19**(2): p. 218-27.
2. Yang, X., et al., *Cholesterol metabolism increases the metabolic pool of propionate in Mycobacterium tuberculosis.* Biochemistry, 2009. **48**(18): p. 3819-21.
3. Thomas, S.T., et al., *Pathway profiling in Mycobacterium tuberculosis: elucidation of cholesterol-derived catabolite and enzymes that catalyze its metabolism.* J Biol Chem, 2011. **286**(51): p. 43668-78.
4. Munoz-Elias, E.J., et al., *Role of the methylcitrate cycle in Mycobacterium tuberculosis metabolism, intracellular growth, and virulence.* Mol Microbiol, 2006. **60**(5): p. 1109-22.
5. Savvi, S., et al., *Functional characterization of a vitamin B12-dependent methylmalonyl pathway in Mycobacterium tuberculosis: implications for propionate metabolism during growth on fatty acids.* J Bacteriol, 2008. **190**(11): p. 3886-95.
6. Upton, A.M. and J.D. McKinney, *Role of the methylcitrate cycle in propionate metabolism and detoxification in Mycobacterium smegmatis.* Microbiology, 2007. **153**(Pt 12): p. 3973-82.
7. McKinney, J.D., et al., *Persistence of Mycobacterium tuberculosis in macrophages and mice requires the glyoxylate shunt enzyme isocitrate lyase.* Nature, 2000. **406**(6797): p. 735-8.

8. Jain, M., et al., *Lipidomics reveals control of Mycobacterium tuberculosis virulence lipids via metabolic coupling.* Proc Natl Acad Sci U S A, 2007. **104**(12): p. 5133-8.

9. Russell, D.G., et al., *Mycobacterium tuberculosis wears what it eats.* Cell Host Microbe, 2010. **8**(1): p. 68-76.

10. Rainwater, D.L. and P.E. Kolattukudy, *Isolation and characterization of acyl coenzyme A carboxylases from Mycobacterium tuberculosis and Mycobacterium bovis, which produce multiple methyl-branched mycocerosic acids.* J Bacteriol, 1982. **151**(2): p. 905-11.

11. Cox, J.S., et al., *Complex lipid determines tissue-specific replication of Mycobacterium tuberculosis in mice.* Nature, 1999. **402**(6757): p. 79-83.

12. Kaur, D., et al., *Chapter 2: Biogenesis of the cell wall and other glycoconjugates of Mycobacterium tuberculosis.* Adv Appl Microbiol, 2009. **69**: p. 23-78.

13. Beatty, W.L., et al., *Trafficking and release of mycobacterial lipids from infected macrophages.* Traffic, 2000. **1**(3): p. 235-47.

14. Beatty, W.L., H.J. Ullrich, and D.G. Russell, *Mycobacterial surface moieties are released from infected macrophages by a constitutive exocytic event.* Eur J Cell Biol, 2001. **80**(1): p. 31-40.

15. Geisel, R.E., et al., *In vivo activity of released cell wall lipids of Mycobacterium bovis bacillus Calmette-Guerin is due principally to trehalose mycolates.* J Immunol, 2005. **174**(8): p. 5007-15.

16. Kim, M.J., et al., *Caseation of human tuberculosis granulomas correlates with elevated host lipid metabolism.* EMBO Mol Med, 2010. **2**(7): p. 258-74.

17. Rhoades, E., et al., *Identification and macrophage-activating activity of glycolipids released from intracellular Mycobacterium bovis BCG.* Mol Microbiol, 2003. **48**(4): p. 875-88.

18. Rhoades, E.R., et al., *Cell wall lipids from Mycobacterium bovis BCG are inflammatory when inoculated within a gel matrix: characterization of a new model of the granulomatous response to mycobacterial components.* Tuberculosis (Edinb), 2005. **85**(3): p. 159-76.

19. Pandey, A.K. and C.M. Sassetti, *Mycobacterial persistence requires the utilization of host cholesterol.* Proc Natl Acad Sci U S A, 2008. **105**(11): p. 4376-80.

20. Brock, M. and W. Buckel, *On the mechanism of action of the antifungal agent propionate.* Eur J Biochem, 2004. **271**(15): p. 3227-41.

21. Millar, A.H., C.J. Leaver, and S.A. Hill, *Characterization of the dihydrolipoamide acetyltransferase of the mitochondrial pyruvate dehydrogenase complex from potato and comparisons with similar enzymes in diverse plant species.* Eur J Biochem, 1999. **264**(3): p. 973-81.

22. Slayden, R.A. and C.E. Barry, 3rd, *Analysis of the Lipids of Mycobacterium tuberculosis.* Methods Mol Med, 2001. **54**: p. 229-45.

23. Rousseau, C., et al., *Virulence attenuation of two Mas-like polyketide synthase mutants of Mycobacterium tuberculosis.* Microbiology, 2003. **149**(Pt 7): p. 1837-47.

24. Abramovitch, R.B., et al., *aprABC: a Mycobacterium tuberculosis complex-specific locus that modulates pH-driven adaptation to the macrophage phagosome.* Mol Microbiol, 2011. **80**(3): p. 678-94.

25. Minnikin, D.E., et al., *The methyl-branched fortifications of Mycobacterium tuberculosis.* Chem Biol, 2002. **9**(5): p. 545-53.

26. Jackson, M., G. Stadthagen, and B. Gicquel, *Long-chain multiple methyl-branched fatty acid-containing lipids of Mycobacterium tuberculosis: biosynthesis, transport, regulation and biological activities.* Tuberculosis (Edinb), 2007. **87**(2): p. 78-86.

27. Rohde, K.H., et al., *Linking the Transcriptional Profiles and the Physiological States of Mycobacterium tuberculosis during an Extended Intracellular Infection.* PLoS Pathog, 2012. **8**(6): p. e1002769.

28. Munoz-Elias, E.J. and J.D. McKinney, *Mycobacterium tuberculosis isocitrate lyases 1 and 2 are jointly required for in vivo growth and virulence.* Nat Med, 2005. **11**(6): p. 638-44.

29. Honer Zu Bentrup, K., et al., *Characterization of activity and expression of isocitrate lyase in Mycobacterium avium and Mycobacterium tuberculosis.* J Bacteriol, 1999. **181**(23): p. 7161-7.

30. Desbois, A.P. and V.J. Smith, *Antibacterial free fatty acids: activities, mechanisms of action and biotechnological potential.* Appl Microbiol Biotechnol, 2010. **85**(6): p. 1629-42.

31. Dubos, R.J., *The effect of organic acids on mammalian tubercle bacilli.* J Exp Med, 1950. **92**(4): p. 319-32.

32. Trivedi, O.A., et al., *Dissecting the mechanism and assembly of a complex virulence mycobacterial lipid.* Mol Cell, 2005. **17**(5): p. 631-43.

CHAPTER THREE

Phenotypic profiling for defining genes essential for propionate and fatty acid metabolism

Adapted from

Intracellular *Mycobacterium tuberculosis* exploits host-derived fatty acids to limit metabolic stress. Lee W, VanderVen BC, Fahey RJ, Russell DG .J Biol Chem. 2013 Mar 8; 288 (10):6788-800.

ABSTRACT

M. tuberculosis has evolved strategies for reprogramming its carbon metabolism with the nutrients in the environment encountered during infection. The intracellular survival and replication of the bacterium relies on the ability to coordinate metabolic pathways in response to carbon sources available inside its host cell. Cholesterol and fatty acids appear key carbon sources, and their 3 carbon product propionyl-CoA can lead a metabolic stress. Relieving of the metabolic stress is central to the realignment of *M. tuberculosis* metabolism to these host-derived lipids. In this study, we employed TraSH analysis, a global genome profiling method, to define the genes involved in propionate and fatty acid metabolism. We identified the pathways and enzymes necessary for the detoxification of propionyl-CoA. Our data demonstrate the metabolic ability of *M. tuberculosis* to limit propionyl-CoA stress by incorporation into cell wall lipids. These data provide verification that biosynthesis of methyl branched lipids serves as a sink for propionyl-CoA, and presents comprehensive genetic characterization of the pathways that impact propionate metabolism.

3.1 Introduction

Nutrient acquisition is crucial for growth and persistence of *M. tuberculosis* in host. Host lipids have long been implicated as primary carbon source during infection [1, 2]. Thus, as a new drug target for drug development, lipid metabolism in the bacterium is attractive. Conventional drugs target biosynthetic pathways involved in cell growth. While these drugs kill efficiently *M. tuberculosis* grown *in vitro*, they are less active against bacteria in a vegetative, non-replicating state in the host [3, 4]. As carbon flow from host nutrients is a significant determinant of the ability of *M. tuberculosis* to replicate and persist in host, these catabolic pathways could also be important targets for therapeutic intervention [2, 5-8]. Therefore, information about the catabolic metabolism in *M. tuberculosis* during infection is critical to understanding *M. tuberculosis* pathogenesis and as a novel theme for new chemotherapeutic agents that could also be active against drug resistant strains.

In order to monitor carbon metabolism, transcriptional profiling has been used. Transcriptional expression analysis reveals invaluable information about global responses of the bacterium at any given condition and time. In particular, it provides critical information for identifying metabolic pathways that *M. tuberculosis* activates and is depend on during infection [9, 10], and for better understanding how drugs and drug candidates works in cells and organisms and what gene may be studied further as a potential targets [11]. However, this approach generates correlative data and may be misleading in situation where message abundance and proteins levels are at variance. These limitations can be addressed by using other global genome analysis methods

such as transposon insertion-site mapping. For these analyses, mutant pools are generated by transposon mutagenesis prior to monitoring survival of each individual mutant in a pool following selection [12, 13]. For example, signature tagged mutagenesis (STM) which uses a series of sequence tagged transposons, allows accurate quantitation of individual mutants in a defined pool[14]. Alternately, Transposon Site Hybridization (TraSH), which combines microarray hybridization and transposon mutagenesis, provides a genome-wide analysis of all essential genes or genomic regions that are required for survival under different conditions [15-18]. This latter method is not reliant on a previously characterized signature tag but involves the quantitative analysis of input and output pools to identify those mutants enriched or depleted by selection through the amplification of the sites of insertion of the transposon.

As noted in earlier chapter (Chapter 2), the pathways of lipid degradation and cell wall synthesis play a critical role in the modulation of the relative levels of 3-carbon intermediates such as propionyl-CoA, and this regulation is critical to the survival of intracellular *M. tuberculosis*. These data were generated from a very targeted approach that artificially controlled carbon flux through the MCC, the MMP and into MB cell wall lipids. The simplicity of the resultant phenotypes is, however, somewhat misleading because the bacterium undoubtedly possesses complex feedback loops and regulatory circuits to control both upstream and downstream pathways of central carbon metabolism and biosynthetic pathways. To expand our study and incorporate a more holistic understanding of other bacterial gene products that impact propionyl-CoA metabolism we exploited our experimental system to construct a

forward genetic screen to identify other genes implicated in this metabolic process. For this screen, we used TraSH to identify genes required in detoxification of propionate. In this chapter, by using TraSH, we generate a comprehensive set of genes that impact propionate metabolism. In conditions of propionate stress, the important roles of biosynthesis of methyl-branched polyketides revealed by TraSH demonstrate that metabolic adaptation of *M, tuberculosis* through carbon re-routing is critical in utilization of host derived lipids.

3.2 MATERIAL and METHODS

Bacterial strains and culture conditions

Mycobacterial strains were maintained in Middlebrook 7H9 medium (Difco) supplemented with 0.2% glycerol, OADC (oleate 0.5% BSA, 0.2% dextrose, 0.085% NaCl) and 0.05% tyloxapol. Kanamycin (20 μg/ml) or hygromycin (50 μg/ml) were used where necessary. *Mycobacterium smegmatis mc2–155* was cultured on LB agar. *M. tuberculosis* H37Rv were cultured on Middlebrook 7H10 agar supplemented with OADC.

For growth on defined carbon sources, strains were grown without shaking in minimal medium (0.5 g/L asparagine, 1.0 g/L KH_2PO_4, 2.5 g/L Na_2HPO_4, 50 mg/L ferric ammonium citrate, 0.5 g/L $MgSO_4$,$7H_2O$, 0.5 mg/L $CaCl_2$ and 0.1 mg/L $ZnSO_4$, 10 mM glycerol, and 0.05% tyloxapol) containing propionate or fatty acids (Sigma).

Long chain fatty acids were prepared as described in Chapter 2. Bacterial growth was monitored by measuring optical density at 600 nm.

Mutant Strains

The *acs*:Tn mutant (Transposon insertion at 866 bp), the *prpD*:Tn mutant (Transposon insertion at 643 bp), and *prpC*:Tn mutant (Transposon insertion at 1019 bp) were constructed using *MycomarT7* in H37Rv in a *Δicl1* background. To construct a PDIM- (or SL-1) deficient mutant in the *Δicl1* background, an internal 1066-bp fragment of *ppsD* (Rv2934) and an internal 1044-bp fragment of *pks2* (Rv3825) was PCR amplified and cloned into the plasmid pMV307 (Km^R), a derivative of pMV306 without the *int* gene, which was used to construct the *ppsD* knockout mutant by single crossover. Then plasmid DNA was UV irradiated and electroporated into the *Δicl1* strain. Transformants were selected on Kanamycin and confirmed by PCR. To quantify survival of *M. tuberculosis* in macrophage infection experiments we transformed the relevant H37Rv strains with pVV16-*smyc'::mCherry* expressing the fluorescent protein mCherry driven by the *smyc* promoter.

Construction of Transposon Mutant Libraries

Transposon libraries were made by using the Transposon donor phagemid *ϕMycoMarT7* (GenBank accession no. AF411123) in the *Δicl1* H37Rv background as described. For preparation of high concentration stock of phagemid ($1x10^{11}$/PFU), the

phagemid was transduced into *M. smegmatis* MC2, and incubated to allow form plaque at 30°C, 20 of plaques of which were tested for temperature sensitivity at 37°C. The isolated plaque which was temperature sensitive was amplified and concentrated by re-tranduction into *M. smegmatis*. For *M. tuberculosis* transduction, the bacterial cultures grown to OD_{600} of 0.8-1.0 in liquid culture were washed twice with MP buffer (50 mM Tris, pH7.5/ 150 mM NaCl/ 10 mM $MgSO_4$ / 2 mM $CaCl_2$) and concentrated in 1/10 of the original culture volume in MP buffer. Then cells were infected with $1x10^{10}$ phage per ml of bacterial culture for 4 hours at 37°C. The mixture was plated on 7H10 OADC 20 μg/ml kanamycin, and libraries were collected by scraping colonies from plates. Each library consisted of at least $1x10^5$ independent mutants.

Transposon site hybridization (TraSH)

Approximately $2x10^6$ CFUs from an aliquot of the library were inoculated into minimal media either containing 10 mM glycerol, or 10 mM glycerol with 0.05 mM propionate and 0.05 mM stearic acid, 2mM acetate, or palmitic acid. To limit the over-selection of fast growers, the cultures were only allowed to grow up to an OD_{600} 0.3. Then, the control pool and the propionate/fatty acid rescue pool were compared, two biological replicates and two technical replicates, using TraSH.

Construction of high density microarray A custom-designed, high-density microarray was used to identify the insertion sites. This array, synthesized by Agilent Technologies, consisted of 60 mer oligos every 350 bp of the *M. tuberculosis* H37Rv

chromosome. We calculated that this oligo density would allow size-selected (200-500 bp) labeled probes to hybridize to at least one oligo and therefore provide sufficient coverage to identify the majority of insertion sites.

Generation of labeled RNA for TraSH analysis Genomic DNA was isolated from mutant pools as described. Fragment from 500 bp to 2000 bp by digested partially by *HinP*I and *Msp*I (New England Biolabs) was ligated to the adapter. To amplify the transposon junctions, PCR reaction was followed with the ligated DNA.

Table 3.1 PCR condition for probe amplification

Primer 1 and adapter primer			**Primer 2 and adapter primer**		
temp (°C)	**min**	**cycle**	**temp (°C)**	**min**	**cycle**
95	10	1	95	10	1
94	0.5	5	94	0.5	5
69	0.5		72	2	
72	1.5				
94	0.5	5	94	0.5	5
67	0.5		70	2	
70	1.5				
94	0.5	15-25	94	0.5	15-25
65	0.5		68	2+	
68	1.5 + 5s /cycle			5s /cycle	
72	5	1	72	5	1

Then, PCR products from 250bp to 500bp was used as for *in vitro* transcription with T7 polymerase to make template RNA (Ambion, Austin, TX). After transcription, RNA was labeled with fluorescein (Alexa-555 and 647). The generated probe was hybridized as described. Images from the signal from hybridized RNA was detected with a Scanarray microarray scanner and analyzed with GeneSpring GX software

(Agilent). Mutants that were significantly over- (or under-) represented after screen were defined using the following criteria: arbitrary fluorescence intensity >300 in one of the channels, fluorescence ratio >3 and *t* test *p* value <0.05.

Table 3.2 Bacterial strains and plasmids

Strains	Relevant characteristics	reference
Icl1	H37Rv *Δicl1(Rv0467)*	
ppsD	H37Rv *Δicl1 , ppsD(Rv2934):: KO:: Km^R*	This study
Pks2	H37Rv *Δicl1 , pks2(Rv3825):: KO:: Km^R*	This study
Acs Tn	H37Rv *Δicl1 , acs(Rv3667)::Tn Km^R*	This study
prpD Tn	H37Rv *Δicl1 , prpD(Rv1130)::Tn Km^R*	This study
prpC Tn	H37Rv *Δicl1 , prpC(Rv1131)::Tn Km^R*	This study
Plasmids		
Name	Relevant characteristics	reference
pMV307	Km^R	This study
ϕMycoMarT7	Km^R	[16]
Primers		
Name	Oligo nucleotide sequence, 5`→ 3`	use
ppsD –F	GACGATGAACCGCGAACTGGACC	Knock out ppsD
ppsD- R	GCTTTCGGTCCATTCGGCATCG	Knock out ppsD
ppsD-CF	GCTTATCGACGGCGACGAGGTGGT	Confirm ppsD KO
ppsD-CR	AGCACCCGCACCAGCCCTTTCAA	Confirm ppsD KO
Pks2-F	GCTGACGGATCTGCACAACGCTG	Knock out pks2
Pks2-R	TACAGGCCCTGCTGCGAACGA	Knock out pks2
Pks2-CF	AGGAGTGCTGTCAGCCGAAGATGGGG	Confirm pks2 KO
Pks2-CR	GGTAGCGGTCACATCAGAGGCAGCG	Confirm pks2 KO
Adaptor prim	GTCCAGTCTCGCAGATGATAAGG	TraSH
TN 1	CCCGAAAAGTGCCACCTAAATTGTAAGCG	TraSH
TN 2	CGCTTCCTCGTGCTTTACGGTATCG	TraSH
Adapter 1	CGACCACGACCA 3′ C6-TFA	TraSH
Adapter 2	AGTCTCGCAGATGATAAGGTGGTCGTGGT	TraSH

3.3 RESULTS and DISCUSSION

3.3.1 Genetic profiling of propionate, stearic acid (C18:0) and palmitic acid (C16:0) metabolism

To identify loci of interest we designed a TraSH screen to reveal mutants that were incapable of detoxifying propionyl-CoA, and that were unable to grow in the presence of propionate when provided long chain fatty acids as a means of rescue (Figure 3.1). We focused on saturated C18 and C16 fatty acid to provide metabolic rescue because we have shown previously that these chain length fatty acids are an effective primer for synthesis of PDIM, and are known to be one of the more abundant fatty acid species in the granulomatous lesion of TB as well as in the mammalian host [19]. We constructed a 10^5 CFU library in *H37Rv Δicl1* using the mariner transposon (*MycomarT7*). This library was grown in minimal medium containing 10 mM glycerol (input pool) versus minimal medium containing 10 mM glycerol, 0.05 mM propionate, and 0.05 mM stearic acid (output pool).

To identify genes that impact the metabolism of fatty acid (stearic acid, palmitic acid, or acetate) or propionate, we compared the input and output pools of mutants to quantify those mutations that were under-, or over-represented following selection. As shown in Figure 3.2, the acetate, stearic acid and palmitic acid TraSH analysis revealed core over-represented mutations and under-represented mutations that satisfied our statistical cut-off (3-fold change, $P<0.05$, intensity 300<) (Table 1-4). These genes are arranged diagrammatically in context of their annotation and assignment to known metabolic pathways (Figure 3.3). We hypothesized that those

mutants lost during selection will include genes that are required for the fatty acid uptake and rescue from propionyl-CoA-mediated toxicity, whilst those mutants enriched in the screen would include genes that mitigate propionyl-CoA-mediated toxicity and facilitate growth. Not surprisingly, the most dominant themes to emerge from the screen are loci involved in methyl-branched lipid biosynthesis, the MCC, and β-oxidation (Figure 3.3).

To validate the TraSH data, we generated and determined the phenotype of 2 double mutants; *Δicl1:KO-ppsD* (PDIM synthesis) and *Δicl1: KO-pks2* (SL-1 synthesis). While both mutants grew normally on control medium, neither the PDIM- nor SL-1-deficient double mutants could grow in propionate-containing medium supplemented by either acetate or stearic acid (Figure 3.4A-C), whereas the parent *Δicl1* mutant grew in propionate supplemented with either acetate or stearic acid. These results both validate the genetic screen and provide biochemical verification of the phenotypes of the double mutants.

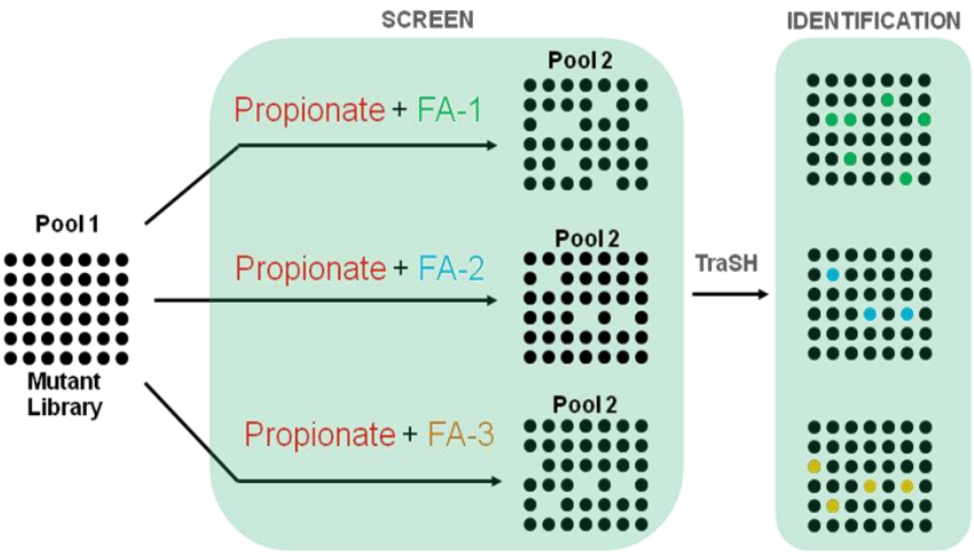

Figure 3.1 Schematic draw for TraSH screen. Mutants that are incapable of detoxifying propionyl-CoA in presence of fatty acids, or unable to grow in the presence of propionate will be less represented in Pool 2 than Pool 1, and these mutations can be identified by TraSH analysis.

3.3.2 Under represented mutants

Prominent among under-represented mutations were those genes involved in the biosynthesis of MB-lipids; locus Rv2930-Rv2950 for PDIM synthesis, Rv3820-Rv3825c for SL-1 synthesis, Rv1180-Rv1185 for PAT and DAT synthesis, and Rv1527c/*Pks5*-Rv1528c/*PapA4,* which are related to mycobacterial lipooligosaccharide (LOS) biosynthetic genes in *M. marinum* and *M. canetti*. While *M. tuberculosis* is not reported to make LOS, *pks5* has been implicated in mycocerosoic acid synthesis, and mutants defective in expression of *pks5* have a marked growth defect in mice [20]. These data provide independent verification that the biosynthesis of MB lipids provides a sink for excess propionyl-CoA and is consistent with the observation that increases in propionate pools enhances the biosynthesis of PDIM and SL-1 or longer MB-lipids. In addition, mutants of a transcriptional regulator, *phoP* (phoP 10.1X P=0.00007, phoR 2.2X P=0.003), were also enriched following selection. We found previously that *phoP* mutants exhibit a marked enhancement in the production of PDIM and other mycocerosates [21], which is consistent with a previous report that documented that *PhoP* mutants exhibited enhanced resistance to both propionate toxicity and to 3-nitropropionate, a known inhibitor of ICL activity [22].

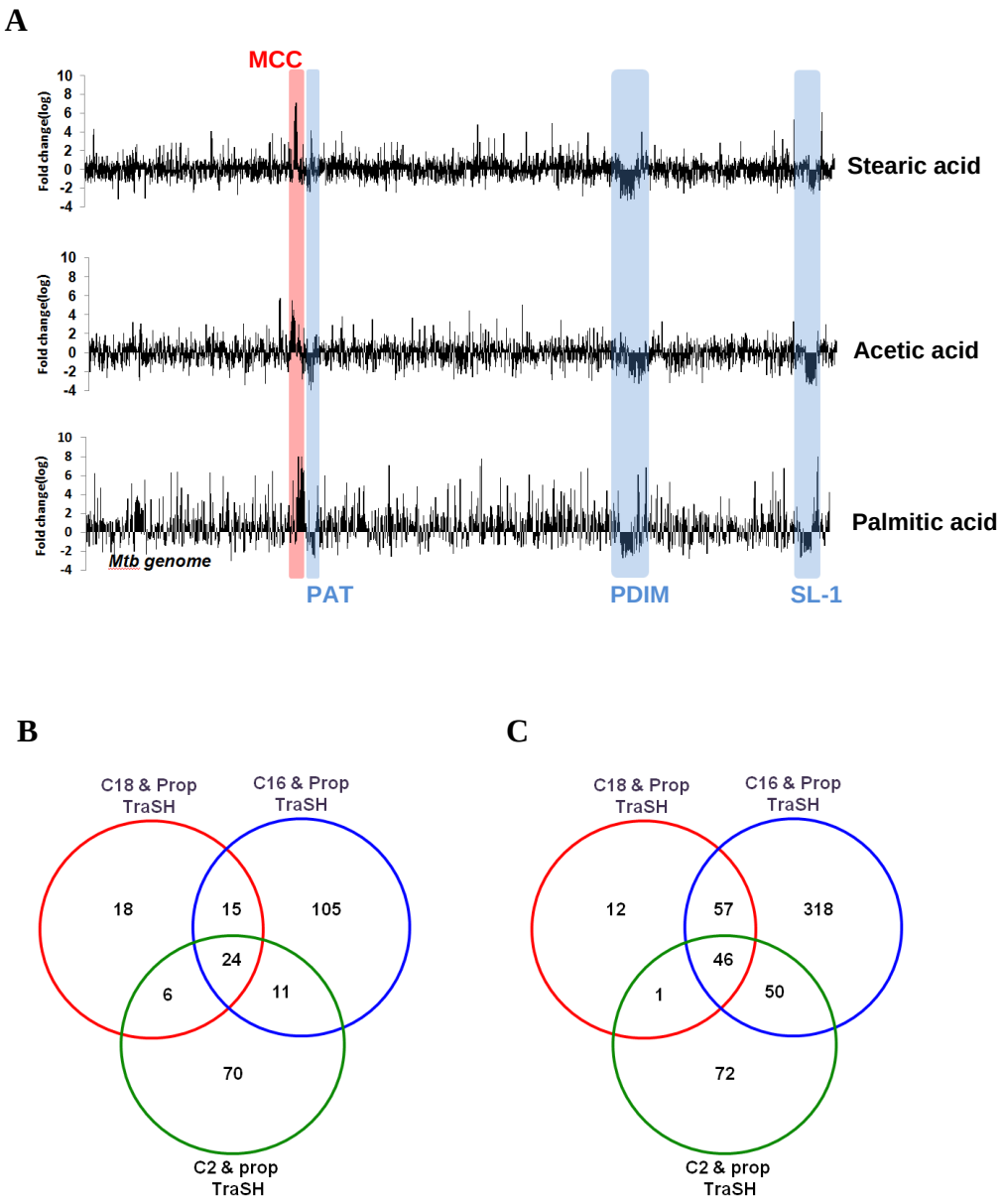

Figure 3.2 TraSH analysis. (A) Fold change cross the *M. tuberculosis* genome. In all three screens, the locus for biosynthesis of PAT, PDIM, and SL-1 were commonly underrepresented (highlighted by blue) while mutations in genes of MCC were over-represented (highlighted by red). Comparison of under-representors (B) or over-representors (C) from acetate (C2) & propionate, palmitic acid (C16) & propionate, and stearic acid (C18) & propionate TraSH.

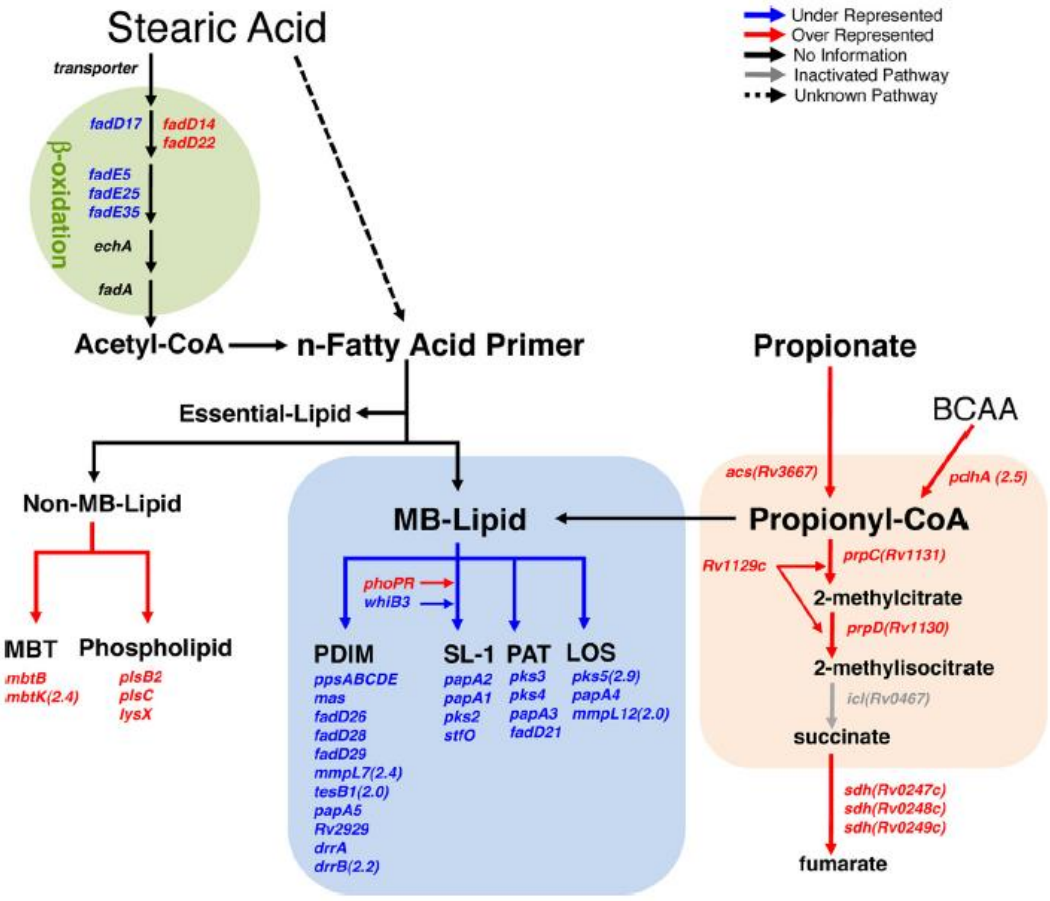
Under Represented
Over Represented
No Information
Inactivated Pathway
Unknown Pathway
Stearic Acid
transporter
β-oxidation
fadD17
fadD14
fadD22
fadE5
fadE25
fadE35
echA
fadA
Acetyl-CoA
n-Fatty Acid Primer
Propionate
BCAA
Essential-Lipid
acs(Rv3667)
pdhA (2.5)
Non-MB-Lipid
MB-Lipid
Propionyl-CoA
Rv1129c
prpC(Rv1131)
2-methylcitrate
prpD(Rv1130)
2-methylisocitrate
icl(Rv0467)
succinate
sdh(Rv0247c)
sdh(Rv0248c)
sdh(Rv0249c)
fumarate
phoPR
whiB3
MBT
Phospholipid
mbtB
mbtK(2.4)
plsB2
plsC
lysX
PDIM
SL-1
PAT
LOS
ppsABCDE
mas
fadD26
fadD28
fadD29
mmpL7(2.4)
tesB1(2.0)
papA5
Rv2929
drrA
drrB(2.2)
papA2
papA1
pks2
stfO
pks3
pks4
papA3
fadD21
pks5(2.9)
papA4
mmpL12(2.0)

Figure 3.3 Phenotypic TraSH screen identifies genes involved in propionate utilization and toxicification. Graphical illustration of the differentially-represented genes in context of the metabolic pathways most relevant to propionate utilization and detoxification. Genes required for *Δicl1 M. tuberculosis* growth in the presence propionate and long chain fatty acids as a means of propionate toxicity rescue are indicated in blue text. Genes that when mutated, enhance *Δicl1 M. tuberculosis* growth in the presence propionate and long chain fatty acids indicated in red text. The differentially represented genes are shown in relation to the relevant carbon metabolic pathways; synthesis of non-essential MB-lipids, synthesis of non-MB-lipids, the MMC, and genes involved in the β-oxidation breakdown of long chain fatty acids. All genes selected were >3x-fold over-represented or >3x-fold under-represented with *P*-values < 0.05. The full list of over-represented and under-represented genes is provided in supplemental material, Table 3.1-4.

3.3.3 Over represented mutants

Amongst those mutations that were over-represented, or positively-selected in the screen, the most striking were those genes implicated in the metabolism of propionate through MCC (Figure 3.3). The screen was conducted in a *Δicl1* mutant background, thus the MCC was inactivated at the 2-methylisocitrate to succinate and pyruvate step. This suggests strongly that the accumulation of all three upstream intermediates, propionyl-CoA, 2-methylcitrate and 2-methylisocitrate are, individually or collectively, toxic to *M.tuberculosis*. The inactivation of Rv1129c, Rv1130/*prpD*, or Rv1131/*prpC* resulted in marked enhancement of growth, which implies that 2-methycitrate and/or 2-methylisocitrate are more toxic than propionyl-CoA; Rv1129c (103.7X, P=0.003), Rv1130 (136.8X, P=0.0002), Rv1131 (15.6X, P=0.01), and Rv3667 (17.7X, P=0.04). This is consistent with the putative mechanism of propionate toxicity in *Salmonella* where 2-methlycitrate is believed toxic [23].

Finally, we also found that a mutation in Rv2497c (*pdhA*) encoding a subunit of the branched-chain keto acid dehydrogenase [24] was advantageous to growth. It is therefore possible that a significant fraction of propionyl-CoA in *M. tuberculosis* may be produced via catabolism of MB-amino acids such as valine and isoleucine, in addition to the breakdown of cholesterol. To validate those loci identified as over-represented in the TraSH screen, we examined the phenotypes of the double knockout mutants, *Δicl1: Tn::Rv3667* (an acetyl-CoA synthase), *Δicl1: Tn::prpC* (citrate synthase, GLTA1), and *Δicl1: Tn::prpD* (methylcitrate synthase).

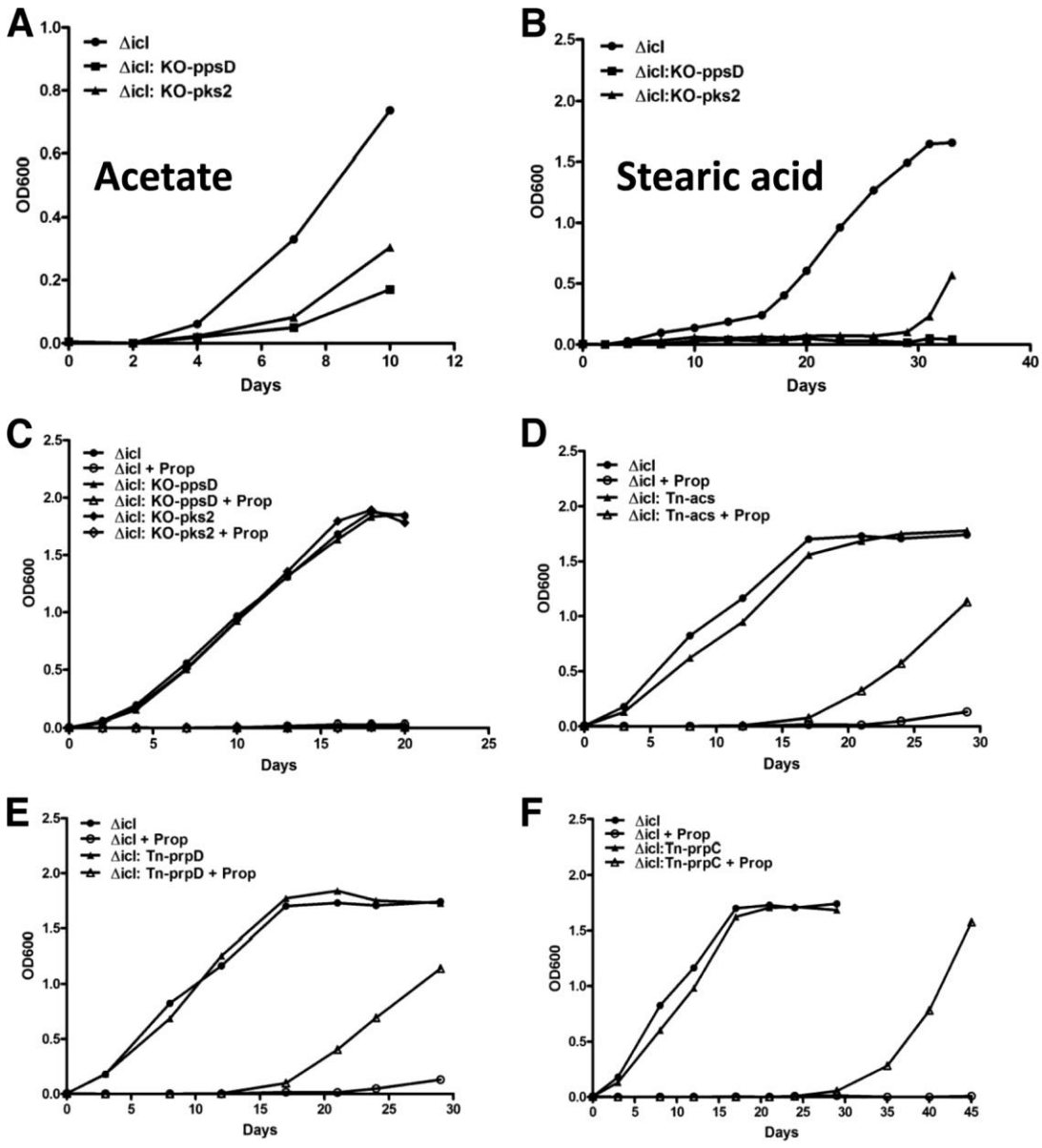
A
Δicl
Δicl: KO-ppsD
Δicl: KO-pks2
Acetate
OD600
Days
B
Δicl
Δicl:KO-ppsD
Δicl:KO-pks2
Stearic acid
OD600
Days
C
Δicl
Δicl + Prop
Δicl: KO-ppsD
Δicl: KO-ppsD + Prop
Δicl: KO-pks2
Δicl: KO-pks2 + Prop
OD600
Days
D
Δicl
Δicl + Prop
Δicl: Tn-acs
Δicl: Tn-acs + Prop
OD600
Days
E
Δicl
Δicl + Prop
Δicl: Tn-prpD
Δicl: Tn-prpD + Prop
OD600
Days
F
Δicl
Δicl + Prop
Δicl:Tn-prpC
Δicl:Tn-prpC + Prop
OD600
Days

Figure 3.4 Validation of the genes implicated in propionate utilization and detoxification in *Δicl M. tuberculosis*. Genes identified by TraSH screen were validated through the generation of double mutants and characterized by growth phenotype (A-C) Genes negatively-selected for involved in MB-containing lipid biosynthesis. Growth of the *Δicl1* parental strain and *Δicl1*:KO-*ppsD* (PDIM biosynthesis), and *Δicl1*:KO-*pks2* (SL-1 biosynthesis) double mutant strains were assessed in minimal media containing glycerol, propionate and (A) 1 mM acetate, or (B) 0.05mM stearic acid, or (C) absent any fatty acid supplement. In each instance the mutants exhibited defective growth in fatty acid with propionate (A and B) yet grew normally in minimal medium with glycerol (C). (D-F) Genes positively-selected as being involved in propionate utilization and the generation of toxic intermediates. Growth of the *Δicl1* parental strain (D) *Δicl1*:Tn *acs* (Rv3667) (E) *Δicl1*:Tn *prpD* (Rv1130), (F) *Δicl1*:Tn *prpC* (Rv1131) in minimal media containing glycerol and 0.05 mM propionate (D-E) or 0.1 mM propionate (F). These mutants all grew normally in minimal medium and each of the second mutations conferred partial resistance to propionate toxicity, consistent with their enrichment under propionate selection. Results are representative of three experiments.

We included Rv3667 in this analysis because, although it is annotated as an acetyl-CoA synthase, it was strongly selected for in the TraSH screen (enriched almost 18 fold) and may function as a propionyl-CoA synthetase, required for the conversion of propionate to propionyl-CoA. All 3 double mutant strains exhibited resistance to propionate toxicity (0.05 mM and 0.01 mM) and were able to grow to varying degrees in propionate-containing medium, while the growth of the parent, *Δicl1* parent strain was strongly inhibited (Figure 3.4D-F). The prolonged lag period observed in the growth of these mutants is not due to suppressor mutations because similar lag periods are observed on the passing of the mutants into fresh culture medium. Again, these data provide biochemical verification of the phenotypes of the double mutants.

3.3.4 Fatty acid metabolism

The above themes have been selected because they validate the TraSH screen and the selection pressure applied to the mutant pools, however, there are other, less obvious sets of genetic loci that have been enriched or depleted from the mutant pool. Notably, several *fadD* and *fadE* genes appeared as under-represented, suggesting these may be involved in stearic acid catabolism and expansion of the acetyl-CoA pool, in addition to stearic acids role as an acyl primer. This finding is particularly interesting given the high redundancy of genes thought to be involved in β-oxidation of fatty acids [25] because it implies that there may be at least a measure of substrate specificity within this pathway.

For further identification of a set of genes for a fatty acid catabolism, we constructed a 10^5 CFU library in CDC1551 using the mariner transposon (*MycomarT7*). This library was grown in minimal medium containing 10 mM glycerol (input pool) versus minimal medium containing 0.05 mM stearic acid (output pool-1). To exclude genes that are related to stearic acid toxicity, we included a culture containing 10 mM glycerol and 0.05 mM stearic acid (output pool-2). To identify genes that impact the utilization of stearic acid, we compared the input and output pools of mutants as described in the propionate TraSH data. The TraSH analysis revealed most of genes that were significant in stearic acid utilization were also presented under the condition of stearic acid toxicity. However, we found a subset of genes that are under-represented in stearic acid utilization, but are over-represented (or not represented), which were likely involved in stearic acid utilization such as its import (3-fold change, $P<0.05$, intensity 300<) (Table 3, 4).

3.3.5 Competition for fatty acid primer

Finally we found that mutations in genes involved in the synthesis of certain non-MB-lipids such as mycobactin (*mbtB*, *mbtK*) [26], and phospholipid (*lysX*, *plsC*) [27], conferred a growth advantage, which was unexpected. However *M. tuberculosis* requires C16-C20 fatty acids (or C12 in mycobactin) to synthesize phospholipids and mycobactin [28], as well as MB-lipids such as PDIM [29]. Therefore, because biosynthesis pathways of non-MB-lipids and MB-lipids likely compete for these fatty acid primers, the reduced carbon flow into biosynthesis of non-MB lipids may lead to

the increased availability of fatty acid primers that can be redirected into MB-lipids, thus enhancing detoxification.

3.4 Concluding remarks

The TraSH data provide insights into the re-routing of carbon flow to limit propionate toxicity, which is consistent with the observations shown in Chapter 2. The data suggest that the biosynthesis of methyl branched polyketides such as PDIM, SL-1, and PAT, plays important roles in reducing propionyl-CoA level by incorporating propionyl-CoA into their phthioceranic acids in form of methyl groups. We also found that transposon mutants with insertions in any gene in the methyl citrate cycle were over-represented, suggesting that the toxic intermediates in the methyl citrate cycles likely include 2 methyl (iso)citrate or propionyl-CoA rather than propionate. Furthermore, TraSH data revealed a subset of genes, which may be involved in filling missing pathways in methyl-branched lipid synthesis, propionate detoxification or fatty acid processing.

Acknowledgement

The authors thank Christopher Sassetti for providing the phagimid, *ϕMycomarT7*.

Table 3.3 Under represented mutants in stearic acid TraSH

Gene Name	probe-ID	Ratio	Function
Rv0147	Rv0147-1/5	-4.49	aldehyde dehydrogenase
Rv0180c	Rv0180c-1/4	-9.21	conserved transmembrane protein
Rv0244(fadE5)	Rv0244c-1/5	-5.50	acyl-coa dehydrogenase fade5
	Rv0244c-2/5	-5.92	
	Rv0244c-3/5	-4.34	
Rv0295c	Rv0295c-2/2	-3.35	conserved hypothetical protein
Rv0315	Rv0315-1/2	-3.19	possible beta-1,3-glucanase
Rv0544c	Rv0544c-1/1	-5.59	conserved transmembrane protein
Rv0545c(pitA)	Rv0545c-2/4	-4.64	low affinity inorganic phosphate transporter
Rv0554(bpoC)	Rv0554-1/2	-3.08	possible peroxidase bpoc
Rv0686	Rv0686-2/2	-3.24	probable membrane protein
Rv0691c	Rv0691c-1/1	-4.97	probable transcriptional regulator
BT-v0804&Rv0805		-6.65	tn>rv0805 : bt-rv0804&rv0805
Rv0820(phoT)	Rv0820-2/3	-3.02	probable phosphate-transport abc transporter
Rv0996	Rv0996-2/3	-3.03	conserved transmembrane protein
Rv1161(narG)	Rv1161-9/10	-3.11	probable respiratory nitrate reductase
Rv1180(pks3)	Rv1180-4/4	-3.27	polyketide synthase 3
Rv1181(pks4)	Rv1181-10/14	-5.22	polyketide synthase 4
Rv1182(papA3)	Rv1182-1/4	-3.99	probable polyketide synthase associated protein
Rv1185c(fadD21)	Rv1185c-2/5	-3.12	probable fatty-acid--coa ligase
	Rv1185c-3/5	-3.47	
	Rv1185c-5/5	-5.29	
Rv1253(deaD)	Rv1253-4/5	-3.27	cold-shock dead-box protein a homolog
Rv1256c(cyp130)	Rv1256c-3/4	-3.14	proba ble cytochrome p450 130
Rv1457c	Rv1457c-2/3	-3.66	probable integral membrane abc transporter
Rv1528c(papA4)	Rv1528c-2/2	-3.31	polyketide synthase associated protein
Rv1566c	Rv1566c-1/2	-3.93	possible inv protein
Rv1626	Rv1626-1/2	-5.82	probable tcs transcriptional regulator
Rv1709	Rv1709-1/2	-3.28	conserved hypothetical protein
Rv1761c	Rv1761c-1/1	-3.19	hypothetical exported protein
BT-PPE27&PE19		-3.42	tn>rv1791 : bt-ppe27&pe19
Rv1946c(lppG)	Rv1946c-1/1	-3.43	possible lipoprotein
Rv2027c(dosT)	Rv2027c-5/5	-3.60	tcs sensor histidine kinase
Rv2135c	Rv2135c-1/2	-4.50	conserved hypothetical protein
Rv2418c	Rv2418c-1/2	-3.19	hypothetical protein
BT-fas&Rv2525c		-3.37	tn>rv2524c : bt-fas&rv2525c
Rv2535c(pepQ)	Rv2535c-1/3	-4.10	probable cytoplasmic peptidase
	Rv2535c-3/3	-4.95	probable cytoplasmic peptidase
Rv2625c	Rv2625c-1/3	-3.02	probable transmembrane protein
Rv2710(sigB)	Rv2710-1/3	-7.54	rna polymerase sigma factor
Rv2723	Rv2723-1/3	-3.25	conserved transmembrane protein
Rv2752c	Rv2752c-5/5	-3.86	conserved hypothetical protein
Rv2781c	Rv2781c-3/3	-3.38	possible ala rich oxidoreductase
Rv2867c	Rv2867c-1/2	-3.66	gcn5-related n-cetyltransferase
Rv2929	Rv2929-1/1	-5.03	hypothetical protein
Rv2930(fadD26)	Rv2930-2/5	-8.71	fatty-acid-coa ligase
	Rv2930-3/5	-5.04	
	Rv2930-5/5	-3.77	
Rv2931(ppsA)	Rv2931-11/16	-6.67	phenolpthiocerol synthesis type-i
	Rv2931-12/16	-7.28	polyketide synthase ppsa

	Rv2931-7/16	-4.82	
Rv2932(ppsB)	Rv2932-11/13	-3.17	phenolpthiocerol synthesis type-i
	Rv2932-2/13	-6.38	polyketide synthase ppsb
	Rv2932-8/13	-4.88	
Rv2933(ppsC)	Rv2933-10/19	-5.84	phenolpthiocerol synthesis type-i
	Rv2933-13/19	-4.45	polyketide synthase ppsc
	Rv2933-2/19	-7.13	
	Rv2933-7/19	-7.28	
	Rv2933-8/19	-4.34	
Rv2934(ppsD)	Rv2934-10/16	-5.63	phenolpthiocerol synthesis type-i
	Rv2934-16/16	-10.2	polyketide synthase ppsd
	Rv2934-8/16	-4.25	phenolpthiocerol synthesis type-i
Rv2935(ppsE)	Rv2935-11/13	-5.94	polyketide synthase ppsd
	Rv2935-12/13	-5.43	
	Rv2935-2/13	-3.46	
	Rv2935-3/13	-3.39	
	Rv2935-4/13	-3.49	
	Rv2935-5/13	-3.24	
	Rv2935-6/13	-5.63	
Rv2936(drrA)	Rv2936-2/3	-4.61	probable daunorubicin-dim-transport atp-binding protein
Rv2939(papA5)	Rv2939-1/4	-9.39	polyketide synthase associated protein
Rv2940(mas)	Rv2940c-10/18	-7.08	probable multifunctional
	Rv2940c-14/18	-3.37	mycocerosic acid synthase
	Rv2940c-17/18	-3.17	
	Rv2940c-18/18	-4.31	
	Rv2940c-3/18	-3.26	
	Rv2940c-7/18	-4.32	
Rv2941(fadD28)	Rv2941-1/5	-4.80	fatty-acid-coa ligase fadd28
	Rv2941-4/5	-9.08	
Rv2950(fadD29)	Rv2950c-4/5	-3.98	probable fatty-acid-coa ligase fadd29
	Rv2950c-5/5	-4.08	
Rv3028c(fixB)	Rv3028c-3/3	-4.91	probable electron transfer flavoprotein
Rv3110(moaB1)	Rv3110-1/1	-3.29	probable pterin-4-alpha-carbinolamine dehydratase
Rv3126c	Rv3126c-1/1	-4.07	hypothetical protein
BT-PPE50&PPE51		-3.88	tn>rv3136 :
Rv3193c	Rv3193c-3/9	-3.43	probable conserved transmembrane protein
	Rv3193c-6/9	-3.50	
	Rv3193c-9/9	-4.25	
Rv3220c	Rv3220c-2/4	-5.96	probable tcs sensor kinase
Rv3255c(manA)	Rv3255c-4/4	-4.05	probable mannose-6-p isomerase
Rv3274c(fadE25)	Rv3274c-1/3	-3.28	acyl-coa dehydrogenase
Rv3403c	Rv3403c-1/5	-3.96	hypothetical protein
BT-v3415c&whiB3		-4.60	rv3415c<tn>rv3416
Rv3506(fadD17)	Rv3506-5/5	-3.05	fatty-acid-coa synthetase
Rv3530c	Rv3530c-1/2	-3.03	possible oxidoreductase
Rv3649	Rv3649-1/6	-3.49	probable helicase
Rv3682(ponA2)	Rv3682-4/7	-5.89	probable penicillin binding protein
Rv3698	Rv3698-1/5	-4.11	conserved hypothetical protein
Rv3732	Rv3732-1/3	-3.69	conserved hypothetical protein
Rv3755c	Rv3755c-2/2	-4.29	conserved hypothetical protein

Rv3820c(papA2)	Rv3820c-1/4	-4.32	possible polyketide synthase
	Rv3820c-3/4	-3.13	associated protein papA2
Rv3824c(papA1)	Rv3824c-4/5	-5.16	probable polyketide synthase
	Rv3824c-5/5	-4.31	associated protein papA1
Rv3825c(pks2)	Rv3825c-1/18	-4.01	probable polyketide synthase pks2
	Rv3825c-12/18	-4.07	
	Rv3825c-13/18	-3.67	
	Rv3825c-16/18	-3.40	
	Rv3825c-17/18	-3.44	
	Rv3825c-4/18	-4.65	
	Rv3825c-8/18	-5.12	
	Rv3825c-9/18	-6.42	

List of genes that are under-represented by TraSH analysis in the stearic acid rescue screen. All genes have >3 fold under representation in the pool of stearic acid and propionate screen condition with a *P*-value <0.05. Genes listed in red are related to PDIM or SL-1. Probes in intergenic regions are shown as BT *Rvxxxx& Rvxxxx*. The numbers beside the genes indicate the position of probe within the gene; for example, Rv3825c-1/18 means that this probe is the first probe out of 18 internal probes within Rv3825c.

Table 3.4 Over represented mutants in stearic acid TraSH

Gene name	probe-ID	Ratio	Function
Rv0041(leuS)	Rv0041-7/8	12.79	leucyl-tRNA synthetase
Rv0042c	Rv0042c-1/1	12.65	possible transcriptional regulatory protein
Rv0174(mce1F)	Rv0174-1/4	3.60	mce-family protein mce1f
Rv0199	Rv0199-1/2	4.33	conserved membrane protein
Rv0236c	Rv0236c-12/12	4.18	conserved membrane protein
Rv0238	Rv0238-1/1	3.28	possible transcriptional regulator
Rv0247c	Rv0247c-1/2	5.31	probable succinate dehydrogenase
	Rv0247c-2/2	3.08	
Rv0248c	Rv0248c-1/6	3.53	probable succinate dehydrogenase
	Rv0248c-3/6	3.48	
Rv0249c	Rv0249c-1/2	6.35	probable succinate dehydrogenase
Rv0346c(ansP2)	Rv0346c-4/4	4.53	possible l-asparagine permease
BT-purA&Rv0358		5.75	rv0357c<tn>rv0358
Rv0384c(clpB)	Rv0384c-1/8	5.98	probable endopeptidase
BT-mmpS1&fadD30		3.51	rv0403c<tn>rv0404
BT-lpqL&lpqM		4.46	tn>rv0419
Rv0426c	Rv0426c-1/1	7.24	possible transmembrane protein
Rv0455c	Rv0455c-1/1	7.22	conserved hypothetical protein
Rv0485	Rv0485-1/4	7.21	possible transcriptional regulatory protein
	Rv0485-2/4	5.51	
Rv0654	Rv0654-3/5	16.73	probable dioxygenase
Rv0655(mkl)	Rv0655-1/3	10.93	possible ribonucleotide-transport
	Rv0655-2/3	9.87	abc transporter
Rv0731c	Rv0731c-3/3	6.12	possible s-adenosylmethionine-dependent methyltransferase.
BT-Rv0756c&phoP		10.13	rv0756c<tn>rv0757
Rv0785	Rv0785-2/5	5.29	conserved hypothetical protein
Rv0877	Rv0877-1/3	4.68	conserved hypothetical protein
Rv0908(ctpE)	Rv0908-3/7	4.69	probable metal cation transporter atpase p-type ctpe
Rv0986	Rv0986-1/2	3.06	probable adhesion component transport abc transporter
Rv0987	Rv0987-5/7	6.61	probable adhesion component transport abc transporter
Rv0993(galU)	Rv0993-1/2	7.55	probable utp--glucose-1-puridylyltransferase
Rv1002c	Rv1002c-2/4	14.40	conserved membrane protein
Rv1013	Rv1013-1/4	3.01	putative polyketide synthase pks16
Rv1058(fadD14)	Rv1058-3/5	10.19	probable fatty-acid-coa ligase
Rv1072	Rv1072-1/3	3.25	conserved transmembrane protein
	Rv1072-2/3	6.40	
Rv1094(desA2)	Rv1094-1/2	7.48	possible acyl desaturase
Rv1099c	Rv1100-1/3	4.76	conserved hypothetical protein
Rv1108c(xseA)	Rv1108c-1/3	4.45	probable exodeoxyribonuclease vii
BT-Rv1128c&Rv1129c		35.60	tn>rv1128c : bt-rv1128c&rv1129c
Rv1129c	Rv1129c-1/4	9.16	probable transcriptional regulator protein
	Rv1129c-2/4	17.28	
	Rv1129c-3/4	103.73	
	Rv1129c-4/4	8.43	
Rv1130(prpD)	Rv1130-1/4	8.44	conserved hypothetical protein
	Rv1130-2/4	136.86	

	Rv1130-3/4	98.29	
	Rv1130-4/4	17.72	
Rv1131(prpC)	Rv1131-2/4	15.67	probable citrate synthase
	Rv1131-3/4	11.72	
	Rv1131-4/4	5.38	
Rv1166(lpqW)	Rv1166-3/5	6.56	probable conserved lipoprotein
BT-Rv1194c&PE13		9.89	rv1194c<tn>rv1195
Rv1194c	Rv1194c-3/4	17.44	conserved hypothetical protein
	Rv1194c-4/4	4.86	
Rv1202(dapE)	Rv1202-1/3	3.40	probable succinyl-diaminopimelate desuccinylase
Rv1231c	Rv1231c-1/2	3.04	probable membrane protein
Rv1250	Rv1250-4/5	7.16	probable integral membrane protein
Rv1315(murA)	Rv1315-4/4	8.38	probable udp-n-acetylglucosamine 1-carboxyvinyltransferase
Rv1339	Rv1339-2/2	16.86	conserved hypothetical protein
Rv1344	Rv1344-1/1	3.13	probable acyl carrier protein
Rv1348	Rv1348-7/8	6.96	probable abc transporter
Rv1349	Rv1349-1/5	3.42	probable abc transporter
Rv1415(ribA2)	Rv1415-3/4	5.40	riboflavin biosynthesis protein
Rv1430(PE16)	Rv1430-4/5	5.21	pe family protein
Rv1432	Rv1432-1/4	3.83	probable dehydrogenase
Rv1469(ctpD)	Rv1469-3/5	3.21	probable cation transporter
Rv1530(adh)	Rv1530-2/3	3.40	probable alcohol dehydrogenase adh
Rv1562c(treZ)	Rv1562c-1/5	7.03	maltooligosyltrehalose trehalohydrolase
Rv1609(trpE)	Rv1609-1/4	7.34	probable anthranilate synthase component
Rv1640(lysX)	Rv1640c-4/10	4.31	possible lysyl-trna synthetase 2
	Rv1640c-5/10	3.92	
	Rv1640c-7/10	3.27	
Rv1647	Rv1647-2/2	5.94	conserved hypothetical protein
Rv1699(pyrG)	Rv1699-5/5	3.07	probable ctp synthase
Rv1890c	Rv1890c-1/2	3.03	hypothetical protein
Rv1896c	Rv1896c-1/2	3.17	conserved hypothetical protein
Rv1941	Rv1941-2/2	5.01	probable short-chain type dehydrogenase/reductase
Rv1992c(ctpG)	Rv1992c-5/7	3.62	probable metal cation transporter
Rv2071c(cobM)	Rv2071c-1/2	7.01	probable precorrin-4 c11-methyltransferase
BT-0000&prcA		7.44	rv2108>tn<rv2109c
Rv2156c(murX)	Rv2156c-1/4	10.53	probable phospho-n-acetylmuramoyl -pentappeptidetransferase murx
Rv2173(idsA2)	Rv2173-3/3	3.16	probable geranylgeranyl pyrophosphate synthetase
Rv2191	Rv2191-4/6	9.73	conserved hypothetical protein
Rv2225(panB)	Rv2225-1/2	3.34	probable 3-methyl-2-oxobutanoate hydroxymethyltransferase
Rv2238c(ahpE)	Rv2238c-1/1	14.57	probable peroxiredoxin
Rv2351c(plcA)	Rv2351c-2/5	3.34	probable phospholipase c 1
Rv2383c(mbtB)	Rv2383c-9/12	16.34	phenyloxazoline synthase
Rv2482c(plsB2)	Rv2482c-7/7	3.28	probable glycerol-3-phosphate acyltransferase
Rv2483c(plsC)	Rv2483c-1/5	4.00	possible transmembrane phospholipid
	Rv2483c-3/5	3.51	biosynthesis enzyme

	Rv2483c-5/5	4.25	
BT-Rv2506&Rv2507		30.90	tn>rv2507
Rv2507	Rv2507-2/2	5.24	conserved pro rich membrane protein
Rv2559c	Rv2559c-3/4	6.06	conserved hypothetical protein
Rv2586c(secF)	Rv2586c-4/4	3.16	protein-export membrane protein
BT-Rv2596&Rv2597		6.95	tn>rv2597 : bt-rv2596&rv2597
Rv2634c(PE_PGRS46)	Rv2634c-2/7	4.15	pe-pgrs family protein
Rv2677c(hemY)	Rv2677c-3/4	3.54	probable protoporphyrindogen oxidase
Rv2682c(dxs1)	Rv2682c-1/6	8.10	probable 1-deoxy-d-xylulose 5-phosphate synthase
BT-ppgK&sigA		3.20	tn>rv2703 : bt-ppgk&siga
Rv2727c(miaA)	Rv2727c-2/2	6.08	probable trna delta(2) -isopentenylpyrophosphate transferase
Rv2841c(nusA)	Rv2841c-2/3	3.38	probable n utilization protein a
Rv2903c(lepB)	Rv2903c-3/3	3.36	probable signal peptidase i
Rv2948c(fadD22)	Rv2948c-2/6	3.42	probable fatty-acid-coa ligase
Rv2969c	Rv2969c-1/2	15.70	possible conserved membrane
Rv3003c(ilvB1)	Rv3003c-1/5	3.65	probable acetolactate synthase
Rv3005c	Rv3005c-1/2	4.27	conserved hypothetical protein
	Rv3005c-2/2	4.25	
Rv3051c(nrdE)	Rv3051c-3/6	6.08	ribonucleoside-di-p reductase
Rv3091	Rv3091-2/5	4.41	conserved hypothetical protein
Rv3222c	Rv3222c-1/1	4.53	conserved hypothetical protein
Rv3311	Rv3311-1/3	3.33	conserved hypothetical protein
Rv3388(PE_PGRS52)	Rv3388-6/7	7.25	pe-pgrs family protein
Rv3394c	Rv3394c-1/4	3.01	conserved hypothetical protein
Rv3494c(mce4F)	Rv3494c-4/5	7.77	mce-family protein
Rv3624c(hpt)	Rv3624c-1/2	3.57	hypoxanthine-guanine phosphoribosyltransferase
BT-Rv3660c&Rv3661		5.70	rv3660c<tn>rv3661 : bt-rv3660c&rv3661
Rv3667(acs)	Rv3667-2/6	3.77	acetyl-coenzyme a synthetase
	Rv3667-3/6	17.69	
	Rv3667-5/6	4.10	
Rv3703c	Rv3703c-2/4	9.15	conserved hypothetical protein
Rv3710(leuA)	Rv3710-4/6	3.12	2-isopropylmalate synthase
Rv3723	Rv3723-1/2	4.54	conserved transmembrane protein
Rv3728	Rv3728-5/9	3.57	probable conserved membrane protein
Rv3752c	Rv3752c-1/2	39.72	possible cytidine/deoxycytidylate deaminase
Rv3860	Rv3860-4/4	17.18	conserved hypothetical protein
Rv3865	Rv3865-1/1	67.73	conserved hypothetical protein
Rv3913(trxB2)	Rv3913-2/3	3.26	probable thioredoxin reductase

List of genes that are over-represented by TraSH analysis in the stearic acid rescue screen. All genes have >3 fold over representation in the pool of stearic acid and propionate screen condition with a *P*-value <0.05.

Table 3.5 Under represented mutants only in palmitic acid TraSH

Gene	probe-ID	Fold	Function
Rv0791c	Rv0791c-1/3	-8.17	conserved hypothetical protein
atsD	Rv0663-5/7	-6.66	possible arylsulfatase atsd
Rv0161	Rv0161-4/4	-6.39	possible oxidoreductase
alkA	Rv1317c-1/5	-5.48	probable ada regulatory protein alka
gabD2	Rv1731-3/4	-5.20	succinate-semialdehyde dehydrogenase
pbpA	Rv0016c-4/4	-5.18	probable penicillin-binding protein pbpa
Rv1813c	Rv1813c-1/1	-5.07	conserved hypothetical protein
bglS	Rv0186-2/6	-4.97	probable beta-glucosidase bgls
Rv1501	Rv1501-2/3	-4.89	conserved hypothetical protein
dacB1	Rv3330-2/3	-4.77	probable penicillin-binding protein dacb1
Rv1730c	Rv1730c-1/5	-4.73	possible penicillin-binding protein
Rv1366	Rv1366-2/2	-4.51	hypothetical protein
Rv0988	Rv0988-2/3	-4.49	possible conserved exported protein
Rv1823	Rv1823-2/3	-4.47	conserved hypothetical protein
pip	Rv0840c-2/3	-4.45	probable proline iminopeptidase pip
Rv2095c	Rv2095c-3/3	-4.43	conserved hypothetical protein
Rv0141c	Rv0141c-1/2	-4.30	hypothetical protein
Rv2949c	Rv2949c-2/2	-4.28	conserved hypothetical protein
Rv0100	Rv0100-1/1	-4.26	conserved hypothetical protein
Rv1771	Rv1771-1/3	-4.18	l-gulono-1,4-lactone dehydrogenase
devR	Rv3133c-2/2	-4.14	two component transcriptional regulator
Rv0127	Rv0127-4/4	-4.02	conserved hypothetical protein

List of genes that are under-represented by TraSH analysis in the stearic acid rescue screen. All genes have >4 fold under representation in the pool of stearic acid and propionate screen condition with a *P*-value <0.01.

Table 3.6 Over representors only in palmitic acid TraSH

Synonym	probe-ID	Fold	Function
dxs1	Rv2682c-1/6	81.93	p1-deoxy-d-xylulose 5-phosphate synthase
folB	Rv3607c-1/1	41.22	probable dihydroneopterin aldolase
fadE24	Rv3139-3/4	39.90	probable acyl-coa dehydrogenase
Rv1856c	Rv1856c-2/2	36.55	possible oxidoreductase
Rv3055	Rv3055-1/1	32.11	possible transcriptional regulator
Rv1444c	Rv1444c-2/2	30.48	hypothetical protein
icd1	Rv3339c-3/4	27.21	probable isocitrate dehydrogenase
hycD	Rv0084-1/3	26.69	possible formate hydrogenlyase hycd
Rv2603c	Rv2603c-1/2	25.25	highly conserved hypothetical protein
asd	Rv3708c-2/3	20.76	aspartate-semialdehyde dehydrogenase
efpA	Rv2846c-2/5	20.55	possible integral membrane efflux protein
pks12	Rv2048c-6/36	19.61	probable polyketide synthase pks12
	Rv2048c-12/36	8.21	
	Rv2048c-27/36	7.98	
	Rv2048c-26/36	3.90	
	Rv2048c-1/36	3.27	
yrbE1A	Rv0167-1/2	19.08	conserved integral membrane protein
dfp	Rv1391-3/4	17.84	flavoprotein homolog dfp
Rv2305	Rv2305-4/4	17.50	hypothetical protein
hemL	Rv0524-3/4	16.39	glutamate-1-semialdehyde 2,1-aminomutase
mce4A	Rv3499c-2/3	16.06	mce-family protein mce4a
echA7	Rv0971c-2/3	15.43	probable enoyl-coa hydratase echa7
Rv3015c	Rv3015c-1/3	15.33	conserved hypothetical protein
Rv0452	Rv0452-1/3	13.71	possible transcriptional regulator
Rv1125	Rv1125-3/4	13.25	conserved hypothetical protein
Rv2747	Rv2747-2/2	13.24	gcn5-related n-acetyltransferase
sodA	Rv3846-1/2	13.09	superoxide dismutase]
Rv0897c	Rv0897c-1/5	13.00	probable oxidoreductase
mycP5	Rv1796-1/5	12.92	probable membrane-anchored mycosin
Rv3603c	Rv3603c-1/3	12.20	conserved ala and leu rich protein
Rv2060	Rv2060-2/2	12.19	conserved integral membrane protein
Rv0064	Rv0064-8/8	12.14	conserved transmembrane protein
Rv1779c	Rv1779c-2/5	12.06	hypothetical integral membrane protein
cyp126	Rv0778-3/4	11.91	possible cytochrome p450 126 cyp126
bpoA	Rv3473c-2/2	11.80	possible peroxidase
Rv2413c	Rv2413c-1/3	11.59	conserved hypothetical protein
pckA	Rv0211-4/5	11.46	phosphoenolpyruvate carboxykinase
PPE6	Rv0305c-8/8	11.24	ppe family protein
Rv2778c	Rv2778c-1/1	10.75	conserved hypothetical protein
mce2D	Rv0592-5/5	10.52	mce-family protein mce2d

List of genes that are under-represented by TraSH analysis in the stearic acid rescue screen. All genes have >10 fold under representation in the pool of stearic acid and propionate screen condition with a *P*-value <0.01.

Table 3.7 Under representors only in acetate TraSH

Synonym	probe-ID	Fold	Function
Rv3083	Rv3083-4/5	-9.04	probable monooxygenase
Rv1639c	Rv1639c-2/4	-7.38	conserved hypothetical membrane protein
fadD31	Rv1925-3/5	-7.12	probable acyl-coa ligase
mutT2	Rv1160-2/2	-6.99	probable mutator protein mutt
Rv2568c	Rv2568c-3/3	-6.54	conserved hypothetical protein
Rv2716	Rv2716-1/2	-6.30	conserved hypothetical protein
Rv0110	Rv0110-2/2	-6.27	conserved integral membrane protein
Rv2030c	Rv2030c-3/5	-6.20	conserved hypothetical protein
lprJ	Rv1690-2/2	-6.07	probable lipoprotein
menC	Rv0553-3/3	-5.42	probable muconate cycloisomerase
fadE34	Rv3573c-2/6	-5.17	probable acyl-coa dehydrogenase
Rv3228	Rv3228-2/3	-5.00	conserved hypothetical protein
Rv3161c	Rv3161c-2/3	-4.96	possible dioxygenase
Rv1998c	Rv1998c-1/2	-4.72	conserved hypothetical protein
Rv3727	Rv3727-5/5	-4.67	possible oxidoreductase
Rv1957	Rv1957-1/1	-4.65	hypothetical protein
Rv1496	Rv1496-1/3	-4.56	possible transport system kinase
moeB2	Rv3116-3/4	-4.26	molybdenum cofactor biosynthesis protein
Rv2751	Rv2751-1/2	-4.22	conserved hypothetical protein
Rv1112	Rv1112-3/3	-4.17	probable gtp binding protein
Rv0919	Rv0919-2/2	-4.16	gcn5-related n-acetyltransferase
PE31	Rv3477-1/1	-4.10	pe family protein
mshB	Rv1170-2/2	-4.07	glcnac-ins deacetylase
Rv3114	Rv3114-1/1	-4.06	conserved hypothetical protein
cyp139	Rv1666c-1/4	-4.02	probable cytochrome p450 139
Rv0195	Rv0195-1/2	-4.02	possible two component transcriptional regulator

List of genes that are over-represented by TraSH analysis in the stearic acid rescue screen. All genes have >4 fold over representation in the pool of stearic acid and propionate screen condition with a *P*-value <0.01.

Table 3.8 Over representors only in acetate TraSH

Synonym	probe-ID	Fold	Function
Rv2015c	Rv2015c-1/3	22.30	conserved hypothetical protein
Rv1371	Rv1371-1/4	14.22	probable conserved membrane protein
narX	Rv1736c-5/5	12.66	probable nitrate reductase narx
Rv2186c	Rv2186c-1/1	11.99	conserved hypothetical protein
katG	Rv1908c-2/7	9.60	catalase-peroxidase-peroxynitritase t katg
Rv1819c	Rv1819c-5/6	7.42	probable atp-binding protein abc transporter
lldD1	Rv0694-3/4	6.73	possible l-lactate dehydrogenase
senX3	Rv0490-2/3	6.50	putative two component sensor histidine kinase
Rv0998	Rv0998-3/3	5.84	conserved hypothetical protein
Rv2978c	Rv2978c-4/4	5.33	probable transposase
lppH	Rv3576-2/2	5.28	possible conserved lipoprotein lpph
Rv2030c	Rv2030c-4/5	4.76	conserved hypothetical protein
cysQ	Rv2131c-3/3	4.55	possible monophosphatase cysq
Rv3629c	Rv3629c-2/3	4.43	conserved integral membrane protein
Rv0688	Rv0688-3/3	4.10	putative ferredoxin reductase
Rv0955	Rv0955-4/4	3.92	conserved integral membrane protein
PE_PGRS22	Rv1091-7/7	3.71	pe-pgrs family protein
tgs1	Rv3130c-3/4	3.64	Triacylglycerol synthase
Rv0906	Rv0906-2/3	3.48	conserved hypothetical protein
Rv3134c	Rv3134c-1/3	3.45	conserved hypothetical protein
Rv0431	Rv0431-1/1	3.44	putative tuberculin related peptide
lgt	Rv1614-4/4	3.36	possible prolipoprotein diacylglyceryl transferases
PPE60	Rv3478-2/4	3.27	pe family protein
Rv2910c	Rv2910c-2/2	3.17	conserved hypothetical protein
Rv0540	Rv0540-1/2	3.07	conserved hypothetical protein

List of genes that are over-represented by TraSH analysis in the stearic acid rescue screen. All genes have >3 fold over representation in the pool of stearic acid and propionate screen condition with a *P*-value <0.01. Genes listed in red are related to propionate metabolism.

3. 5 References

1. Peyron, P., et al., *Foamy macrophages from tuberculous patients' granulomas constitute a nutrient-rich reservoir for M. tuberculosis persistence.* PLoS Pathog, 2008. **4**(11): p. e1000204.
2. Schnappinger, D., et al., *Transcriptional Adaptation of Mycobacterium tuberculosis within Macrophages: Insights into the Phagosomal Environment.* J Exp Med, 2003. **198**(5): p. 693-704.
3. Sacchettini, J.C., E.J. Rubin, and J.S. Freundlich, *Drugs versus bugs: in pursuit of the persistent predator Mycobacterium tuberculosis.* Nat Rev Microbiol, 2008. **6**(1): p. 41-52.
4. Koul, A., et al., *The challenge of new drug discovery for tuberculosis.* Nature, 2011. **469**(7331): p. 483-90.
5. Marrero, J., et al., *Gluconeogenic carbon flow of tricarboxylic acid cycle intermediates is critical for Mycobacterium tuberculosis to establish and maintain infection.* Proc Natl Acad Sci U S A, 2010. **107**(21): p. 9819-24.
6. McKinney, J.D., et al., *Persistence of Mycobacterium tuberculosis in macrophages and mice requires the glyoxylate shunt enzyme isocitrate lyase.* Nature, 2000. **406**(6797): p. 735-8.
7. Russell, D.G., C.E. Barry, 3rd, and J.L. Flynn, *Tuberculosis: what we don't know can, and does, hurt us.* Science, 2010. **328**(5980): p. 852-6.
8. Shi, L., et al., *Carbon flux rerouting during Mycobacterium tuberculosis growth arrest.* Mol Microbiol, 2010. **78**(5): p. 1199-215.

9. Rohde, K.H., R.B. Abramovitch, and D.G. Russell, *Mycobacterium tuberculosis invasion of macrophages: linking bacterial gene expression to environmental cues.* Cell Host Microbe, 2007. **2**(5): p. 352-64.

10. Rohde, K.H., et al., *Linking the transcriptional profiles and the physiological states of Mycobacterium tuberculosis during an extended intracellular infection.* PLoS Pathog, 2012. **8**(6): p. e1002769.

11. Wilson, M., et al., *Exploring drug-induced alterations in gene expression in Mycobacterium tuberculosis by microarray hybridization.* Proc Natl Acad Sci U S A, 1999. **96**(22): p. 12833-8.

12. Sassetti, C. and E.J. Rubin, *Genomic analyses of microbial virulence.* Curr Opin Microbiol, 2002. **5**(1): p. 27-32.

13. van Opijnen, T. and A. Camilli, *Transposon insertion sequencing: a new tool for systems-level analysis of microorganisms.* Nat Rev Microbiol, 2013. **11**(7): p. 435-42.

14. Mei, J.M., et al., *Identification of Staphylococcus aureus virulence genes in a murine model of bacteraemia using signature-tagged mutagenesis.* Mol Microbiol, 1997. **26**(2): p. 399-407.

15. Griffin, J.E., et al., *High-resolution phenotypic profiling defines genes essential for mycobacterial growth and cholesterol catabolism.* PLoS Pathog, 2011. **7**(9): p. e1002251.

16. Sassetti, C.M., D.H. Boyd, and E.J. Rubin, *Comprehensive identification of conditionally essential genes in mycobacteria.* Proc Natl Acad Sci U S A, 2001. **98**(22): p. 12712-7.

17. Sassetti, C.M., D.H. Boyd, and E.J. Rubin, *Genes required for mycobacterial growth defined by high density mutagenesis.* Mol Microbiol, 2003. **48**(1): p. 77-84.

18. Sassetti, C.M. and E.J. Rubin, *Genetic requirements for mycobacterial survival during infection.* Proc Natl Acad Sci U S A, 2003. **100**(22): p. 12989-94.

19. Kim, M.J., et al., *Caseation of human tuberculosis granulomas correlates with elevated host lipid metabolism.* EMBO Mol Med, 2010. **2**(7): p. 258-74.

20. Rousseau, C., et al., *Virulence attenuation of two Mas-like polyketide synthase mutants of Mycobacterium tuberculosis.* Microbiology, 2003. **149**(Pt 7): p. 1837-47.

21. Abramovitch, R.B., et al., *aprABC: a Mycobacterium tuberculosis complex-specific locus that modulates pH-driven adaptation to the macrophage phagosome.* Mol Microbiol, 2011. **80**(3): p. 678-94.

22. Gonzalo-Asensio, J., et al., *PhoP: a missing piece in the intricate puzzle of Mycobacterium tuberculosis virulence.* PLoS One, 2008. **3**(10): p. e3496.

23. Rocco, C.J. and J.C. Escalante-Semerena, *In Salmonella enterica, 2-methylcitrate blocks gluconeogenesis.* J Bacteriol, 2010. **192**(3): p. 771-8.

24. Venugopal, A., et al., *Virulence of Mycobacterium tuberculosis depends on lipoamide dehydrogenase, a member of three multienzyme complexes.* Cell Host Microbe, 2011. **9**(1): p. 21-31.

25. Cole, S.T., et al., *Deciphering the biology of Mycobacterium tuberculosis from the complete genome sequence.* Nature, 1998. **393**(6685): p. 537-44.

26. Krithika, R., et al., *A genetic locus required for iron acquisition in Mycobacterium tuberculosis.* Proc Natl Acad Sci U S A, 2006. **103**(7): p. 2069-74.

27. Maloney, E., et al., *Alterations in phospholipid catabolism in Mycobacterium tuberculosis lysX mutant.* Front Microbiol, 2011. **2**: p. 19.

28. Bhatt, A., et al., *The Mycobacterium tuberculosis FAS-II condensing enzymes: their role in mycolic acid biosynthesis, acid-fastness, pathogenesis and in future drug development.* Mol Microbiol, 2007. **64**(6): p. 1442-54.

29. Minnikin, D.E., et al., *The methyl-branched fortifications of Mycobacterium tuberculosis.* Chem Biol, 2002. **9**(5): p. 545-53.

CHAPTER FOUR

Using the lipid droplet-loaded macrophages to elucidate propionyl-CoA assimilation during intracellular infection

Adapted from

Intracellular *Mycobacterium tuberculosis* exploits host-derived fatty acids to limit metabolic stress. Lee W, VanderVen BC, Fahey RJ, Russell DG. J Biol Chem. 2013 Mar 8; 288(10):6788-800

Infection of macrophages with *Mycobacterium tuberculosis* induces global modifications to phagosomal function. Podinovskaia M, Lee W, Caldwell S, Russell DG. Cell Microbiol. 2013 Jun; 15(6):843-59.

ABSTRACT

M. tuberculosis infection leads to the alternation of host lipid metabolism, and in the macrophage, one key change is the induction of foam cell formation by retention of fatty acids in intracellular lipid bodies. This lipid-rich host cell likely provides a privileged environment for *M. tuberculosis* and facilitates acquisition of fatty acids by the bacterium. In this work, we demonstrate that the induction of oleate-containing lipid droplets in macrophages rescued the growth of an *M. tuberculosis Δicl1* mutant. Metabolic labeling of macrophages with radioactive fatty acids revealed that *M. tuberculosis* inside the oleate loaded macrophage exploits fatty acids derived from host to synthesize the cell wall lipids of the bacterium. Monitoring the lipid droplet we observed the metabolic interplay between the host cells and *M. tuberculosis* whereby mycobacterial infection causes retention of lipid droplets in infected versus uninfected macrophages. These data provide further confirmation that a significant stress from propionyl-CoA for *M. tuberculosis* inside host cells can be relieved by the routing of propionyl-CoA into the cell wall lipids of the bacterium, and suggests that a balanced lipid diet from the host cell is important to intracellular fitness and growth of *M. tuberculosis*.

4.1 Introduction

Macrophages filled with lipid bodies, called foamy macrophages, are found in granulomas in human patients as well as macrophage infection in culture, and the tight interplay between *Mycobacterium tuberculosis* and the foamy macrophage has been noted previously [1-4]. Recent studies showed the tight apposition of the *M. tuberculosis*-containing phagosome to the lipid bodies [5]. This suggests that *M. tuberculosis* has access to host lipids, in the form of lipid bodies. Moreover, it has been shown that utilization of the triacylglycerol from the foamy macrophage resulted in up-regulation of genes associated with dormancy, and that this re-programing allowed intracellular *M. tuberculosis* to develop resistance against antibiotics such as isoniazid and rifampicin [6].

Therefore, foamy macrophages provide a nutrient reservoir and play important roles in growth and persistence of *M. tuberculosis* in the host. The accumulation or sequestration of host lipids and their utilization by *M. tuberculosis* is part of the metabolic re-programing of the host cell that has been documented both in cell culture models and in human tuberculosis granulomas [5-8].

M. tuberculosis mutants defective in cholesterol utilization or in the expression of ICL1 exhibit reduced survival in macrophages and mice, and this defect is exacerbated further by activation of the host macrophages or the development of an effective immune response [9-11]. The similarity in phenotype between *M. tuberculosis* mutants defective in cholesterol utilization and mutants defective in expression of ICL1 is intriguing because it could result from related metabolic defects. *M. tuberculosis* mutants defective in utilization of cholesterol will starve if dependent

on the sterol as a carbon source, whereas mutants defective in ICL1 expression will be vulnerable to propionate toxicity should they metabolize cholesterol.

In Chapters 2 and 3, we showed that long chain fatty acids rescued the *Δicl* mutant from propionyl-CoA toxicity by facilitating methyl-branched lipid synthesis *in vitro* culture. Recently, Daniel and colleagues reported that intracellular *M. tuberculosis* can access and metabolize fatty acids from lipid droplet stores in their host cell [6]. This key observation suggests that it is feasible to establish whether or not *M. tuberculosis* experiences propionyl-CoA toxicity under the physiological conditions within its host cell and whether the bacterium manipulates the host lipid stores to provide metabolic rescue.

In this current study we manipulated the formation of lipid bodies in macrophages to elucidate the metabolic shift in *M. tuberculosis* in response to host-lipid derived stresses. We demonstrate that *M. tuberculosis* faces a significant amount of propionyl-CoA during macrophage infection, and that through biochemical rescue, *M. tuberculosis* can access and metabolize the lipid stores in its host cell to shunt propionyl-CoA through favored, non-intoxicating routes of degradation or synthesis. Moreover, we demonstrate the tight interplay between the lipid metabolism of both host and pathogen during tuberculosis infection. Consistent with this result is the finding in the earlier chapters (Chapter 2 and 3). Our results provide mechanistic insights that the pathways of lipid degradation and cell wall synthesis play a critical role in the modulation of the relative levels of 3-carbon intermediates, propionyl-CoA and that this regulation is critical to the survival of intracellular *M. tuberculosis*.

4.2 MATERIAL and METHODS

Bacterial strains and culture conditions

M. tuberculosis and *M. bovis* strains were maintained in Middlebrook 7H9 medium supplemented with 0.2% glycerol, 10% OADC and 0.05% tyloxapol. Kanamycin (20 μg/ml) or hygromycin (50 μg/ml) were used where necessary. All chemicals were purchased from Sigma unless otherwise stated.

Mutant Strains

To quantify survival of *M. tuberculosis* and *M. bovis* strains in macrophage infection experiments we transformed the relevant H37Rv and BCG strains with pVV16-*smyc'::mCherry* expressing the fluorescent protein mCherry driven by the *smyc* promoter [12].

Metabolic Labeling and Lipid Analysis

Metabolic radiolabeling of mycobacterial cell wall lipids were performed as described [12]. For intracellular labeling, lipid droplets were induced in macrophages ($2x10^8$) by addition of 400 μM oleate and 20 μCi of [1-^{14}C] oleic acid, 20μCi [1 ^{14}C] stearic acid, or [1-^{14}C] sodium propionate for 24 hours as described. The cells were washed and infected either *Δicl1* or Erdman (MOI=10:1) for 4 hours at 37°C. After 4 days,

macrophages were washed and harvested in PBS. Lipids from intracellular *M. tuberculosis* lipids were isolated as detailed by Singh et al [13] whereby infected macrophages were washed twice with PBS, followed by methanol wash to remove lipids derived from macrophage. Mycobacterial lipids were then extracted with $CHCl_3/CH_3OH$ (2:1 v/v) for 48 hrs. The organic phase was collected, washed twice with water and dried (Folch wash). The total lipids were resuspended in $CHCl_3/CH_3OH$ (2:1 v/v), and ^{14}C incorporation was determined by a Scintillation Counter.

TLC analysis

To analyze lipid species we used 100, 000 counts per minute of the sample at TLC plates (10cm x 10cm silica gel 60 aluminum sheets). The TLC was developed with petroleum ether: ethyl acetate (98:2, v/v) solvent system, and followed by exposing to a phosphor screen and scanning by using a Storm Imager to detect and quantify the radiolabeled lipids.

Lipid Droplet Induction and Macrophage Infection

C57BL/6 mouse bone marrow-derived macrophages were cultured in DMEM containing 15% L929-conditioned medium, 10% fetal bovine serum, and 2 mM glutamate for 7 days. Lipid droplet induction was preformed as described [14]. Briefly, 400 μM oleate, conjugated to de-fatted BSA (1:5), was added to the macrophage

medium. To monitor lipid droplet formation, these macrophages were transferred to 24 wells containing sterile cover slips and incubated up to 5 days in the presence of 400 μM oleate.

To assess the impact of lipid droplet formation on the survival of the *Δicl1* mutant, lipid droplets were induced in macrophages by incubation with 400 μM oleate for 24 hrs prior to infecting the cells with *Δicl1* (MOI=10) for 4 hours at 37°C. The cultures were washed extensively and the intracellular bacterial load was assessed over a period of 8-9 days. The bacterial load was quantified either by lysing the macrophages, plating the lysate on Middlebook 7H10 medium supplemented with 0.2% glycerol, 10% OADC, and counting cfus. Or, alternatively, the infection was performed in 96 well plates at comparable MOI with *Δicl1* (*smyc`::mCherry*), and the mCherry fluorescence was measured by a Perkin-Elmer EnVision plate reader over a period of 9 days. Cultures were manipulated through the addition of Vitamin B12 to 50 μg/ml and maintained throughout the infection.

Confocal microscopy

Macrophages were washed with PBS twice and fixed with 4% parpformaldehyde in PBS for 30min at room temperature, followed by staining with a 1μg/ml BODIPY 493/503 (Invitrogen) dissolved in 150mM NaCl. After 10min incubation at room temperature, cells were washed with PBS twice and mounted in ProLong Gold Antifade Reagent (Molecular Probes). Images were obtained by using Leica TCS SP5

Confocal laser scanning microscople (Leica Microsystem) using 63 x oil immersion lens.

4.3 RESULTS and DISCUSSION

4.3.1 Intracellular *M. tuberculosis* can exploit host lipid stores to alleviate propionate-mediated stress.

To determine the physiological significance of propionyl-CoA toxicity during infection, we induced lipid droplet formation in macrophages through the addition of 400 μM oleate to the culture medium [14]. The resultant lipid droplets, detected by BODIPY 493/503, saturated within 1 day of culture (Figure 4.1). These macrophages, and control, untreated macrophages were subsequently infected with the *Δicl1* mutant (containing *smyc'::mCherry*) (MOI=10), and bacterial growth was monitored in parallel by both CFU counts and by the fluorescent signal from mCherry. As reported previously, the growth of the *Δicl1* mutant was severely impaired in the control, untreated macrophages (Figure 4. 2).

In contrast, growth of the *Δicl1* mutant was rescued in the macrophages preloaded with lipid droplets induced by addition of oleate. Moreover, the addition of VitB12, which opens the methylmalonyl pathway of propionyl-CoA processing, to the culture medium was also capable of restoring intracellular growth to the *Δicl1* mutant. The trends were comparable in both the CFU and the fluorescence readouts (Figure 4.2), although the CFU count likely under-estimates bacterial viability due to

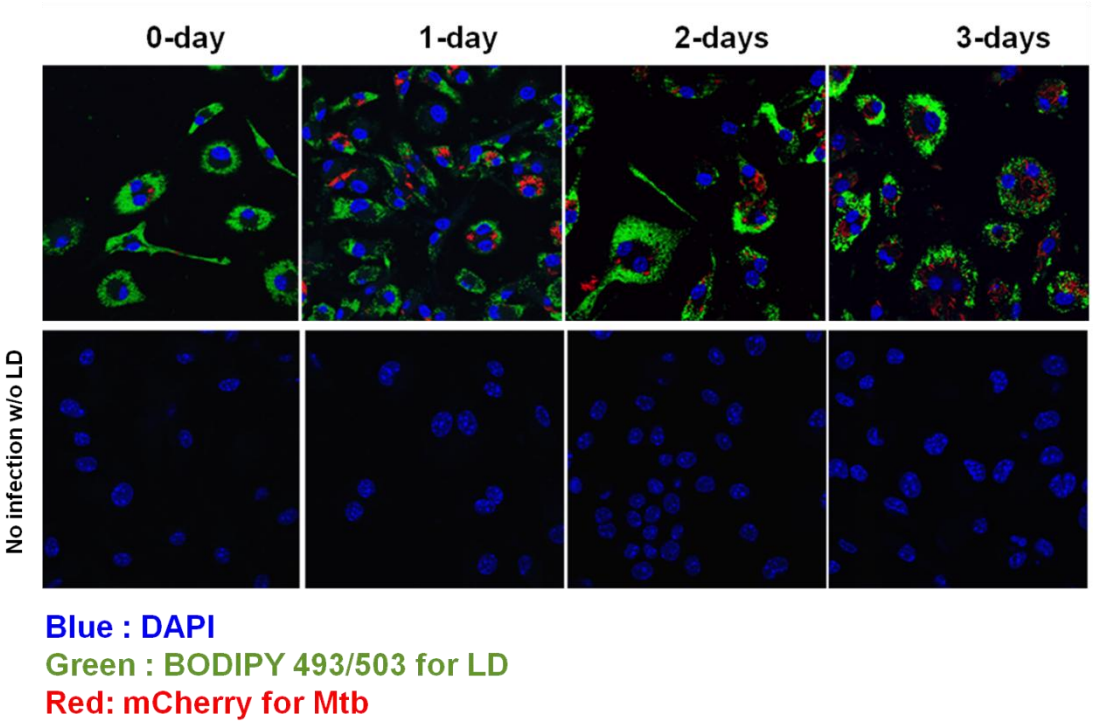

Figure 4.1 Lipid droplet induction in macrophage by addition of oleate. Figure illustrates the induction and persistence of lipids droplets, detected with BODIPY 493/503 (green), *Δicl1* strain expressing pVV16-mCherry (*smyc`::mCherry*) (red), and nuclei (blue) in oleate-loaded macrophages versus untreated macrophages over the duration of the experimental period.

A

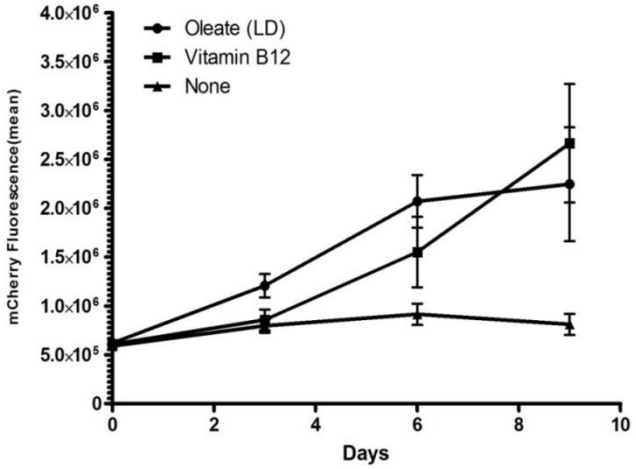
Oleate (LD)
Vitamin B12
None
mCherry Fluorescence(mean)
4.0×10⁶
3.5×10⁶
3.0×10⁶
2.5×10⁶
2.0×10⁶
1.5×10⁶
1.0×10⁶
5.0×10⁵
0
0
2
4
6
8
10
Days

B

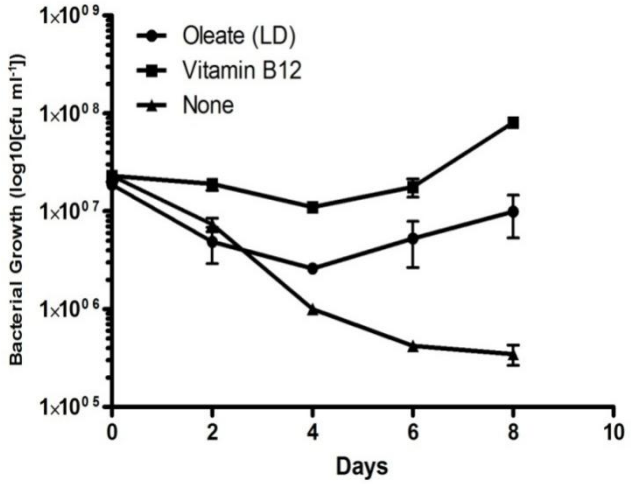
Oleate (LD)
Vitamin B12
None
Bacterial Growth (log10[cfu ml⁻¹])
1×10⁰⁹
1×10⁰⁸
1×10⁰⁷
1×10⁰⁶
1×10⁰⁵
0
2
4
6
8
10
Days

Figure 4.2 Intracellular growth is restored to the *Δicl1* mutant through the induction of oleate-containing lipid droplets in the infected cell. The survival of the *Δicl1* mutant was seriously impaired in macrophages, however, growth could be restored through loading the host cells with oleate, or through the addition of VitB12 to the medium to facilitate operation of the MMP. (A) The CFUs were determined at 2 day intervals for an 8-day period for the *Δicl1* mutant in untreated, control macrophages (triangle), in lipid droplet-containing, oleate-loaded macrophages (circle), and in macrophage supplemented by the addition of VitB12 to the medium (square). Results are representative of three replicates. (B) The experiment was repeated with an *Δicl1* strain expressing pVV16-mCherry (*smyc`::mCherry*) and bacterial survival and growth was determined by measurement of fluorescence. Both methods demonstrated the enhanced growth and survival of the *Δicl1* mutant in the presence of either oleate-induced droplets or Exogenous VitB12. Error bars indicate standard error of the mean from 3 replicates.

stress inflicted during bacterial isolation, while the fluorescence readout probably over-estimates viability due to persistent signal from dying bacteria.

4.3.2 Metabolic labeling of macrophage

In order to demonstrate the incorporation of host-derived fatty acids into PDIM, we metabolically labeled macrophage lipid droplets with ^{14}C-propionate, ^{14}C-oleate, and ^{14}C-stearic acid prior to infection with *M. tuberculosis*. Subsequent analysis of *M. tuberculosis* cell wall lipids post-infection revealed that ^{14}C label from the ^{14}C-propionate, ^{14}C-oleate, and ^{14}C-stearic acid was incorporated into PDIM (Figure 4.3) providing biochemical confirmation of the intracellular growth phenotype shown in Figure 3. These data confirm and extend three issues that are critical to our understanding of the physiology of *M. tuberculosis* within its host macrophage. First, propionyl-CoA metabolism, and the relative balance of 2- and 3-carbon intermediates is a significant problem for *M. tuberculosis* within the environment of the host macrophage. Second, the routing of propionyl-CoA through MM-CoA and into MB cell wall lipids such as PDIM is an important detoxification pathway to intracellular *M. tuberculosis*. And, finally, the balance of lipids in the lipid droplets in the host macrophage may have considerable bearing on the fitness and growth potential of the bacterium within its host cell.

A

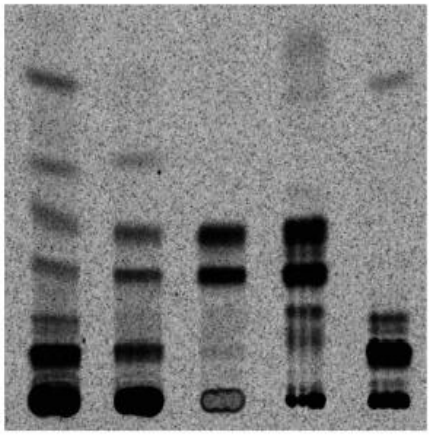

Mtb Erdman in macrophages	+	+	+	-	-
[1 -^{14}C] Oleic acid	+	-	-	-	+
[1 -^{14}C] Stearic acid	-	+	-	-	-
[1- ^{14}C] Propionate	-	-	+	+	-
Macrophage control	-	-	-	-	+
Broth control	-	-	-	+	-

B

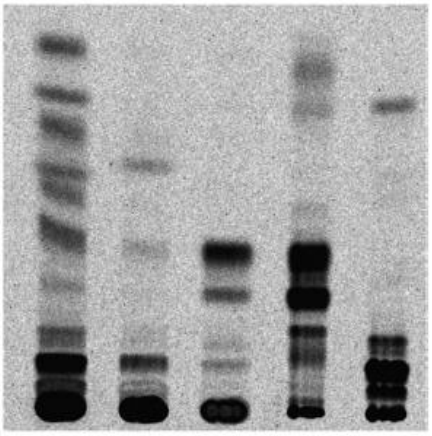

H37Rv Δicl1in macrophages	+	+	+	-	-
[1 -^{14}C] Oleic acid	+	-	-	-	+
[1 -^{14}C] Stearic acid	-	+	-	-	-
[1- ^{14}C] Propionate	-	-	+	+	-
Macrophage control	-	-	-	-	+
Broth control	-	-	-	+	-

Figure 4.3. *M. tuberculosis* inside lipid droplet-loaded macrophage incorporates the host-derived fatty acids into PDIM. Using radio-labeled fatty acid precursors, we demonstrate the incorporation of the fatty acids and propionate into PDIM species in both the wt Erdman (A) and the *Δicl1* mutant (B) strains. Lipid droplets were induced in macrophages with oleic acid containing [1-^{14}C] oleic acid (lane 1), [1-^{14}C] stearic acid (lane 2), or [1-^{14}C] propionate (lane 3) for 24 hours. Then, the lipid-loaded macrophages were infected with either Erdman or H37Rv *Δicl1* at a MOI of 5:1 for 4 hours. At 5 day post infection, *M. tuberculosis* cell wall lipids were extracted from macrophage and analyzed on TLC. The bands labeled correspond to (1) triacylglycerol, (2) phthiocerol A dimycocerate and (3) phthiodiolone dimycocerate. The identity of the PDIM bands had been established previously by mass spectrometry [12]. Control labeling experiments were run with *M. tuberculosis* Erdman grown in broth culture labeled with [1-^{14}C] propionate (lane 4) and macrophages alone labeled with [1-^{14}C] oleic acid (lane 5).

4.3.3 *M. tuberculosis* infection leads to retention of lipids and the maintenance of foamy macrophage phenotype

As noted, lipid droplets in the macrophage also can be induced by infection, by hypoxia, or by feeding high concentration of lipid [6, 15]. Our data suggests that *M. tuberculosis* can exploit the host droplet to relieve metabolic stresses. Then, it is intriguing to consider whether or not the formation of lipid droplet is consequence of decreased turnover of lipids in the infected macrophage. To test this possibility, we decided to monitor lipid droplet retention in macrophage upon *M. tuberculosis* infection. Macrophages were preincubated in macrophage media supplemented with 400 μM oleate conjugated in BSA for 24 h. Subsequently, the macrophages loaded with lipid droplets were infected with either *M. tuberculosis* CDC1551 or *M. bovis* expressing mcherry protein at multiplicity of infection (moi) of 10:1, or incubated without infection. Lipid droplets in macrophages were monitored by treatment with the BODIPY 493/503 prior to imaging by confocal microscope over several days. As observed in Figure 4.4, there was a significant increase in retention of lipid droplet in the macrophages infected *M. tuberculosis*. A marginal retention of the lipid was observed in the infection with *M. bovis*, comparable to that of infection with *M. tuberculosis*. In contrast, uninfected macrophages showed rapid lost of the lipid droplets within 48hrs.

A

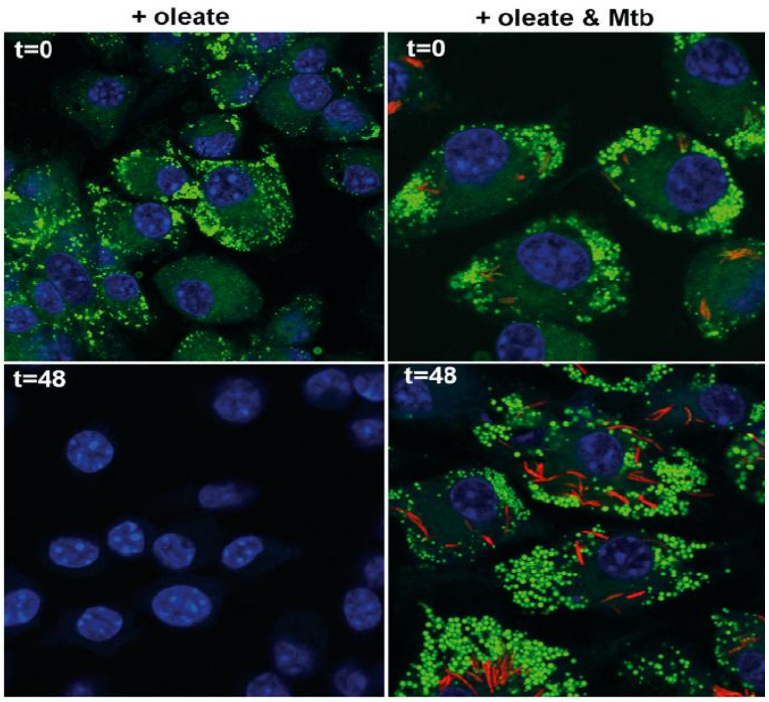

B

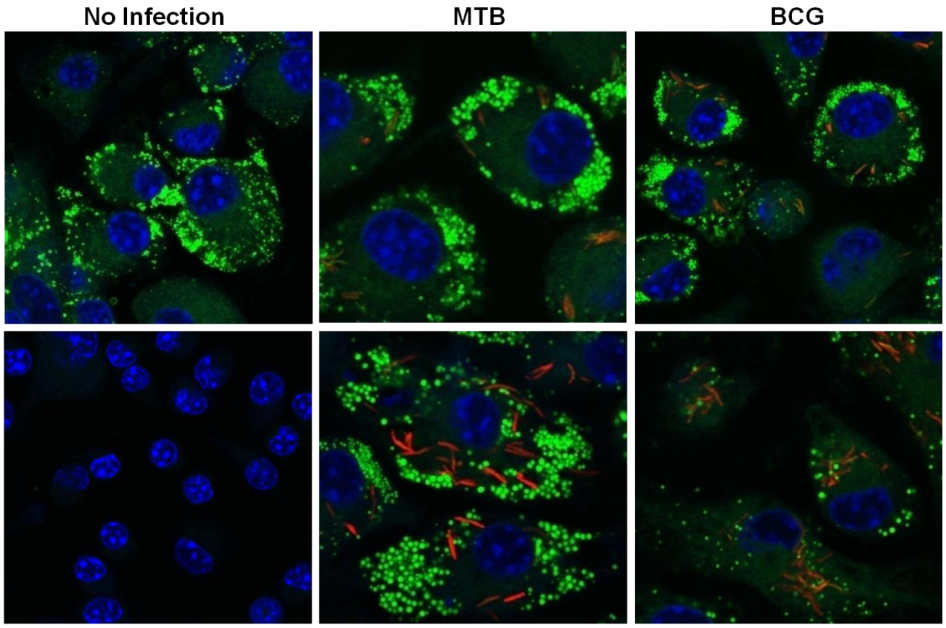

Blue : DAPI Green : BODIPY 493/503 for LD Red: mCherry for Mtb

Figure 4.4 *M. tuberculosis* infection leads to retention of the foamy macrophage phenotype and facilitates bacterial access to host-derived lipids. Murine bone marrow-derived macrophages were induced to form foam cells through incubation with 400 μM oleate for 24 h. The cells were subsequently infected with *M. tuberculosis*, *M. bovis*, or left uninfected. (A) At 0 h and 48 h after infection (t=0 and t=48) cells were fixed and stained with BODIPY 493/503. (B) Retention of lipid bodies by *M. tuberculosis* was compared with that of *M. bovis*. *M. tuberculosis* and *M. bovis* are displayed in red, BODIPY 493/503 is displayed in green and DAPI-stained nuclei are shown in blue. Absence of green stain in uninfected cells at 48 h indicates loss of oleate-induced lipid droplets.

It is unclear if this retention represents a decreased degradation of the droplets through a reduction of phagosomal lipolysis or an increased trafficking of the droplets into the endosome. Nonetheless, these data are significant because such reprogramming in host lipid metabolism may provide a privileged niche for the bacterium in acquisition of nutrients [3, 5, 7, 16]. As noted, *M. tuberculosis* can exploit host lipids to synthesis virulence-associated polyketides, and as a carbon source for growth following reactivation [6, 9, 11, 17]. Moreover, *M. tuberculosis* containing lipid droplets have been postulated to represent a dormant non-replicative stage, which is innately resistant to antibiotics [6]. However, much of this host-pathogen metabolic crosstalk during infection remains to be elucidated.

4.4 Concluding remarks

In macrophage infection, *M. tuberculosis* can access and exploit host lipids in forms of fatty acids from lipid droplets to provide acyl-primers required for the biosynthesis of methyl-branched polyketides. This is significant because the metabolic re-programming that we demonstrated through fatty acid-mediated rescue from propionate toxicity in *in vitro* culture also has validity within a macrophage infection model. These data also suggest that the tight control of the propionyl-CoA pool is critical to growth and persistence of the intracellular *M. tuberculosis,* and that lipid droplets serve as a well-balanced diet for *M. tuberculosis* because they contain a lipid mixture that providew balanced levels of acetyl-CoA and propionyl-CoA. Moreover,

lipid droplet retention in macrophages by *M. tuberculosis* infection provides insight into the metabolic interplay between the host cell and the intercellular bacterium.

Acknowledgment

The authors are grateful to Joo-yong Jung for his help and advice with lipid droplet experiments.

4.5 References

1. Houben, E.N., L. Nguyen, and J. Pieters, *Interaction of pathogenic mycobacteria with the host immune system.* Curr Opin Microbiol, 2006. **9**(1): p. 76-85.
2. Caceres, N., et al., *Evolution of foamy macrophages in the pulmonary granulomas of experimental tuberculosis models.* Tuberculosis (Edinb), 2009. **89**(2): p. 175-82.
3. Russell, D.G., et al., *Foamy macrophages and the progression of the human tuberculosis granuloma.* Nat Immunol, 2009. **10**(9): p. 943-8.
4. Caire-Brandli, I., et al., *Reversible lipid accumulation and associated division arrest of Mycobacterium avium in lipoprotein (VLDL)-induced foamy macrophages may resemble key events during latency and reactivation of tuberculosis.* Infect Immun, 2013.
5. Peyron, P., et al., *Foamy macrophages from tuberculous patients' granulomas constitute a nutrient-rich reservoir for M. tuberculosis persistence.* PLoS Pathog, 2008. **4**(11): p. e1000204.
6. Daniel, J., et al., *Mycobacterium tuberculosis uses host triacylglycerol to accumulate lipid droplets and acquires a dormancy-like phenotype in lipid-loaded macrophages.* PLoS Pathog, 2011. **7**(6): p. e1002093.
7. Kim, M.J., et al., *Caseation of human tuberculosis granulomas correlates with elevated host lipid metabolism.* EMBO Mol Med, 2010. **2**(7): p. 258-74.

8. Podinovskaia, M., et al., *Infection of macrophages with Mycobacterium tuberculosis induces global modifications to phagosomal function.* Cell Microbiol, 2013. **15**(6): p. 843-59.

9. McKinney, J.D., et al., *Persistence of Mycobacterium tuberculosis in macrophages and mice requires the glyoxylate shunt enzyme isocitrate lyase.* Nature, 2000. **406**(6797): p. 735-8.

10. Munoz-Elias, E.J., et al., *Role of the methylcitrate cycle in Mycobacterium tuberculosis metabolism, intracellular growth, and virulence.* Mol Microbiol, 2006. **60**(5): p. 1109-22.

11. Pandey, A.K. and C.M. Sassetti, *Mycobacterial persistence requires the utilization of host cholesterol.* Proc Natl Acad Sci U S A, 2008. **105**(11): p. 4376-80.

12. Abramovitch, R.B., et al., *aprABC: a Mycobacterium tuberculosis complex-specific locus that modulates pH-driven adaptation to the macrophage phagosome.* Mol Microbiol, 2011. **80**(3): p. 678-94.

13. Singh, A., et al., *Mycobacterium tuberculosis WhiB3 maintains redox homeostasis by regulating virulence lipid anabolism to modulate macrophage response.* PLoS Pathog, 2009. **5**(8): p. e1000545.

14. Listenberger, L.L. and D.A. Brown, *Fluorescent detection of lipid droplets and associated proteins.* Curr Protoc Cell Biol, 2007. **Chapter 24**: p. Unit 24 2.

15. Eoh, H. and K.Y. Rhee, *Multifunctional essentiality of succinate metabolism in adaptation to hypoxia in Mycobacterium tuberculosis.* Proc Natl Acad Sci U S A, 2013. **110**(16): p. 6554-9.

16. Singh, V., et al., *Mycobacterium tuberculosis-driven targeted recalibration of macrophage lipid homeostasis promotes the foamy phenotype.* Cell Host Microbe, 2012. **12**(5): p. 669-81.

17. Russell, D.G., et al., *Mycobacterium tuberculosis wears what it eats.* Cell Host Microbe, 2010. **8**(1): p. 68-76.

CHAPTER FIVE

Final discussion

Bacterial infection involves multiple adaptations to the host environments, and these processes play critical roles in mediating the host/pathogen interactions. Such activities include modification of the phagosomal compartments of the host cells, and modulation of the host immune responses. Metabolic realignment of the pathogen in response to the host environment is also an essential adaptation for intracellular survival. In the *M. tuberculosis* infection, in order to persist and replicate in the host cells, the bacterium has adapted its metabolism to the host-derived nutrients and physical conditions, and coordinated its metabolic status with its life cycle. As demonstrated by the requirement of the isocitrate lyase (ICL1) and PhoPR of *M. tuberculosis* for intracellular survival and *in vivo* infection, it has abilities to sense its environment and respond by modulating its cellular processes such as carbon metabolism, cell wall integrity, and energy metabolism.

A large and growing body of literature has emerged on metabolic reprogramming of *M. tuberculosis* during infection and this information is now being applied to define the major intracellular nutrients and the mycobacterial catabolic pathways required to metabolize them. It is well recognized that fatty acids derived from host lipids are dominant and important carbon sources for *M. tuberculosis* during infection, and most of these studies have been devoted to understanding how acquires and processes the nutrients. Relatively little is known regarding the realignment of the metabolic

pathways of *M. tuberculosis* to reduce metabolic stress during utilization of the host lipids. However, it has been shown that *Mycobacterium tuberculosis'* metabolic flexibility allows for increased capacity to survive in host cells. This discussion will reiterate those aspects of the modulation of the carbon flow associated with the utilization of host lipids, and will emphasize those observations made over the course of this study that may serve to guide future research into the coupled metabolism of host and pathogen.

5.1 Metabolic stress during infection

As discussed in chapter 2, *M. tuberculosis* is sensitive to increases in propionyl-CoA, which is a major product of cholesterol catabolism and the bacterium has three pathways to metabolize this intermediate [1, 2]. To verify that a functional methylcitrate cycle is essential for alleviating the increased propionyl-CoA pool, the growth of *Δicl* mutant was monitored in medium with alternative carbon sources. Whereas the growth of wild type H37Rv in medium with glycerol and glucose was unimpaired by the addition of propionate, the growth of the ICL1 mutant was inhibited strongly in the same conditions, suggesting that MCC function to detoxify propionyl-CoA rather than to utilize propionate as a carbon source. Data from carbon supplementation of propionate-containing medium revealed that acetate rescued the propionate toxicity. Additionally, pyruvate was shown to rapidly accumulate upon propionate treatment. These data suggest that propionyl-CoA or its intermediates inhibited pyruvate dehydrogenase as reported in response to propionate by *Aspergillus*

[3] in contrast to *Salmonella* [4, 5]. Together, these observations demonstrate that, despite of absence of a functional MCC, propionate toxicity can be relieved by balancing between 3-carbon (propionyl-CoA) and 2-carbon (Acetyl-CoA) units. Moreover, long chain fatty acids (C4-C24) were shown to rescue propionate toxicity, implying that acetyl-CoA was consumed during detoxification of propionate. Metabolic labeling with ^{14}C-propionate revealed the molecular mechanism for fatty acids rescue from the propionate toxicity. The fatty acids added to the medium functioned as primers for methyl-branched polyketides (such as PDIM), which enabled the bacterium to incorporate excess propionate into the polyketides. *M. tuberculosis* was shown to incorporate long chain fatty acid (stearic acid) into PDIM without catabolic β-oxidation confirming that the fatty acids were utilized as primers and not through degradation and expansion of the acetyl-CoA pool. Together, these findings demonstrate that *M. tuberculosis* PDIM is an important "sink" for the detoxification of propionate, and that the balance between propionyl-CoA and acyl-primers is critical to activate or sustain the flux of propionyl-CoA into PDIM.

As discussed in Chapter 3, the genetic profiling of propionate and stearic acid metabolism by TraSH verified these interpretations. Analysis of the output pool revealed both positive and negative selection of mutants involved in relieving or intensifying propionate-mediated toxicity. The biosynthesis of methyl-branched lipids appears to be required to relieve propionyl-CoA toxicity: PDIM, SL-1, PAT, and DAT. Additionally, in the MCC, the accumulation of all three intermediates, propionyl-CoA, 2-methylcitrate, and 2-methylisocitrate were shown to be toxic to *M. tuberculosis*, which is consistent with observations for propionate toxicity in *Salmonella enterica*

and *Aspergillus nidulans*[4, 5]. Although we found that one key to propionate toxicity seems to be an inhibition of PDH by propionyl-CoA, perhaps, 2-methylcitrate and 2-methylisocitrate could be toxic to *M. tuberculosis* as shown in a *Salmonella* model where these intermediates inhibit fructose 1,6 bisphosphatase (FBP). However, as shown in Figure 2. 3, glucose was unable to rescue *Δicl* mutant from propionate toxicity suggesting that these intermediate of MCC are unlikely to inhibit any enzymes involved in gluconeogenesis including FBP. Alternatively, these toxic intermediates may inhibit one of three components of PDH complex. Additionally, the TraSH data revealed both known genes and novel pathways that control propionate metabolism and generation of acyl-primers for the synthesis of mycobacterial lipids. Moreover, mutants of a transcriptional regulator, PhoP were shown to be enriched in the selection, which further validates our model because a *phoP* mutant was shown to exhibit enhanced production of PDIM [6, 7]. Lastly, the TraSH data also identified a regulator, Rv1626, which may involve in a coordinated interplay between the MCC, MMP, and methyl-branched lipid synthesis.

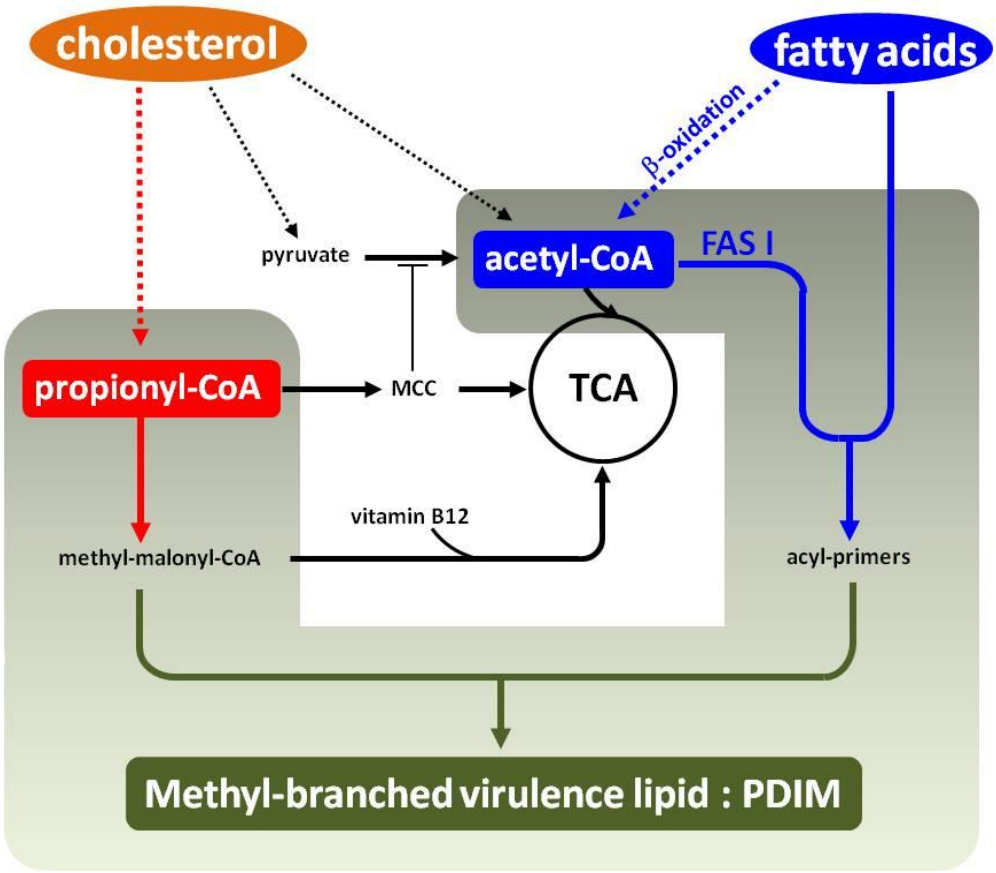

Figure 5.1 The model of assimilation of host lipids and fatty acids into methyl-branched *M. tuberculosis* virulence Lipids. *M. tuberculosis* has access to both cholesterol and fatty acids from the intracellular stores of its host macrophage. Degradation of cholesterol expands the propionyl-CoA pool, which is thought deleterious to the generation of acetyl-CoA from pyruvate through the activity of PDH. This places more pressure on the acetyl-CoA pool, which may be utilized for the generation of malonyl-CoA primers used in the assembly of *M. tuberculosis* cell wall lipids. These MB cell wall lipids can be built from primers generated from either acetyl-CoA or from pre-formed long chain fatty acids imported by the bacterium. The balance of these 2- and 3-carbon intermediates is clearly critical to the growth of *M. tuberculosis*, and its success within its host cell environment.

As discussed in chapter 4, this metabolic process to relieve the propionate stress was also observed in *M. tuberculosis* infected in macrophages loaded with lipid droplets. Metabolic labeling with ^{14}C fatty acids demonstrated that intercellular M. *tuberculosis* can access and utilize fatty acids from lipid droplets of macrophage, and that fatty acids from the lipid droplet likely serve as acyl-primers to facilitate synthesis of methyl branched polyketide (PDIM). These data suggest that our model for metabolic realignment to limit propionate toxicity is also valid in a host cell infection model (Figure 5.1).

M. tuberculosis is a metabolically-flexible bacterium [8-10]. This ability is believed to contribute to its extraordinary success, allowing it to persist and replicate within the host environment[9]. Current work focuses on the metabolic plasticity of *M. tuberculosis* by studying how the bacterium re-routes its carbon flow to adapt host nutrients. Our conclusion that *M. tuberculosis* has abilities to exploit host-derived fatty acids to limit metabolic stress from propionate toxicity was based on several lines of evidences. First, in *in vitro* culture, propionyl-CoA, a product of cholesterol, leads metabolic stress and this can be relieved by gating the synthesis of methyl-branched lipids (such as PDIM) through provision of acyl-primers. Secondly, in a macrophage infection model, *M. tuberculosis* is exposed in a significant stress derived from propionyl-CoA, and this metabolic stress can be alleviated through the induction of a foamy macrophage where the bacterium accesses and utilizes the host fatty acids to facilitate incorporation of propionyl-CoA into PDIM.

5.2 Ongoing experiments and future directions

5.2.1. Fatty acids transporters

Our finding that fatty acids rescue the *Δicl* mutant from propionate toxicity brings up several questions to be addressed in future studies. For example, observations such as this could be applied to a forward genetic screen to identify mutants defective in the uptake and processing of short and long chain fatty acids. As discussed earlier, it has been believed that host lipids are critical to the survival of *M. tuberculosis* during infection [9, 11-13]. However, the fatty acids uptake and metabolic processing still remain to be elucidated. As detailed in Chapter 3, the screen that exploited the propionate toxicity identified several genes that may involve in stearic acid processing and uptake. In addition, mutants defective in survival in this screen (under-represented) may be more susceptible to stearic acid because, as shown in Chapter 2, similar to other saturated fatty acids, stearic acid also appeared to have a growth inhibitory effect. Indeed, most of under-represented genes that have been followed appear to be involved in susceptibility to stearic acid rather than its utilization (data not shown).

In order to precisely define the genes that are required for the stearic acid uptake and metabolic processing, we designed another TraSH-based screen to reveal mutants that were incapable of utilizing stearic acid, but were also resistant to its growth inhibition. For this screen, we constructed a 10^5 CFU library in CDC1551 using the mariner transposon as shown in Chapter 3.

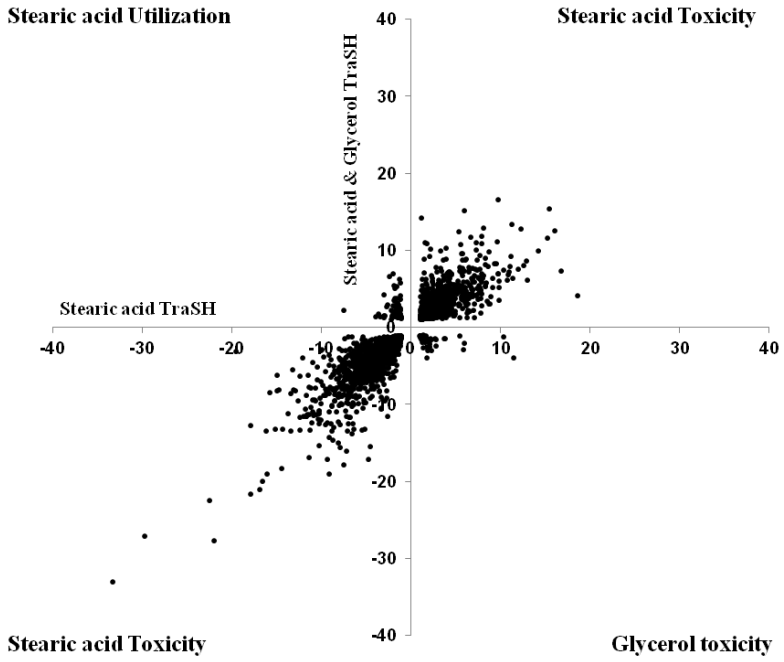

Figure 5.2 TraSH screen for defining genes for stearic acid utilization. S and SG represent TraSH screen on stearic acid, and stearic acid plus glycerol, respectively. All genes selected were >3x-fold over-represented or >3x-fold under-represented with *P*-values < 0.05. Significant genes in the subset of the second quadrant (upper left) are provided in Table 5.1

Table 5.1 Under representors in TraSH screen for stearic acid utilization

Gene	Function	Stearic acid & glycerol TraSH	Stearic acid TraSH
Rv1242	conserved hypothetical protein	1.71	-10.7
Rv2411c	conserved hypothetical protein	2.06	-9.27
Rv1156	conserved hypothetical protein	3.08	-6.59
Rv3401	hypothetical protein	1.35	-6.58
Rv1099c	conserved hypothetical protein	1.86	-5.65
Rv2097c	conserved hypothetical protein	1.46	-5.31
Rv0794c	probable oxidoreductase	4.17	-5.22
Rv1151c	probable transcriptional regulator	1.77	-4.76
Rv0163	conserved hypothetical protein	2.93	-4.7
Rv2459	probable integral membrane transporter	1.41	-4.62
Rv2339	probable conserved transmembrane transporter	1.71	-4.58
Rv0150c	conserved hypothetical protein	2.21	-4.02
Rv2525c	conserved hypothetical protein	3.14	-3.89
Rv3239c	probable conserved transmembrane transporter	1.33	-3.84
Rv1072	probable conserved transmembrane protein	1.91	-3.42
Rv1249c	probable transmembrane protein	3.32	-3.42
Rv2953	conserved hypothetical protein	2.55	-3.38
Rv3123	hypothetical protein	3.1	-3.34
Rv2517c	conserved hypothetical protein.	1.73	-3.3
Rv0918	conserved hypothetical protein	1.55	-3.2

List of genes that have >3 fold under representation in the pool of stearic acid condition but not under-represented in stearic acid and glycerol condition with a *P*-value <0.05.

This library was grown in minimal medium containing 10mM glycerol (input pool) versus minimal medium containing stearic acid (output pool for stearic acid utilization: S) or strearic acid and 10mM glycerol (output pool for growth inhibition of stearic acid: SG). To identify genes that only impact the utilization of stearic acid, we compared the input and output pools of mutants to quantify the mutations that were under-represented or over-represented. As shown Figure 5.2, the TraSH analysis revealed that the under (or over) -representors from S screen were largely shared with those from SG, suggesting that the most dominant themes to emerge from both S and SG screen are genes involved in growth inhibition of stearic acid. However, we found a subset of genes that were likely involved in stearic acid processing (Table 5.1), and currently we are following those genes for further characterization.

5.2.2 Isocitrate dehydrogenase regulator, Rv2170

As discussed earlier, the metabolic flexibility of *M. tuberculosis* relies on the enzyme isocitrate lyase (ICL) [14-16]. Due to the dual role of ICL in the glyoxylate shunt and methylcitrate cycle in *M. tuberculosis*, a functional ICL is required for growth of the bacterium in propionate or fatty acids [17, 18]. Moreover, under hypoxic conditions ICL was shown to play an important role in production of succinate that was required for ATP generation [19]. As shown in other bacteria, isocitrate, the substrate of ICL, is the entry point into glyoxylate cycles, and its flow is known to be regulated by isocitrate dehydrogenase (ICD), which converts isocitrate to α-ketoglutarate in the TCA cycles [20]. Despite the critical importance of understanding

this metabolic node in *M. tuberculosis*, the regulatory mechanism(s) impacting the metabolic flux downstream of isocitrate remain to be elucidated. Like other bacteria [21, 22], *M. tuberculosis* is likely to modulate the isocitrate flow through regulation of ICD activity. Therefore we are interested in identifying potential ICD suppressor(s) that repress ICD activity in the presence of fatty acids and facilitates carbon flow into the glyoxylate cycle.

We hypothesized that if the growth *Δicl* mutant on fatty acid was slowed or delayed by an ICD suppressor, then the mutation of such a hypothetical suppressor would allow the mutant to grow on the fatty acid medium. To identify potential regulators for ICD a library of 10^5 transposon mutants generated in H37Rv *Δicl* was grown on minimal medium containing 0.05mM stearic acid. In this screen, we identified the GCN5-related N-acetyltransferase (Rv2170) as being positively selected for increased growth. We selected 36 colonies and 27 of which have transposon insertion in upstream of Rv2170. As key regulatory mechanism, protein acetylation has been known to modulate enzyme activity involved in metabolic pathways [23-25]. In mycobacteria, protein acetylation is known to control diverse metabolic enzymes including acetyl-CoA synthetase [26-28].

To validate Rv2170 as an ICD suppressor, we examined the phenotypes of the mutant, H37Rv *Δicl Tn::Rv2170*. As shown in Figure 5.3, the double mutant *Δicl Tn::Rv2170* was able to grow in stearic acid-containing medium, while the growth of the parent *Δicl* mutant strain was delayed with a marked initial lag phase.

A

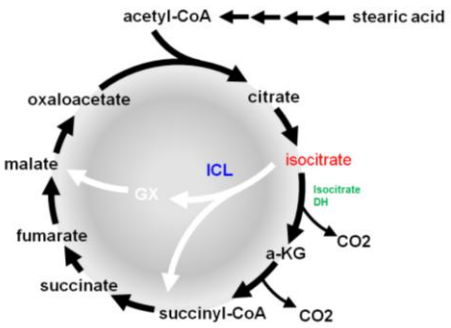

B

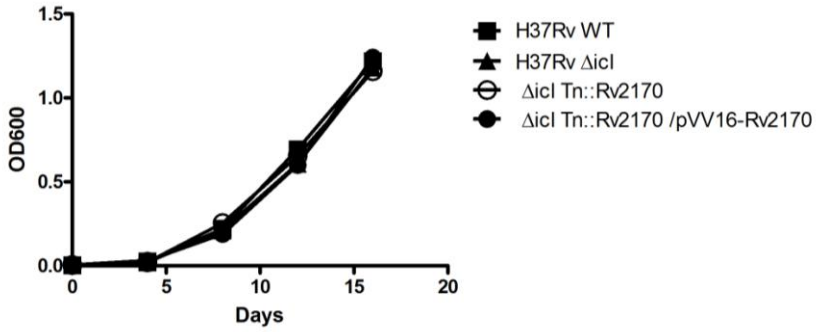

C

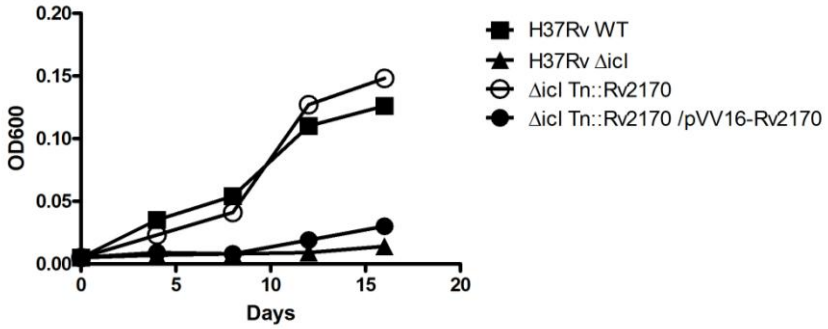

Figure 5.3 Mutation of Rv2170 allows *Δicl* mutant to grow on fatty acids without initial lag phase. The *Δicl1* mutant strain exhibits long initial lag phase on fatty acids but growth can be restored by inactivation of Rv2170. (A) TCA and glyoxylate cyles (B) and (C) Bacterial growth, measured by absorbance at 600 nm, was determined for H37Rv wt, *Δicl* , *Δicl Tn::Rv2170* , *Δicl Tn::Rv2170* / pVV16-Rv2170 strains grown in minimal media containing 10mM glycerol (B) or 0.05mM stearic acid (C) as primary carbon source.

A

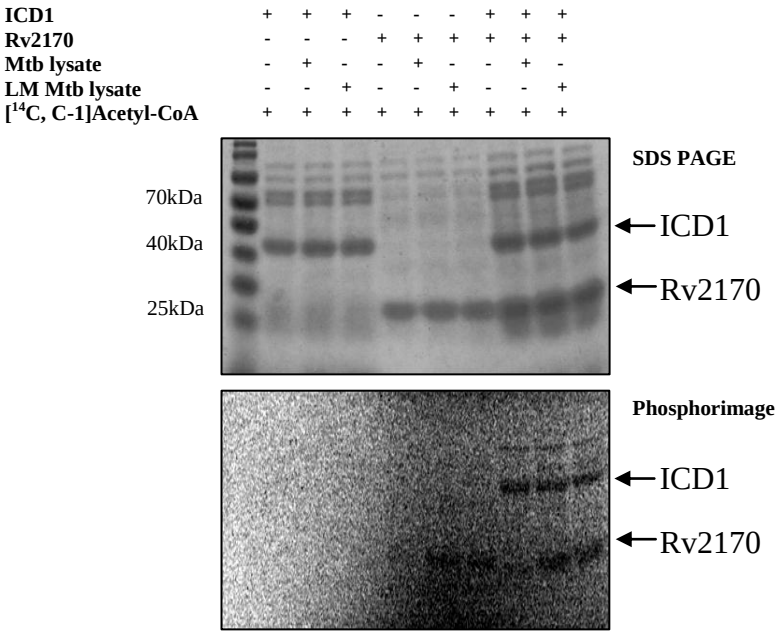
ICD1 + + + - - - + + +
Rv2170 - - - + + + + + +
Mtb lysate - + - - + - - + -
LM Mtb lysate - - + - - + - - +
[14C, C-1]Acetyl-CoA + + + + + + + + +
SDS PAGE
70kDa
40kDa
25kDa
ICD1
Rv2170
Phosphorimage
ICD1
Rv2170

B

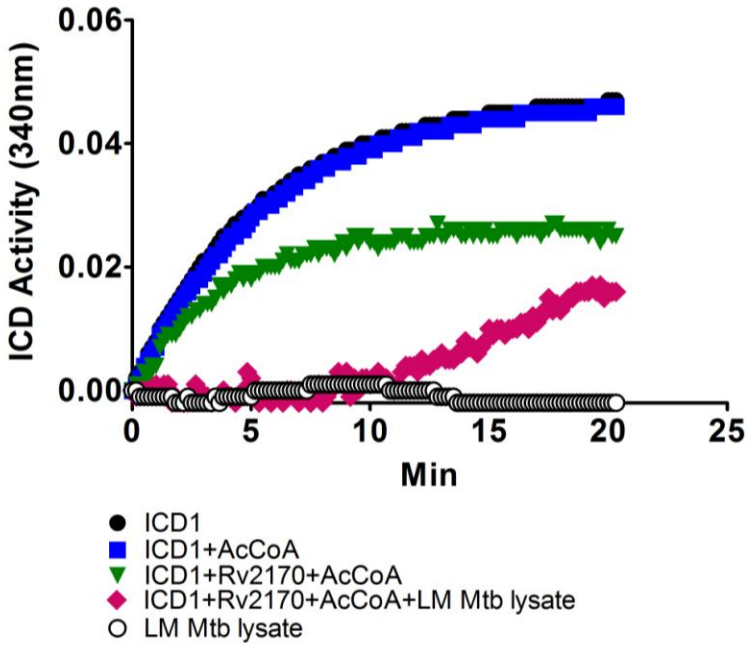
ICD Activity (340nm)
0.06
0.04
0.02
0.00
0
5
10
15
20
25
Min
ICD1
ICD1+AcCoA
ICD1+Rv2170+AcCoA
ICD1+Rv2170+AcCoA+LM Mtb lysate
LM Mtb lysate

Figure 5.4 Rv2170 represses ICD1 activity through acetylation. (A) Rv2170 protein acetylates ICD1 in *M. tuberculosis* lysate dependent manner by using [14C, C-1] acetyl-CoA as substrate. *M. tuberculosis* lysate was prepared from wt H37Rv grown on acetate as sole carbon. The lysate was depleted of proteins by passage through 2kDa size exclusion column (LM Mtb lysate). Upper gel, Coommassie-stained SDS-PAGE gel. Lower gel, phosphorimage of the upper gel. (B) ICD1 (0.5μg) activity was suppressed by addition of Rv2170 (0.3μg) in *M. tuberculosis* lysate (LM Mtb lysate) dependent manner in presence of 50μM acetyl-CoA. ICD1 activity was monitored by measuring NADP reduction at 340nm.

To study this regulatory mechanism further, we tested whether recombinant Rv2170 could acetylate ICD *in vitro.* To achieve this, *M. tuberculosis* ICD1 (Rv3339c) and ICD2 (Rv0066c) were purified to homogeneity and incubated with purified Rv2170 in the presence of [^{14}C, 1-C]-Acetyl-CoA. Following the failure of initial experiments we included *M. tuberculosis* lysate because cofactors such as cyclic AMP may be required for protein acetylation [27]. A bacterial lysate was prepared from *M. tuberculosis* H37Rv culture grown on 10mM acetate. The lysate was depleted of proteins by passage through a size exclusion column (2 kDa). As shown Figure 5.4A, Rv2170 acetylated ICD1 in the presence of the bacterial lysate, suggesting that Rv2170, as a protein acetyltransferase, was dependent on cofactors. Next, we assessed whether this interaction through protein acetylation would impact ICD1 activity. To do this, we measured ICD activity with or without Rv2170. The ICD activity was monitored by the generation of NADPH which is cofactor of the ICD reaction. We also included the *M. tuberculosis* lysate. As shown in Figure 5.4B, the activity of ICD1 was suppressed in the presence of Rv2170 and the bacterial lysate, demonstrating that acetylation of ICD1 by Rv2170 leaded a reduction of ICD1 activity in *M. tuberculosis* lysate-dependent manner. These data provide biochemical verification of the phenotype of the double mutant, *Δicl Tn::Rv2170*. Currently, we are following the Rv2170 to further elucidate a regulatory mechanism for isocitrate flow in central carbon pathway by studying potential lysine residues of ICD1 targeted by Rv2170, and by identifying cofactors that may be involved in this acetylation reaction.

5.3 Concluding remarks

The result presented in this study has clarified some key issues that are critical to our understanding of a metabolic reprogramming in *M. tuberculosis* during the course of infection. Our data by using *in vitro* culture and macrophage infection model has established how *M. tuberculosis* limit propionate mediated metabolic stress. Additionally, the genetic profiling by TraSH in this work provides a comprehensive characterization of fatty acid and propionate metabolism in *M. tuberculosis*; transport into the bacterial cell, the degradation and conversion of the fatty acids into primary metabolites. Lastly, the present work provides insights that extend our appreciation of carbon metabolism of *M. tuberculosis* within its host cell and to develop novel chemotherapeutic strategies.

5.4 References

1. Griffin, J.E., et al., *Cholesterol catabolism by Mycobacterium tuberculosis requires transcriptional and metabolic adaptations.* Chem Biol, 2012. **19**(2): p. 218-27.
2. Pandey, A.K. and C.M. Sassetti, *Mycobacterial persistence requires the utilization of host cholesterol.* Proc Natl Acad Sci U S A, 2008. **105**(11): p. 4376-80.
3. Brock, M. and W. Buckel, *On the mechanism of action of the antifungal agent propionate.* Eur J Biochem, 2004. **271**(15): p. 3227-41.
4. Horswill, A.R., A.R. Dudding, and J.C. Escalante-Semerena, *Studies of propionate toxicity in Salmonella enterica identify 2-methylcitrate as a potent inhibitor of cell growth.* J Biol Chem, 2001. **276**(22): p. 19094-101.
5. Rocco, C.J. and J.C. Escalante-Semerena, *In Salmonella enterica, 2-methylcitrate blocks gluconeogenesis.* J Bacteriol, 2010. **192**(3): p. 771-8.
6. Gonzalo-Asensio, J., et al., *PhoP: a missing piece in the intricate puzzle of Mycobacterium tuberculosis virulence.* PLoS One, 2008. **3**(10): p. e3496.
7. Abramovitch, R.B., et al., *aprABC: a Mycobacterium tuberculosis complex-specific locus that modulates pH-driven adaptation to the macrophage phagosome.* Mol Microbiol, 2011. **80**(3): p. 678-94.
8. Eisenreich, W., et al., *Carbon metabolism of intracellular bacterial pathogens and possible links to virulence.* Nat Rev Microbiol, 2010. **8**(6): p. 401-12.
9. Russell, D.G., et al., *Mycobacterium tuberculosis wears what it eats.* Cell Host Microbe, 2010. **8**(1): p. 68-76.

10. Shi, L., et al., *Carbon flux rerouting during Mycobacterium tuberculosis growth arrest.* Mol Microbiol, 2010. **78**(5): p. 1199-215.

11. Rohde, K.H., et al., *Linking the transcriptional profiles and the physiological states of Mycobacterium tuberculosis during an extended intracellular infection.* PLoS Pathog, 2012. **8**(6): p. e1002769.

12. Russell, D.G., et al., *Foamy macrophages and the progression of the human tuberculosis granuloma.* Nat Immunol, 2009. **10**(9): p. 943-8.

13. Russell, D.G., H.C. Mwandumba, and E.E. Rhoades, *Mycobacterium and the coat of many lipids.* J Cell Biol, 2002. **158**(3): p. 421-6.

14. McKinney, J.D., et al., *Persistence of Mycobacterium tuberculosis in macrophages and mice requires the glyoxylate shunt enzyme isocitrate lyase.* Nature, 2000. **406**(6797): p. 735-8.

15. Munoz-Elias, E.J. and J.D. McKinney, *Mycobacterium tuberculosis isocitrate lyases 1 and 2 are jointly required for in vivo growth and virulence.* Nat Med, 2005. **11**(6): p. 638-44.

16. Rhee, K.Y., et al., *Central carbon metabolism in Mycobacterium tuberculosis: an unexpected frontier.* Trends Microbiol, 2011. **19**(7): p. 307-14.

17. Gould, T.A., et al., *Dual role of isocitrate lyase 1 in the glyoxylate and methylcitrate cycles in Mycobacterium tuberculosis.* Mol Microbiol, 2006. **61**(4): p. 940-7.

18. Munoz-Elias, E.J., et al., *Role of the methylcitrate cycle in Mycobacterium tuberculosis metabolism, intracellular growth, and virulence.* Mol Microbiol, 2006. **60**(5): p. 1109-22.

19. Eoh, H. and K.Y. Rhee, *Multifunctional essentiality of succinate metabolism in adaptation to hypoxia in Mycobacterium tuberculosis.* Proc Natl Acad Sci U S A, 2013. **110**(16): p. 6554-9.

20. Cozzone, A.J., *Regulation of acetate metabolism by protein phosphorylation in enteric bacteria.* Annu Rev Microbiol, 1998. **52**: p. 127-64.

21. Garnak, M. and H.C. Reeves, *Purification and properties of phosphorylated isocitrate dehydrogenase of Escherichia coli.* J Biol Chem, 1979. **254**(16): p. 7915-20.

22. Garnak, M. and H.C. Reeves, *Phosphorylation of Isocitrate dehydrogenase of Escherichia coli.* Science, 1979. **203**(4385): p. 1111-2.

23. Starai, V.J., et al., *Sir2-dependent activation of acetyl-CoA synthetase by deacetylation of active lysine.* Science, 2002. **298**(5602): p. 2390-2.

24. Thao, S. and J.C. Escalante-Semerena, *Control of protein function by reversible Nvarepsilon-lysine acetylation in bacteria.* Curr Opin Microbiol, 2011. **14**(2): p. 200-4.

25. Wang, Q., et al., *Acetylation of metabolic enzymes coordinates carbon source utilization and metabolic flux.* Science, 2010. **327**(5968): p. 1004-7.

26. Lee, H.J., et al., *Cyclic AMP regulation of protein lysine acetylation in Mycobacterium tuberculosis.* Nat Struct Mol Biol, 2012. **19**(8): p. 811-8.

27. Nambi, S., N. Basu, and S.S. Visweswariah, *cAMP-regulated protein lysine acetylases in mycobacteria.* J Biol Chem, 2010. **285**(32): p. 24313-23.

28. Nambi, S., et al., *Cyclic AMP-dependent protein lysine acylation in mycobacteria regulates fatty acid and propionate metabolism.* J Biol Chem, 2013. **288**(20): p. 14114-24.